Volume 7 | Number 23 | 7 December 2023

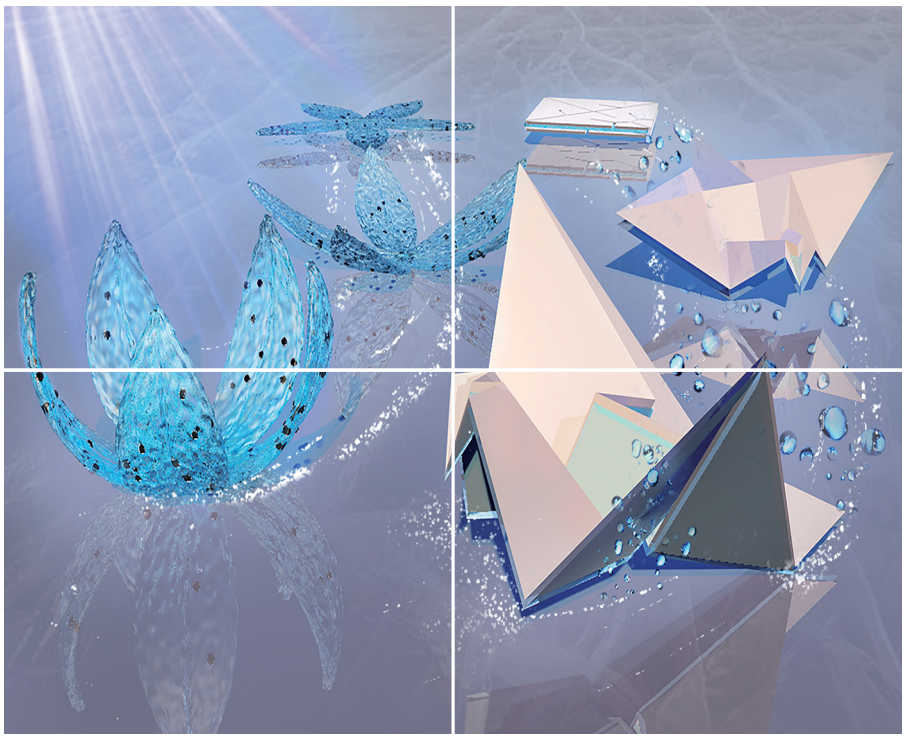

MATERIALS CHEMISTRY

FRONTIERS

CCS 中国化学会 CHINESE CHEMICAL SOCIETY

ICCAS 1956

ROYAL SOCIETY OF CHEMISTRY

rsc.li/frontiers-materials

MATERIALS CHEMISTRY
FRONTIERS

REVIEW

View Article Online
View Journal | View Issue

Cite this: *Mater. Chem. Front.*, 2023, **7**, 5989

3D shape morphing of stimuli-responsive composite hydrogels

Xiao Li, †[a] Minghao Li, †[a] Lisa Tang,[bc] Diwei Shi,[a] Emily Lam[bc] and Jinhye Bae *[abc]

In nature, plants and animals undergo remodeling to adapt to changes in their surroundings. Stimuli-responsive hydrogels, with their abundant water content and inherent responsiveness to environmental stimuli, serve as ideal candidates for mimicking the morphing behavior of living tissues or organisms. When combined with other materials, stimuli-responsive hydrogels extend their shape morphing abilities, along with corresponding functionalities. This review delves into the fundamentals involved in incorporating stimuli-responsive hydrogel matrices and functional additives, exploring the shape morphing mechanism and fabricating stimuli-responsive composite hydrogels. An exploration of recent advances in stimuli-responsive composite hydrogels suggests their potential applications in diverse fields, including soft robotics, information encryption/decryption, biomedical research, flexible electronics, and engineering living materials. As these innovative materials continue to develop, they hold the promise of revolutionizing daily lives and shaping the future of the biosphere.

Received 1st August 2023,
Accepted 25th September 2023

DOI: 10.1039/d3qm00856h

rsc.li/frontiers-materials

1. Introduction

Hydrogels, esteemed as pioneering polymers employed in the progression of new materials, are hydrophilic, cross-linked, three-dimensional polymer structures capable of absorbing, swelling, and maintaining immense quantities of water or aqueous solutions. Gels have traversed a remarkable trajectory since their conception in the late 19th century by Scottish chemist Thomas Graham.[1] He used sol–gel chemistry to make a silica gel. Graham's initial exploration of gel-like colloids opened the door to a plethora of material advancements, although the concept of hydrogels was not mentioned at that time. The term 'hydrogel' was first coined in 1894 to describe a type of colloidal gel.[2] Demonstrating the remarkable water absorption capabilities and distinguished swelling properties

[a] *Materials Science & Engineering Program, University of California San Diego, La Jolla, CA 92093, USA. E-mail: j3bae@ucsd.edu*
[b] *Chemical Engineering Program, University of California San Diego, La Jolla, CA 92093, USA*
[c] *Department of NanoEngineering, University of California San Diego, La Jolla, CA 92093, USA*
† Authors have equal contribution to this review.

Xiao Li

Xiao Li is a PhD student in the Materials Science and Engineering Program under the supervision of Prof. Jinhye Bae. His research interests lie in the stimuli-responsive hydrogels and 3D printing of smart polymers. He received his bachelor's degree at Nanjing Tech University in China. In 2019, he obtained his master's degree at the University of Chinese Academy of Sciences. In 2021, he joined Prof. Bae's lab and started working as a graduate student researcher at the University of California San Diego.

Minghao Li

Minghao Li is a PhD candidate in the Materials Science and Engineering Program, conducting research under the supervision of Prof. Jinhye Bae. His research is primarily focused on the integration of functional additives into stimuli-responsive hydrogels for developing new approaches in shape morphing systems. Minghao completed his undergraduate studies at Iowa State University and went on to earn his master's degree at the University of Florida in 2018. Since 2019, he has worked as a graduate student researcher in the Bae research group at the University of California San Diego.

of hydrogels was instrumental in propelling them into the scientific spotlight. This allowed their humble beginnings to evolve into the multifunctional materials that form the basis of countless biomedical, pharmaceutical, and environmental applications today. Currently, numerous scholarly articles have been published to dissect the properties and applications of hydrogel materials, each providing unique insights. According to the origin, composition, ionic charge, physical structure, crosslinking, and application of hydrogels, they can be classified from different perspectives.[3–5] For instance, hydrogels can be classified as natural, synthetic, and hybrid based on their origin, but they also enable to be categorized into homopolymer hydrogels, copolymer hydrogels, double network (DN) hydrogels, and interpenetrating polymer network (IPN) hydrogels from the perspective of the composition. In past decades, the development of smart or intelligent hydrogels, also known as stimuli-responsive hydrogels, marked a significant milestone in the field and heralded a new era of hydrogel research. Smart hydrogels possess the remarkable ability to respond to environmental factors such as temperature,[6] light,[7] electric,[8] magnetic fields,[9] pH,[10] mechanical force,[11] *etc.* Through a combination of ingenious chemistry, molecular design, and processing techniques, smart hydrogels are capable of exhibiting a dramatic shift in their shape,[12] swelling behavior,[13] color or transparency,[14] mechanical strength,[15] rheology,[16] adhesive property,[17] and conductivity. This provided opportunities to manipulate and control the hydrogel responses in a predictable and desired manner, thus making them ideal for a range of applications spanning from drug delivery systems, where they can control the release of therapeutics,[18] to soft electric sensors, where they can monitor the signals like strain, humidity, pressure, temperature, *etc.*[19] Moreover, the intelligence of these hydrogels goes beyond simple responsive behavior. Advanced smart hydrogels can be programmed to exhibit sequential and logic-gated responses,[20] opening new horizons in the development of active and adaptive materials.

Jinhye Bae

Jinhye Bae is an Assistant Professor in the Department of NanoEngineering at the University of California San Diego. She received her PhD in Polymer Science and Engineering at the University of Massachusetts Amherst in 2015, and then worked as a Postdoctoral Fellow in the School of Engineering and Applied Sciences at Harvard University. Her research focuses on understanding the physical and chemical properties of polymeric materials to program their shape reconfiguration and responsiveness. Her research interests also include the integration of material characteristics into new structural design and fabrication approaches for applications in biomedical devices, soft robotics, actuators, and sensors.

In recent years, composite hydrogels, an effective way to fabricate smart hydrogels, attract significant attention due to their numerous advantages and unique properties that allow them to overcome some limitations, including low strength, limited functionalities, and isotropic volume change, inherent to traditional hydrogels.[19,21,22] Typically, composite hydrogels involve combining a hydrogel matrix with other materials, such as inorganic fillers, organic compounds, or other polymers, significantly enhancing their functionality and performance. One key advantage of composite hydrogels is their improved mechanical properties. Traditional hydrogels, while flexible and soft, often lack sufficient mechanical strength and stability, limiting their applications in load-bearing situations. However, by incorporating additional materials into the hydrogel network, composite hydrogels can demonstrate increased toughness, strength, and resilience.[23] This opens up opportunities for their use in mechanically demanding environments, such as tissue engineering and regenerative medicine.[24] Additionally, composite hydrogels offer the advantage of tailoring their response to external stimuli. By selecting specific materials, these hydrogels can be designed to respond to environmental factors like temperature, pH, light, or biological molecules. This versatility in stimuli-responsiveness expands their potential application spectrum.[25] Notably, the synergistic effects of hydrogel matrices and incorporated functional additives can introduce new functions to the hydrogel, such as magnetic responsiveness, electrical conductivity, or photo- and even mechano-luminescence.[26–29] For instance, Zhang *et al.* introduced ZnS into the fabrication of a sandwich-like actuator, the existence of ZnS endows the hydrogel matrix with electroluminescence. By combining with reasonable control logic, the ability of self-adaptive background color-matching can be observed.[30] Also, Li *et al.* encapsulated biological dinoflagellates, bioluminescent unicellular marine algae, with the hydrogel matrix and eventually realized mechanoluminescence due to the special responsiveness of algae additives, which can be used for optical signaling and illumination.[31] Furthermore, composite hydrogels exhibit improved control over their porous structure. By manipulating the composition and preparation process, the porosity, pore size, and distribution of pores within the hydrogel can be finely tuned.[32] This feature is particularly useful in applications like biomedicine and tissue scaffolding, where pore structure plays a crucial role in cellular behavior and tissue formation, and the biocompatibility of composite hydrogels can be improved through the integration of biological materials, such as proteins or polysaccharides.[33] Overall, composite hydrogels, with their mechanical strength, customizability, enhanced functionality, controlled porosity, and biocompatibility, present significant advantages over traditional hydrogels. As a result, they have been increasingly adopted across diverse fields and hold great promise for future technological advancements.

As one of the most fascinating properties of smart composite hydrogels, their shape morphing behavior, the ability to undergo pre-programmed changes in shape under specific environmental stimuli, represents an exciting frontier in material science, with potential ramifications across interdisciplinary

fields.[34] The fundamental reason for focusing on shape morphing behavior in hydrogels is the significant advancement in functionalities that it offers.[35] In bioengineering and medicine, for instance, shape morphing hydrogels can lead to advancements in minimally invasive procedures and personalized medicine. Hydrogels that can change their shape in response to specific biological signals could potentially deliver drugs more precisely, navigate complex biological structures, or even alter their form to match changing physiological needs.[36] In the realm of soft robotics, shape morphing hydrogels could lead to the creation of robots that can adapt to their surroundings and perform tasks with a sophisticated and delicate level, which is currently unattainable with rigid materials.[37] Additionally, the potential for environmental sensing is exciting, where shape-changing hydrogels could provide visual, real-time indicators of changes in parameters like pH, temperature, or pollutant levels.[38–40] More importantly, the study of shape morphing behavior also offers fundamental insights into the interplay between materials and their environments. This can lead to an in-depth understanding of naturally occurring shape-changing processes, such as using the hydrating/dehydrating induced shape change of hydrogels to study the cavitation of soft materials and observing the shape change of hydrogels that swell in granular medium to investigate why soil can reduce the ability of hydrogels to absorb water and swell.[41,42] Such knowledge could, in turn, inform the design of more efficient materials and systems. In sum, the shape morphing behavior of hydrogels presents an avenue of study with far-reaching implications. From advancing medical procedures to contributing to the rise of soft robotics, this research area promises to reshape our understanding of what materials are capable of achieving.[43]

In this review, we mainly focus on the three-dimensional (3D) shape morphing behavior of stimuli-responsive composite hydrogels and comprehensively discuss their hydrogel matrices, functional additives, interaction between additives and matrices, fabricating techniques, shape morphing mechanisms, as well as different external stimuli-induced shape-morphing complexity of composite hydrogels (Fig. 1). In stark contrast to previous overviews of shape morphing behavior of smart soft materials such as shape memory polymers, liquid crystal elastomers, or pure stimuli-responsive hydrogels,[44–49] we dig much deeper in the contribution of composite hydrogels to shape morphable soft matter and highlight the role of utilizing the chemistry of hydrogel matrix, functionalities of additives, and their interaction to tailor inhomogeneity of synthetic composite hydrogels. For an in-depth understanding of the state-of-art composite hydrogels with shape morphing behaviors, we also compile the emerging fabrication methods, designing mechanisms and recent advances of shape morphable composite hydrogels. These progress in shape morphing of composite hydrogels are categorized by the type of initiating stimuli, ranging from temperature,[50] light,[51] electricity,[8] magnetic field,[52] pH value,[53] solvents[54] to other stimuli like force.[55] Moreover, an exhaustive and up-to-date application scenario of shape morphable composite hydrogels have been depicted, including soft robotics,[56] information encryption,[57] biomedical applications,[58,59] flexible electronics,[60] and engineered living materials.[61] For each application, we discuss in detail a few rationally designed devices, systems, or mechanisms with far-reaching perspectives. Finally, we conclude with insights into the development and barriers in shape-morphable composite hydrogels, providing an effective source to recognize the current developmental limitations and inspire innovative strategies for future smart hydrogel research.

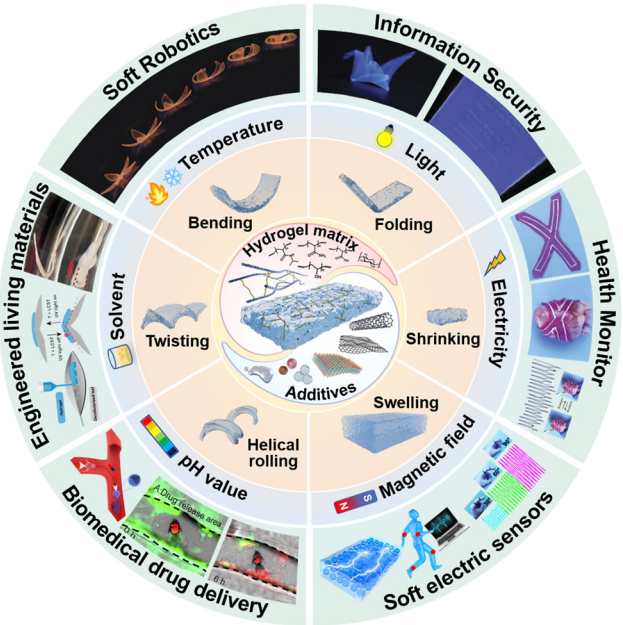

Fig. 1 Representative composition, 3D shape-morphing, types of stimuli that can be responded to, and emerging applications of composite hydrogels. Reproduced with permission.[56–61] Copyrights 2016, Springer Nature, Copyright 2021, 2021 Wiley-VCH, Copyright 2021, 2022, 2022, American Chemical Society.

2. Chemistry of conventional hydrogels and additive components for composite hydrogels

In general, hydrogel matrices and functional additives are the two basic components of fabricating composite hydrogels. The co-existence of hydrogel matrices and functional additives serves as an efficient combination of continuous phases and discrete reinforced phases.[62]

Continuous hydrogel matrices function as a bonding agent between matrices and additives, the crosslinked network of hydrogels can provide structural support and create a stable environment for incorporating various additives.[63] Moreover, hydrogel matrices enable to transfer and distribute the loads between additives. The stronger interaction between matrices and additives contributes to more effective load distribution and energy dissipation, thus improving the mechanical properties of composite hydrogels.[64,65] Additionally, since hydrogels physically entrap or chemically bind additives, these additives are protected by the hydrogel matrices from external destruction and environmental corrosion.[62] Especially, unlike toxic

polymer matrices, hydrogel matrices can supply a bio-friendly, hydrophilic living environment, which is compatible with bio-additives like specific cells, fungi, and bacteria.[66] Notably, different types of hydrogel matrices also endow composite hydrogels with various classification criteria. Specifically, composite hydrogels can be categorized based on their origin, responsiveness, and constitution. They include natural and synthetic composite hydrogels depending on their origin. As for their responsiveness, composite hydrogels can be classified as non-responsive, temperature-responsive, light-responsive, solvent-responsive, and other stimuli-responsive hydrogels. Moreover, based on their constitution, composite hydrogels are divided into single-network, double-network, and multiple-network composite hydrogels.[21]

Regarding functional additives, on the one hand, incorporating stiff additives can strengthen the specific region of the hydrogel matrix,[67] which is commonly accompanied by the decrease of swelling ratios of hydrogels when specific interactions occurred between additives and matrices.[68] It is noteworthy that composite hydrogels exhibit a dependency on additives dispersion.[21] The well-distributed additives are the basic requirement to prepare isotropic composite hydrogels, whereas the concentrated or patterned distribution is a typical technique to create a modulus and sensitivity mismatch throughout the hydrogel matrices. On the other hand, the particular functional additive can integrate the specific sensitivity to new stimuli, thereby expanding the functionality of stimuli-responsive composite hydrogels.[69] Taking into account the diversity of additives, composite hydrogels can also be classified through the composition and sensitivity of additives.[21] For example, based on the composition of additives, composite hydrogels can be categorized as carbon-based, metal-based, and polymer-based additives reinforced composite hydrogels. Similarity, considering the dimension of additives, they can be divided into 0D, 1D, 2D, and 3D fillers reinforced composite hydrogels.

Therefore, selecting or synthesizing proper matrices and additives for composite hydrogels necessitates deeply understanding the chemical structures and properties of different hydrogels and additives. To comprehensively summarize hydrogel matrices and functional additives that are typically used for preparing composite hydrogels, we first elucidate various types of hydrogels, including non-responsive natural hydrogels, non-responsive synthetic hydrogels, and responsive (or smart) hydrogels. For each type of hydrogel, their special chemical structures, common preparation and crosslinking mechanism, outstanding traits, as well as potential limitation are introduced. Afterward, carbon-based, metal-based, polymer-based, Mxene-based, cellulose-based, and other additives are reviewed. Several of the most common examples in these additive families are chosen to showcase their representative functionalities, including morphological structures, sensitivity, mechanisms, stimuli-responsiveness, and shape-morphing behaviors of the corresponding composite hydrogels.

2.1. Chemistry of typical hydrogels for composite matrix

2.1.1. Non-responsive natural hydrogel matrices. Nature is frequently regarded as an eternal, reliable, economic, and productive technique for generating attractive hydrogel matrices. Researchers around the world have extracted and received plenty of biological chemicals that can constitute gel-like structures from animals or plants in various ecological environments, such as cellulose-rich plants, algae, shrimp, and animal collagen. Owing to the bio-friendly origins of these chemicals, favorable biocompatibility can be observed in nearly all natural hydrogels, leading to their promising applications in biomedical fields such as wound healing, drug delivery, tissue regeneration, and more.[70–72]

Alginates (Alg), as one of the most famous natural hydrogels, have been widely studied in past decades.[73] It is typically extracted from brown algae (*i.e.*, Phaeophyceae), which are the major seaweeds of the temperate and polar regions. Over 200 different alginates have been produced, originating from different brown algae species.[74] The chemical structure of alginate is an anionic linear polysaccharide consisting of β-D-mannuronic acid (M) residues and α-L-guluronic acid (G) residues. The carboxylic groups in G and M residues tend to deprotonate in H_2O with a pH value higher than the pK_a of alginates (pK_a value of M and G residues are 3.38 and 3.65, respectively), thereby forming the anion $-COO^-$ and H_3O^+.[73,75] Moreover, the sequential arrangement of these two residues forms three different chain blocks: successive G-block (*e.g.*, -GGGG-), successive B-block (*e.g.*, -BBBB-), and alternating GM-block (*e.g.*, -GMGM-).[73,75] Notably, the content ratio of G-block to B-block differs in more than 200 kinds of existing alginates.[74] Since the gelation and properties of a hydrogel generally depend on the stable network generated *via* physical or chemical interactions, understanding possible crosslinking methods is crucial to designing and tuning their properties. In alginates, there are three typical mechanisms to crosslink polysaccharide chains: (1) acid crosslinking; (2) ion crosslinking; (3) covalent crosslinking.[75] For acid crosslinking, contrary to the aforementioned deprotonation of carboxyl groups, the anionic $-COO^-$ will protonate and return to carboxyl groups if the pH value is below the pK_a of alginates, thus hydrogen bonding and entanglements will be dramatically imposed due to the disappearance of electrostatic repulsion.[76,77] Overall, stronger crosslinking can be obtained in a more acidic environment, but acid crosslinking is hard to control and the strong acids always degrade the alginate chains. Ion crosslinking is the most prevalent approach. Introduced multivalent cations (*e.g.*, Ca^{2+}, Mg^{2+}, Mn^{2+}, Al^{3+}, Fe^{3+}) can be anchored into the cage, where surrounded by $-COO^-$, and interconnect as a ''box-egg'' model.[78] Interestingly, the anion suppliers involved in the ion interaction mainly originate from the G-block, followed by the GM-block, but rarely from the B-block.[71] This can be attributed to the eq–eq linkage present in the B-block, which leads to a flatter three-fold screw symmetry and creates cages too small for cations to occupy.[78] Therefore, alginates with more G-block will fulfill stiffer but more brittle mechanical behaviors. The third method is covalent crosslinking, which is based on the chemical reaction between the bifunctional crosslinker and the carboxyl and hydroxyl groups in alginates. The most well-known crosslinker is diamine; the secondary amine groups can condense with carboxyl

groups in alginates and undergo amidation.[79] With the assistance of catalysts, the chemical network is easily constructed. In addition to the crosslinking controllability and intrinsic biocompatibility of alginates, they can also be used to improve the stretchability and toughness of hydrogels.[80] In 2012, Sun *et al.* proposed a highly stretchable and tough hydrogel *via* hybrid crosslinking (Fig. 2a). The combination of two toughening mechanisms, crack bridging by the network of covalent crosslinks and hysteresis by unzipping the network of ionic crosslinks, increases the stress and stretch at rupture to 156 kPa and 2300%, respectively. These properties are 3.7 kPa and 120% for the parent alginate gel, 11 kPa and 660% for the parent polyacrylamide gel.[81] Despite the outstanding advantages of alginates, several limitations still restrict their development. For example, the stability of alginate hydrogels is easily affected by enzymes (*i.e.*, alginase), surrounding media, pH value, degree of oxidation, and temperature.[73,82] Additionally, the viscous alginate precursor is always used as a thickening agent to prepare adhesive or cohesive substances, but the high viscosity also poses difficulties in processing.[83]

Similar to alginate hydrogels, many other polysaccharides with analogous chemical structures are capable of preparing natural hydrogels. One significant example is agar, which is obtained from the cell walls of red algae. Agar is composed of a mixture of gellable agarose and non-gellable agaropectin. The hydrogen bonds in agarose are the main source of gelation. As the temperature increases, hydrogen bonds will dissociate, leading to the transition from a gel state to a sol state in agar. Owing to the relatively low gel point (37 °C) and excellent biocompatibility, agar has always been applied in food manufacturing and plant biology.[84,85] Another fascinating natural hydrogel is chitosan which is acquired by treating the chitin shells of shrimp, crab, and other crustaceans with an alkaline substance.[86] Chitosan is a linear chain with a random distribution of D-glucosamine and *N*-acetyl-D-glucosamine. The crosslinking of chitosan hydrogels is based on active amino and hydroxyl groups inside. Either strong coordination with metal ions (*e.g.*, Fe^{3+}) or covalent reaction with bifunctional crosslinkers (*e.g.*, dicarboxylic acid) can facilitate chitosan to generate stable networks (Fig. 2b).[87] Normally, the pK_b value of amino groups in chitosan is around 6.5, thus significant protonation occurs in a neutral solution (pH = 7) and chitosan will be water-soluble. In the meantime, protonated amino groups enable it to readily attract negatively charged surfaces such as mucosal membranes, and residual unprotonated amino groups and hydroxyl groups can function as donors to form hydrogen bonding with acceptors on different surfaces. As a result, chitosan has been widely used to improve the bio-adhesion of hydrogels (Fig. 2b), which is meaningful to wound adherence, anti-inflammation, skin protection, and wearable devices.[88–90]

Gelatin, which origins from animal collagen, is another traditional hydrogel matrix. It contains plenty of peptides and proteins, which are linear biomolecules and macromolecules comprised of various amino acid residues.[91] Since gelatin can be referred to as hydrolyzed collagen, the types and contents of various amino acid residues in gelatin are nearly the same as those in collagen, including glycine, proline, hydroxyproline, alanine, glutamic acid, arginine, *etc.* (Fig. 2c).[72] Among these amino acids, glycine dominates the formation of hydrogen bonding between gelatin chains, which eventually assembles to helixes with double or triple strands. Additionally, the existence of H_2O molecules can assist to bridge the interaction between other amino acids in gelatin chains, thus improving the stability of formed helixes. In virtue of the above assembly

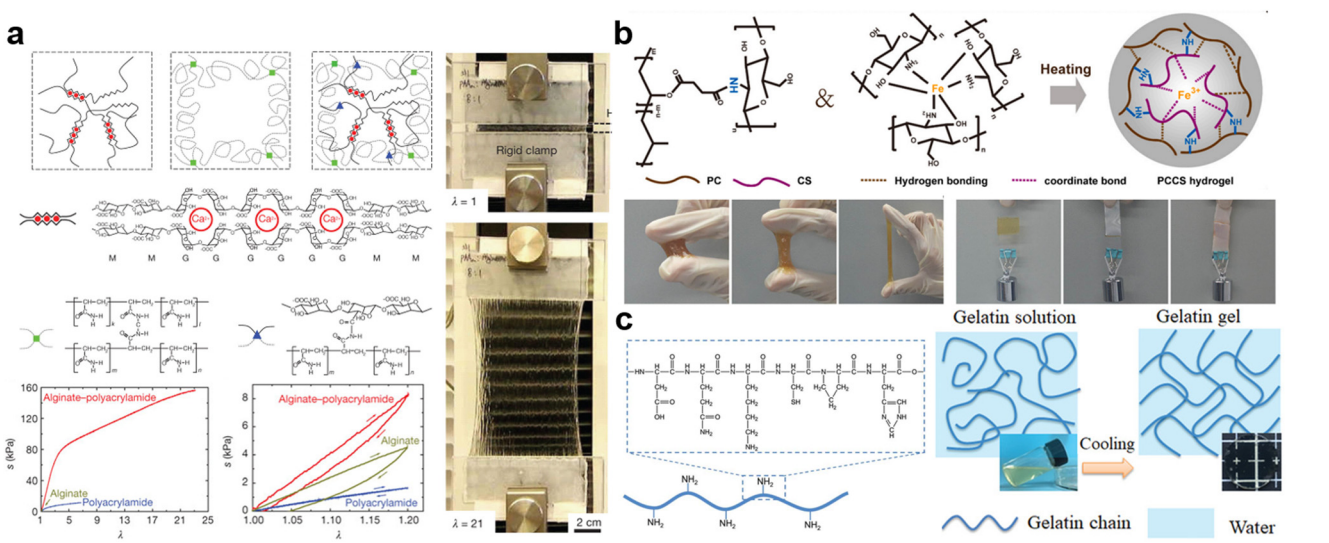

Fig. 2 Representative natural hydrogels: (a) the network comparison of alginate, polyacrylamide, and alginate–polyacrylamide hybrid hydrogels, and their mechanical tensile test and loading–unloading cyclic test (the photograph present stretchability of alginate–polyacrylamide hybrid hydrogel). Reproduced with permission.[81] Copyrights 2012, Springer Nature. (b) The double crosslinked hydrogel based on amidation and coordination bonds from carboxylated polyvinyl alcohol (PC) and chitosan/Fe^{3+}, and photographs exhibit its adhesion property. Reproduced with permission.[87] Copyright 2022, Elsevier. (c) The formula and gelation of gelatin hydrogel. Reproduced with permission.[72,93] Copyright 2020, Wiley-VCH.

mechanism, the gelation of gelatin can be realized *via* assembly-induced crystallization or crosslinking.[92] Typically, owing to the heating-dependent dissociation of the hydrogen bonding, the increasing temperature can destroy the helical conformation of gelatin chains, which means the hydrogel network can be de-crosslinked. Contrarily, the cooling procedure promotes the regeneration of the hydrogen bonding, leading to the recovery of crosslinked network and gelation (Fig. 2c).[93] Another crosslinking approach is creating covalent bonds through the chemical reaction between bifunctional crosslinkers (*e.g.*, diisocyanate) with amino, acid, or amide groups in gelatin. Notably, gelatin-based hydrogels exhibit a broad selection of tensile strength, ranging from 2.4 to 63.25 MPa for samples derived from the pig skin.[94] Actually, the strength of gelatin is determined by double or triple helixes contents, which vary in different origins of gelatin, such as distinct species, tissues, or organs.[94] In addition to widely optional mechanical strength, the hydrolysis of gelatin endows it with biodegradability, so gelatin hydrogels have been mostly used as hard capsules in pharmaceutics, gelling agents in food manufacturing, cartilage replacement, *etc.*[94–97]

2.1.2. Non-responsive synthetic hydrogel matrices. Unlike biodegradable natural hydrogels, hydrogels with stable properties and long lifetimes are also desired in certain engineering fields, like soft robotics, pollutant removal, and wearable electronics. Thus, scientists have developed a series of synthetic hydrogels *via* rational molecular structure design and reasonable chemical synthesis.[98] In synthetic hydrogels, hydrophilic polymer chains are basic units that constitute three-dimensional networks, monomers with plenty of hydroxyl, amide, carboxyl, or amino groups are typically employed to examine polymerization and crosslinking due to their fantastic hydrophilicity. Their molecular weights, conformations, and properties are readily controlled by synthesis procedures. In other words, the high programmability of synthetic hydrogels creates more available choices for hydrogel-based applications. For example, mechanical behaviors in some cases can be regulated *via* simply changing molecular weights, crystallinity, or polymer components.[99] Additionally, although the biocompatibility of these synthetic hydrogels is not as good as natural hydrogels, they are still bio-friendly and non-toxic. Hence, synthetic hydrogels enable to be also applied in biomedical fields like artificial implanting materials, drug release systems, contact lenses, *etc.*[71] Here, to better acknowledge the family of synthetic hydrogels, some representative synthetic hydrogels that always occur as non-responsive hydrogel matrices are briefly introduced.

Poly(vinyl alcohol) (PVA) hydrogels, which are one of the most researched water-soluble polymers, are typically prepared by the base hydrolysis of polyvinyl acetate (PVAc). The preparation of PVAc is achieved through the free radical polymerization of the vinyl acetate monomer. Since a number of hydroxyl groups on PVA chains can establish the intramolecular and intermolecular interaction by complementary hydrogen bonding, several adjacent polymer strands in certain regions are more likely to be oriented, thereby forming the crystallization. These crystallized regions can be viewed as physical-crosslinking sites of PVA hydrogels due to bundled polymer chains. Thus, physical crystallization is the most common way to realize the gelation of PVA.[100] At present, there are three methods that researchers use for generating outnumbered crystallization inside PVA hydrogels: cyclic freezing–thawing,[101–104] solvent exchange,[102,105,106] and salting-out.[105,106] For the cyclic freezing–thawing procedure, the low temperature not only weakens the movement of chains but increases the contact time for PVA chains, resulting in higher crystallinity. Regarding solvents exchange, switching solvents from good solvent to poor solvent promotes the aggregation of PVA chains, the distance between PVA chains is dramatically shrunk and more crystallines can be formed. The salting-out effect is using certain salts to attract H_2O molecules, which can form solvent–chain hydrogen bonding and competes with chain–chain hydrogen bonding. The introduction of salts decreases this competition and thus improves crystalline contents. Furthermore, the molecular weight of PVA chains is another critical factor to determine the crystallinity.[107] Longer polymer chains provide more hydroxyl groups that participate in the crystallization. Interestingly, the crystallinity is closely related to the mechanical behavior of PVA hydrogels.[103] On the one hand, crystallines can block the propagation of crack tips, and PVA hydrogels will be stiffened. On the other hand, extracting polymer chains from crystallines has to dissipate energy, which means PVA hydrogels will be toughened. Therefore, increasing crystallinity is capable of preparing PVA hydrogels with both high strength and large stretchability.[108] For instance, Xu *et al.* fabricated a highly-crystalized PVA hydrogel *via* the synergic effect of solvent exchange and salting-out (Fig. 3a). In virtue of ultrahigh crystallinity of 30%, the resultant PVA hydrogels obtained coordinatively enhanced stiffness (52.3 ± 2.7 MPa) and toughness (120.7 ± 11.7 kJ m^{-2}) respectively.[106] Although PVA hydrogels are well-known for their impressive mechanical behavior, they are hard to function as water purification, actuators, and the driving source of soft robotics. That is because highly crystalized (*i.e.*, physically crosslinked) networks also induce low H_2O absorption and anti-swelling behavior.[109]

Polyacrylamide (PAM) hydrogels are typically fabricated by the free radical polymerization of the acrylamide monomer and crosslinkers (*e.g.*, *N*,*N*′-methylenebisacrylamide, abbreviated as BIS) induced chemical crosslinking.[110] Since PAM chains are characterized by their extremely hydrophilic amide groups, the significant swelling ratio is readily observed in the aqueous environments.[111] Simultaneously, the large volumetric expansion is accompanied by high water contention, making PAM hydrogels commonly used as superabsorbents.[112] Moreover, another feature of PAM hydrogels is their relatively low mechanical strength. Despite the adjustable stretchability realized by the contents of crosslinker, the stress at the fracture point of PAM hydrogels is around 10 KPa, which limits the development of PAM hydrogels.[113] To address this problem, Kim *et al.* proposed a highly-entangled PAM hydrogel in recent years (Fig. 3b). This high entanglement is acquired from the acrylamide precursor with a high concentration of monomers but low concentration of both initiators and crosslinkers. Compared to regular PAM hydrogels, once the polymerization is initiated in this precursor, more monomers will eventually form much

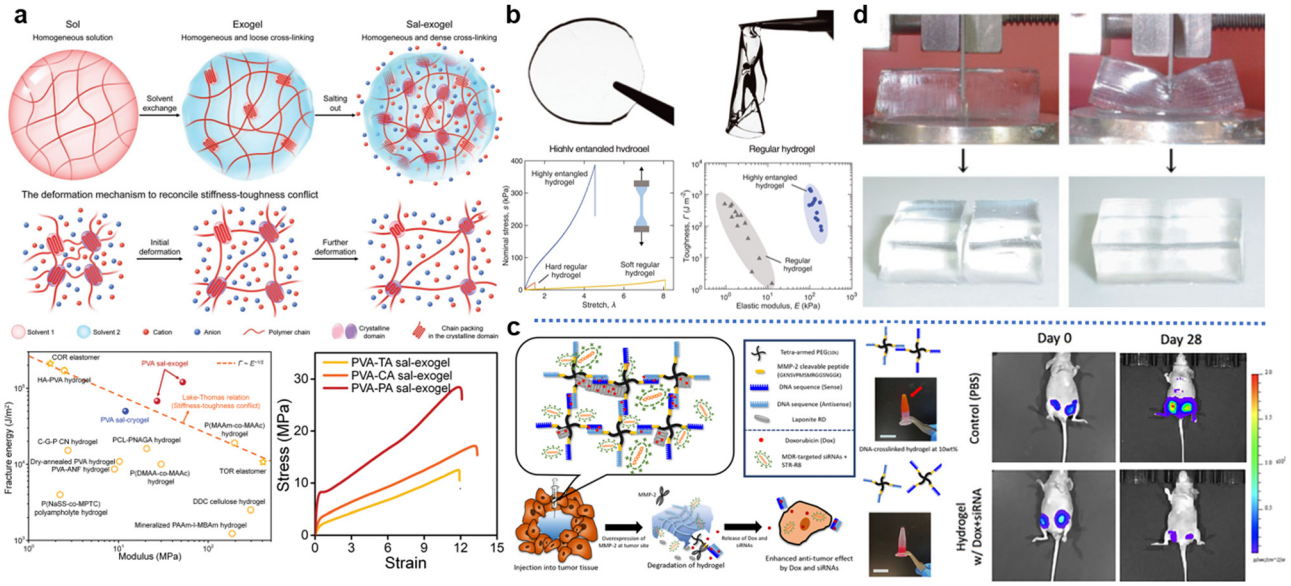

Fig. 3 Representative synthetic hydrogels: (a) The highly-crystalized PVA hydrogel with excellent mechanical performance, which is realized by solvent exchange and salting-out effect. Reproduced with permission.[106] Copyrights 2023, Wiley-VCH. (b) The mechanical comparison between the regular PAM hydrogel and the highly-entangled PAM hydrogel. Reproduced with permission.[114] Copyright 2022, American Association for the Advancement of Science. (c) The DNA crosslinked PEG hydrogel and its degradation mechanism. Triggered by the tumor-specifc enzyme (MMP-2), therapeutic cargos are released in multidrug resistant cancer. Representative images of IVIS spectrum measurement of mice over 28 days present *In vivo* anti-cancer efficacy of the therapeutic hydrogel. Reproduced with permission.[120] Copyright 2020, Elsevier. (d) The strength of a poly(2-acrylamido-2-methylpropanesulfonic acid) (PAMPS)/PAM DN hydrogel that resists slicing with a cutter. Reproduced with permission.[122] Copyrights 2003, Wiley-VCH.

longer PAM chains, and they will be prone to interpenetrate with each other. In this situation, numerous entanglements endow PAM hydrogels with higher breaking stress, and the energy dissipation from sliding and disentanglement between chains contributes to improved stretchability.[114] Overall, the simple synthesis, favorable biocompatibility, and easily-expanded networks of PAM hydrogels facilitate them to be developed in drug sustained-release,[115] tissue engineering,[116] and agriculture.[117]

Polyethylene glycol (PEG), a linear polymer terminated by two hydroxyl groups, is typically synthesized by ring-opening polymerization of ethylene oxide and H_2O. Either acidic or basic catalysts can accelerate the polymerization. The gelation of PEG hydrogels predominantly relies on chemical crosslinking, including chain-growth crosslinking, step-growth crosslinking, and mixed-mode growth crosslinking.[118] For chain-growth crosslinking, adding a certain crosslinker terminated by two ethylene oxides is required. Two ethylene oxides at both ends of the crosslinker enable them to participate in PEG polymerization and connect separate PEG strands, eventually forming a stable network. Regarding step-growth crosslinking, the monomer with tetra-functional groups that can react with hydroxyl groups needs to be used. Based on this reaction, this monomer functions as the linking center, which connects four PEG chains and constitutes the fence-like network. Mixed-mode growth crosslinking refers to PEG chains undergoing free-radical polymerization after their hydroxyl groups were modified by vinyl or other groups enabling chain growth. In this process, a substance that possesses the vinyl group at one end and the group that reacts with hydroxyl at another end (*e.g.*, acrylate acid) is inevitable for the modification, and a crosslinker like BIS is necessary for the following gelation. Owing to the advantage of easy modification for PEG hydrogels, they are broadly applied in the biomedical field, such as tumor treatments.[119] As shown in Fig. 3c, PEG chains are modified by amino acid first and then connect two DNA molecules with complementary sequences. Pairing DNA molecules is viewed as DNA crosslinking, which can be easily degraded after injecting into tissues. Subsequently, the anti-tumor medicine can be released.[120]

Notably, all synthetic hydrogels listed above are based on a single polymeric system. However, integrating functionalities from different hydrogels is one of the challenges that researchers are facing. In recent years, a fascinating and general strategy, DN hydrogels, has been introduced to integrate the advantages of two independent networks.[121] Take using DN hydrogels to fabricate strong and tough hydrogels as an example, Gong *et al.* reported a DN hydrogel with extremely high mechanical strength (Fig. 3d).[122] At the heart of their DN hydrogels lies the DN architecture, which consists of two distinct polymeric networks: a stiff and brittle first network intertwined with a soft and stretchable second network. The first network with high mechanical strength provides the DN hydrogel with rigidity and load-bearing capabilities. In contrast, the second network formed by a more elastic and flexible polymer imparts the DN hydrogel with elasticity and deformability. Eventually, the resultant DN hydrogel exhibits a stress of 17.2 MPa and a fracture strain of 92%, respectively. These values greatly exceed that sustained by the single network gels. Therefore, as an emerging technique for integrating synthetic hydrogels, DN hydrogels provide promising potential for fabricating all-inclusive hydrogel matrices.

2.1.3. Responsive hydrogel matrices. Stimuli-responsive hydrogels are another special hydrogel matrices, which can actively detect external stimuli and feedback certain responsiveness.[123] According to the types of stimuli that can be sensed, the stimuli-responsive hydrogels are divided into temperature-responsive hydrogels, light-responsive hydrogels, pH-responsive hydrogels, *etc.* Next, the preparation, characteristics, and mechanisms of these stimuli-responsive hydrogels will be clarified by combining the introduction of some representative examples.

Temperature-responsive hydrogels, one of the most common smart hydrogels, are mainly received in hydrogels with lower critical solution temperature (LCST) or upper critical solution temperature (UCST).[7,46,124] LCST is the critical temperature below which the components of a mixture are miscible in all proportions. Polymers with LCST have been more extensively studied in aqueous solutions.[6,125] The most famous representative hydrogel possessing LCST is poly(*N*-isopropylacrylamide) (PNIPAM). PNIPAM hydrogels are typically synthesized *via* free radical polymerization of NIPAM monomers and amide crosslinkers.[126,127] When the environmental temperature is below the LCST, PNIPAM chains are hydrophilic and miscible with water due to the formation of hydrogen bonds with water molecules, resulting in a coil-like structure of the chains. Once the temperature is heated up to the LCST, the increased activity of H_2O molecules will break their hydrogen bonds with amide groups, thus invaliding the solvation of PNIPAM chains. Afterward, the intra/interchain hydrophobic interaction will be dominated by the hydrophobic interaction between isopropyl groups, and PNIPAM chains will change to hydrophobic and collapse into a globule structure.[128] Simultaneously, this collapse of PNIPAM chains leads to the volumetric shrinkage of the whole network, and the white color gradually occurs as a result of the phase separation between hydrophobic chains and hydrophilic aqueous environment (Fig. 4a).[129] Contrarily, UCST is the critical temperature above which the components of a mixture are miscible in all proportions. In hydrogels with UCST, the IPN hydrogels of PAM and polyacrylic acid (PAA) is one of the most common examples. Since amide groups in PAM is a better hydrogen acceptor compared to H_2O and carboxyl groups in PAA is a better hydrogen donor compared to H_2O, the complementary hydrogen bonds in the coexisted system of PAM-PAA are more stable than that in PAA-H_2O or PAM-H_2O. In other words, the inclination of chains to form the phase separation instead of the solvation attributes to dominated intra-/inter-chain hydrogen

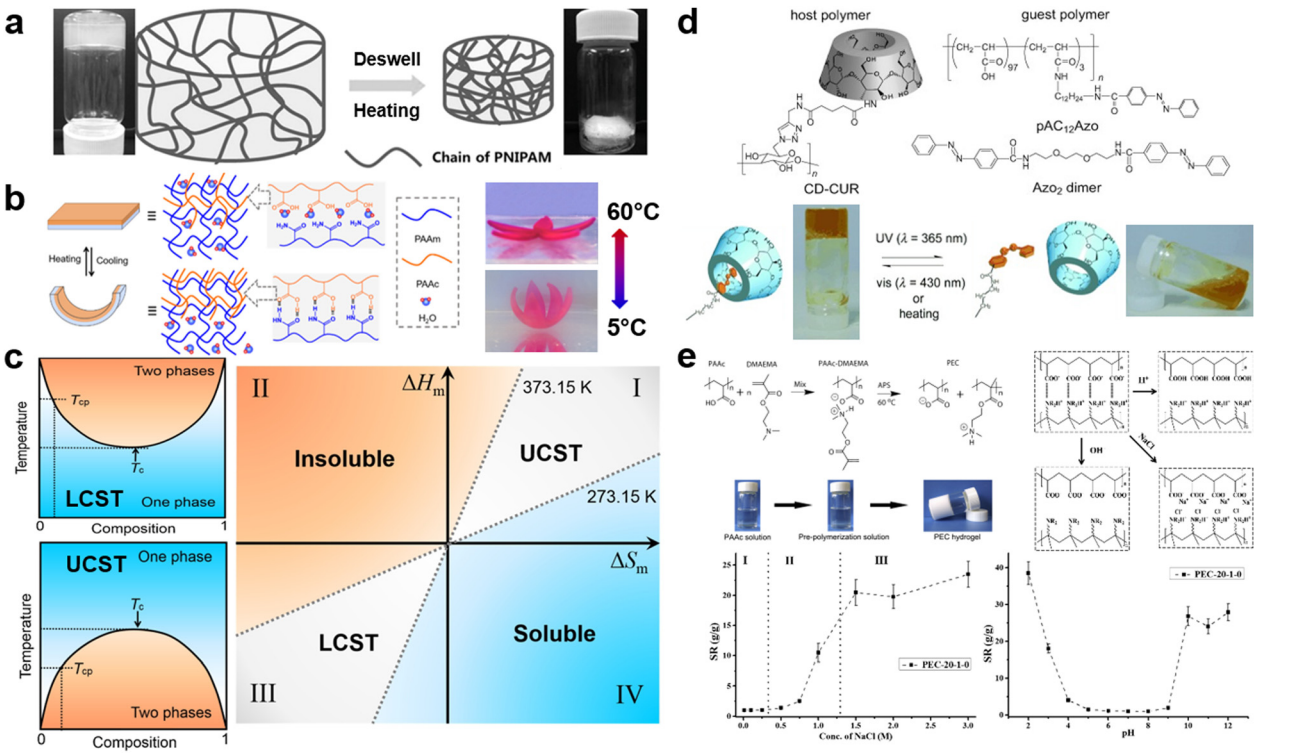

Fig. 4 Representative smart (stimuli-responsive) hydrogels: (a) The swelling/deswelling behavior of PNIPAM hydrogels based on heating/cooling temperature upon its LCST. Reproduced with permission.[129] Copyrights 2015, Wiley-VCH. (b) The dual-layer actuator driven by controlling temperature upon/below UCST of IPN of PAM-*co*-PAA. Reproduced with permission.[130] Copyright 2019, American Chemical Society. (c) Typical phase diagrams of a polymer solution with LCST and UCST behavior (T_c: critical temperature; T_{cp}: cloud point), and the thermodynamic map showing the solubility and solution properties of polymers in water (the ΔH_m–ΔS_m plot is divided into 4 zones depending on the changes of enthalpy (ΔH_m) and entropy (ΔS_m) and the temperature: I – polymers with UCST; II – insoluble non-thermoresponsive polymers; III – polymers with LCST; IV – soluble non-thermoresponsive polymers. Zones I and III are delimited by the freezing and boiling points of water at 273.15 and 373.15 K, respectively). Reproduced with permission.[131] Copyright 2019, Elsevier. (d) vis/UV responsive supramolecular hydrogels based on azobenzene and host–guest interaction. Reproduced with permission.[138] Copyright 2010, Wiley-VCH. (e) The dually-pH-responsive PEC hydrogel consisting of PAA and poly(2-(dimthylamino) ethyl methacrylate) (PDEAEMA). Reproduced with permission.[140] Copyright 2016, Elsevier.

bonds. However, increasing temperature disrupts this domination, because formed hydrogen bonds are broken by enhanced energy. Therefore, PAM/PAA IPN hydrogels recover to be soluble and exhibit UCST transition (Fig. 4b).[130] From a thermodynamical view, the solubility in a binary system can be explained by phase diagrams (Fig. 4c). The phase boundary, also known as binodal curves of binary systems, represents the specific temperature and composition at which a solution transfer from homogeneous to heterogeneous state. The extrema of the binodal curve is the critical temperatures (T_c), including both LCST for the concave case and UCST for the convex case (Fig. 4c).[131] Based on the Flory-Huggins theory, the Gibbs energy of mixing (ΔG_m) is given as $\Delta G_m = RT(n_1 \ln \phi_1 + n_2 \ln \phi_2 + X_{12} n_1 \ln \phi_2)$, where R is the ideal gas constant, n is the molar number, ϕ is the volume fraction, X is the Flory–Huggins interaction parameter, and the subscripts 1 and 2 denote the solvent and the polymer, respectively. Notably, the entropy of mixing (ΔS_m) is $\Delta S_m = -R(n_1 \ln \phi_1 + n_2 \ln \phi_2)$, and enthalpy of mixing (ΔH_m) is $\Delta H_m = RTX_{12} n_1 \ln \phi_2$. For the Gibbs energy of mixing, when $\Delta G_m < 0$, binary systems will spontaneously soluble with each other; when $\Delta G_m > 0$, binary systems will be insoluble; when $\Delta G_m = 0$, the Gibbs energy attains the critical point, the critical temperature T_c can be calculated by $\Delta H_m/\Delta S_m$. Thus, according to the mixing entropy and enthalpy of a polymer–solvent mixture, its solubility can be divided into four regions: (1) insoluble region, where ΔH_m is positive and ΔS_m is negative; (2) soluble region, where ΔH_m is negative and ΔS_m is positive; (3) LCST region, where both ΔH_m and ΔS_m are negative; (4) UCST region, where both ΔH_m and ΔS_m are positive (Fig. 4c).[131] Especially for case (3) and (4), the temperature plays a crucial role in determining solubility. In the LCST region, the polymer is insoluble when $T > T_c$, but it is soluble when $T < T_c$. In the UCST region, the polymer is soluble when $T > T_c$, but it is insoluble when $T < T_c$.[131,132] In a word, designing a temperature-responsive hydrogel is closely relevant to understanding the phase diagram of the polymer–solvent binary system and the effect of intra/interchain interactions on its solubility.

For light-responsive hydrogel matrices, introducing functional groups enabling photochemical reaction into polymer chains, which construct hydrogel networks, is inevitable in their synthesis.[17,133–135] Typically, incorporating photosensitive moieties relies on two approaches: the "click" grafting of moieties onto polymer chains and the polymerizing of monomers modified *via* photosensitive moieties. These photosensitive moieties in polymer structures can reconfigure their molecular structures and affect the properties (*e.g.*, mechanical behavior, rheology, topological structures, fluorescence, adhesive, or responsiveness) of hydrogels by varying the source, intensity, and wavelength of light. For example, the molecular structure of azobenzene is composed of two phenyl rings linked by N=N double bond. Under ultraviolet (UV) light, the structure is nonplanar *cis*-azobenzene, whereas the *cis*-azobenzene will change to planar *trans*-azobenzene once stimulated by visible light or heating.[136,137] Tamesue *et al.* utilized the photosensitive azobenzene and the host–guest interaction to control the gelation and de-gelation reversibly *via* photo irradiation (Fig. 4d). The host polymer can only associate with the *trans*-azobenzene that functions as guest polymers under visible light, this association contributes to physical-crosslinking and realizes the gelation. If the physical-crosslinked hydrogel is irradiated by UV light, the *cis*-azobenzene will dissociate with the host polymer, which means the physical crosslinking will be disrupted.[138]

Regarding pH-responsive hydrogels, cationic or anionic groups, like carboxyl, amino, and sulfonic groups, are needed to realize pH-responsiveness due to the effect of pH value on their protonation or deprotonation.[139] For instance, PAA which is typically synthesized by the free radical polymerization of acrylic acid monomers, is one of the anionic pH-responsive hydrogels. The carboxyl groups on the side chains incline to deprotonate when the pH value is higher than the pK_a of –COOH, thus forming the anion $-COO^-$ and H_3O^+. The existence of the carboxyl anion provides PAA hydrogels with the ability to function as an electrolyte. However, if the pH value is lower than the pK_a of carboxyl groups, the $-COO^-$ anion will protonate and return to carboxyl groups, thereby PAA hydrogels will be neutralized.[111] As an example of pH-responsive hydrogels, C. Wong *et al.* developed a dually-pH-responsive polyelectrolyte complex (PEC) hydrogel consisting of PAA and poly(2-(dimthylamino) ethyl methacrylate) (PDEAEMA) (Fig. 4e). The pH-responsiveness of amino groups is contrary to that of carboxyl groups. When pH value is higher than their pK_a, amino groups will keep the deprotonated neutral form, but the protonation of amino groups will occur once the pH value is lower than their pK_a, eventually generating $-NR_2H^+$ cation. Hence, in this PEC hydrogel, only when the pH value is higher than the pK_a of carboxyl groups and lower than the pK_a of amino groups can the ionic interaction between $-COO^-$ and $-NR_2H^+$ be stable. As a result, the intermolecular interactions, microstructures, and swelling ratio of PEC hydrogels can be regulated *via* controlling the pH value of aqueous environments.[140]

In addition to the representative examples of responsive hydrogels mentioned above, numerous uncommon stimuli-responsive hydrogel matrices have been invented *via* various technologies, such as reasonable molecular design, gradient crosslinking density, and lithography.[141] For example, inspired by the destruction and reconstruction (*i.e.*, mechanical training) of a muscle, Matsuda *et al.* developed a mechanical force-triggered self-growing hydrogel. The mechanical force-responsiveness of this hydrogel relies on the generation of mechanoradicals by mechanical force-induced polymer strand scission. In typical hydrogels, polymer strand breakage leads to crack propagation and eventual failure. However, the DN structure of the hydrogel provides an effective means to preserve mechanoradicals without bulk failure. The brittle first network generates mechanoradicals when it breaks, while the tough second network protects the hydrogel from bulk failure. Simultaneously, these internal mechanoradicals can initiate the polymerization of sustained monomers, which can be regarded as the reconstruction of the first network. With the repetitive loading, the hydrogel can self-grow and be substantially strengthened.[142] Based on the same mechanism, their group exploited a mechanical force stamp to control the self-growing of microstructures on the surface of hydrogels, which engineers the on-demand functions of hydrogels.[143] Moreover, the hydrogels that respond to bio-signals (*e.g.*, peptide, glucose, antibody, and

enzyme) are another set of novel smart hydrogels obtained significant interest.[144] For these bio-signals, their chemical or physical characteristics can affect the crosslinking density, interactions, or molecular conformations of hydrogels, thus achieving bio-responsiveness.[36] For instance, Maitz *et al.* fabricated a thrombin-responsive hydrogel for autoregulating the blood coagulation. Its gelation is based on the reaction between carboxylic acid moieties on heparin, which is a typical anticoagulant that catalyzes the complexation of thrombin with antithrombin, and thrombin-responsive peptides terminated star-PEG. Since thrombin can cleave between the arginine and serine on peptides, crosslinked heparins are immediately released as thrombin increases, resulting in the degradation of hydrogels and the inactivation of the thrombin. Especially, inactivated thrombin cannot cleave inside peptides, thus the release of heparin is gradually terminated and the autoregulation of the blood coagulation is realized.[145] In conclusion, these interesting responsive hydrogel matrices enable them to be promising candidates for fabricating composite hydrogels but also expand the option of functional additives.

2.2. Functional additives for composite hydrogels

Stimuli-responsive hydrogels, prepared by reasonable molecular design, typically exhibit isotropic volume expansion (*i.e.*, swelling) or contraction (*i.e.*, deswelling) in response to one or more stimuli. However, the incorporation of additives into hydrogel matrices provides a way to realize anisotropic responsiveness. Herein lies a great interest in hybrid material systems that combine hydrogels and other materials. Notably, incorporating additives extends far beyond the simple addition of strengthening elements. The potential mismatch in deformation rates or modulus and the susceptibility to temperature and environmental variations enable to creation of discrepancies in composite hydrogels. For example, when materials with disparate deformation behaviors are combined, they may respond differently to applied mechanical forces over time, leading to uneven stress distributions and structural instability. In other words, additive components in composite hydrogels reinforce specific regions, thereby creating a mismatch in a degree of deformation (*i.e.*, swelling or deswelling) or modulus throughout the hydrogel matrices, thus facilitating out-of-plane deformation of composite hydrogels. Alternatively, since the additives and the matrices do not exhibit compatibility with the prevailing environmental conditions, environmental fluctuations (*e.g.*, temperature, light, magnetic field) can induce varying rates of expansion and contraction in the composite hydrogels, potentially causing internal stresses and deformations. Furthermore, certain additives can introduce sensitivity to new stimuli, thereby expanding the functionality of the stimuli-responsive hydrogel. In essence, the mismatch in deformation or modulus, the misfit to environmental changes, and the functionality are three pivotal factors that are worth considering when choosing proper functional additives. Here, we review various types of additives that cooperate with stimuli-responsive hydrogels, such as carbon-based, metal-based, polymer-based, Mxene-based, cellulose-based, and other additives. Representative additives in shape morphing hydrogel systems have been summarized in Table 1.

2.2.1. Carbon-based additives.

As one of the most abundant elements on earth, carbon-based materials have been widely used and investigated due to their low cost and functionalities.[146,147] Carbon-based materials which are related to the unique atomic structures of carbon atoms can be categorized by the dimensionality of carbon-based materials as zero-dimension (*e.g.*, carbon dots), one-dimension (*e.g.*, carbon nanotube), two-dimension (*e.g.*, graphene oxide) and three-dimensional (*e.g.*, carbon sponge).[148] Among various carbon-based materials, carbon nanotubes (CNTs), and graphene oxide (GO) are most intriguing to scientific societies.

For stimuli-responsive hydrogel systems, the major function of carbon-based additives is the photothermal effect for the conversion of heat from light. Typically carbon-based additives such as CNT, GO and reduced graphene oxide (rGO) are black, making them ideal materials to absorb the incident light.[149] Under light irradiation, the photoexcited electron of carbon-based materials will vibrate and interact with others, thereby accumulating heat energy in a short time.[150] As a result, this temperature increase is confined to the light-exposed region. To introduce shape morphing in stimuli-responsive hydrogels, two main approaches are often employed: the anisotropic distribution of carbon-based additives and light localization. By creating heterogeneous structures through techniques such as 3D printing,[151,152] molding[153–155] and photolithography,[156,157] composite hydrogels can achieve designated shape transformation. For example, Shang *et al.* reported on organohydrogels based on rGO-PNIPAM that demonstrated both synergistic shape morphing and color change upon exposure to near-infrared irradiation.[158] Moreover, various methods have been explored to selectively introduce carbon-based materials into the hydrogel matrix, including the infiltration method,[159] electric field[160,161] and UV light irradiation.[162] Researchers have successfully demonstrated complex shape deformation in homogeneous GO-PNIPAM hydrogels by employing local NIR irradiation.[163] Additionally, Wang *et al.* also reported shape morphing of GO-PAM-based trilayer hydrogel by localized NIR light.[164]

In addition to the photothermal effect, carbon-based materials play other essential roles in shaping morphing hydrogel systems. GO, known for its two-dimensional (2D) shape and abundant oxygen-containing groups, has been employed for physical crosslinking within hydrogel networks.[165] This incorporation serves to reinforce the hydrogel structure and reduce swelling/deswelling properties.[166,167] Building on this, Li *et al.* utilized 3-(trimethoxysilyl) propylmethacrylate to modify GO, leading to the synthesis of pH- and temperature-responsive hydrogels with modified GO as a crosslinker.[168] Similarly, Zhang *et al.* utilized the 2D shape of GO to stack and align it in sodium alginate (SA) hydrogels, resulting in a composite hydrogel that exhibits responses to water, humidity, heat, and light.[169] This introduces anisotropic expansion/contraction due to the nacre-like structures. Furthermore, Gregg *et al.* demonstrated a hydrogel actuator by incorporating PNIPAM hydrogel into a patterned CNT forest.[170] The small size of the CNT structure enables a rapid response time of just 70 ms under light exposure. Moreover, Ying *et al.* utilized the conductivity of

Table 1 Representative functional additives in shape morphing stimuli-responsive hydrogel systems

Types of additives	Materials of additives	Hydrogel matrix	Stimuli type	Role of additive	Key properties	Ref.
Carbon-based additives	GO + rGO	PNIPAM + PMAA	Temperature, light, pH, ionic strength	Structural modifier and photothermal effect	Local photoreduction of GO for structural anisotropy	156
	rGO	PNIPAM + organohydrogel	Temperature, light	Photothermal effect	Synergistic color-changing and shape morphing	158
	GO	SA	Water, humidity, light	Structural modifier, photothermal effect	Structural anisotropy by stacking of GO	169
	CNT	P(AMPS-*co*-AA)	Electric field	Conductor	Fast response speed due to additional conductor of CNT	171
Metal-based additives	Cu^{2+}	PNaAc	Solvents	Local crosslinking and stiffening	Electro-driven patterning of ions	173
	AuNP	PNIPAM	Light	Photothermal effect	Biomedical devices, soft actuators	182
	Nd:NP	PAM	Magnetic field	Generation of magnetic torque	Magnetic-field guidance for *in vivo* applications	188
	IONP	PNIPAM	Magnetic field	Magnetothermal effect	Shape deformation under alternating magnetic field	189
Polymer-based additives	PNIPAM microgel	Chitosan	Temperature	Local deswelling	All-hydrogel actuator	193
	PPy	PNIPAM	Light	Photothermal effect	Resistance change with size of hydrogel	194
	Latex microsphere	PNIPAM	Temperature	Local stiffening	Electric-field induced assembly	197
MXene-based additives	MXene	PNIPAM	Light	Photothermal effect	Photopolymerization of Mxene nanomonomer	216
Cellulose-based additives	CNC	PNIPAM	Temperature	Rheological modifier, local stiffening	Shape morphing and antibacterial abilities	225
	NFC	PAA + CMC	Hydration	Local stiffening and change of porosity	Shape morphing owing to hydration and dehydration	229
Other additives	MOFs	PNIPAM	Light	Photothermal effect	Fast response speed due to porous structure of MOF	231
	WS_2 nanosheet	PNIPAM	Light	Photothermal effect and local stiffening	Fast response speed due to ice-templating	232
	NC	PNIPAM	Temperature	Structural modifier and local stiffening	Tunable response speed by intensity-dependent NC structures	233

PMAA = poly(methylacrylic acid); PNaAc = polyelectrolyte (sodium polyacrylate); CMC = sodium carboxymethyl cellulose.

CNT to show shape morphing in CNT-enriched poly(2-acrylamido-2-methyl-1-propanesulfonic acid-*co*-acrylic acid) (P(AMPS-*co*-AA)) hydrogels in response to an electric field.[171] The versatility of carbon-based additives opens up exciting possibilities for creating advanced and responsive hydrogel systems with diverse applications.

2.2.2. Metal-based additives. Metals are known for their stiffness, strength, and density, which contrasts with the soft and flexible nature of hydrogels.[172] This stark difference makes metals highly suitable as functional additives to hydrogel matrices. Incorporating metal-based additives in hydrogels serves two primary roles, offering additional functionalities: (1) stiffening hydrogel matrix; (2) providing additional means to harvest environment stimuli. First, the local embedding of metal ions can crosslink or stiffen hydrogel, thus enabling 3D shape morphing of a single hydrogel sheet. Palleau *et al.* first reported the electrically assisted ionoprinting of hydrogels by introducing copper ions as patterns into poly(sodium acrylate) hydrogels.[173] The patterned hydrogels demonstrated motions such as folding and gripping in response to solvent exchanges between water and ethanol. Other ionoprinted stimuli-responsive hydrogels with 3D shape morphing ability in response to temperature[174] and pH[175] were later reported. Furthermore, other types of responsive particles can be utilized to enhance the mechanical properties of hydrogel matrices in specific ways. For instance, magnetic responsive particles, such as Fe_3O_4, can be selectively localized within the hydrogel under the influence of an external magnetic field. Once positioned, these particles contribute to reinforcing the local hydrogel region, resulting in improved mechanical strength and stiffness. The mismatch between the particle-rich region and hydrogel matrix can lead to out-of-plane shape deformations of the composite hydrogel structures.[176,177] Similarly, electrically responsive particles, such as silver nanoparticles, can be strategically positioned within the hydrogel matrix under an applied electric field. The localized presence of silver nanoparticles enhances the mechanical properties of the hydrogel in the targeted region, allowing out-of-plane deformation.[178]

Secondly, metals can respond to external stimuli, thus triggering the deformation hydrogel matrix in additional means. For instance, metal nanoparticles, including gold nanoparticles (AuNP), iron oxide nanoparticles (IONP), and neodymium-doped nanoparticles (Nd:NP), have the remarkable ability to convert light into heat through a phenomenon known as the photothermal effect.[179–181] This unique property makes metal nanoparticles highly sought after for integration into temperature-responsive hydrogel matrices to harness light-induced deformations.[182–184] When these metal nanoparticles are exposed to light, they efficiently absorb the incident photons, converting the optical energy into localized heat.[185–187] This localized heating raises the temperature of the surrounding hydrogel matrix. As a result, the hydrogel undergoes volume changes due to temperature-induced shrinking, which leads to controlled deformation of the material.

Moreover, the inclusion of Nd:NP and Nickel nanoparticles in hydrogel matrices enables a unique response to magnetic fields, leading to out-of-plane deformations, as these nanoparticles tend to align with the magnetic lines of force[188] or undergo magnetothermal effect,[189] respectively, inducing localized changes in the structures of hydrogels. Hence such structural anisotropy renders shape deformation of the composite hydrogels.

2.2.3. Polymer-based additives. While hydrogel itself is a 3D structure of crosslinked hydrophilic polymers, the addition of other polymer-based materials can be achieved to enhance the mechanical properties of the hydrogel system with physical bonding.[190,191] Microgels with typical diameters ranging from several hundred nanometers to several tens of micrometers are dispersed hydrogel particles that provide the mentioned characteristics. Li *et al.* synthesized calcium-alginate microgels as an additive to the PAM hydrogel matrix and demonstrated enhanced elastic modulus and toughness than pure PAM hydrogel.[192] Hence, the incorporation of stimuli-responsive microgels enhances the volume change of the composite hydrogel than ordinary hydrogel. Furthermore, Anju *et al.* reported that PNIPAM nanogels were added into chitosan hydrogel matrices to introduce anisotropic shape deformation.[193] The PNIPAM nanogels (radius of 60 nm) were synthesized by *in situ* free radical polymerization at 70 °C, above the LCST of PNIPAM. By localization of PNIPAM nanogels, complex shape deformations could be achieved. Therefore, an all-hydrogel-based actuator is prepared without introducing other types of additives.

Besides microgels, other polymer-based materials are also widely used in hydrogel matrices to render additional functionalities. For instance, polypyrrole (PPy) has been loaded into the PNIPAM hydrogel matrix to introduce shape morphing through the photothermal effect.[194] The addition of PPy can further render conductivity to PNIPAM hydrogel which is typically considered an insulator. Therefore, the shape morphing of PPy-PNIPAM composite hydrogels can convert to relative resistance changes, which offers potential in soft robots with a self-sensing ability. Furthermore, rigid polymer additives such as nylon spring,[195] and starch[196] have been incorporated with stimuli-responsive hydrogels. Daniel *et al.* reported PNIPAM hydrogel sheets with electric-field-guided latex microspheres.[197] These microspheres were driven, collected and patterned at the electrode due to the dielectrophoretic force. Owing to the rigid, nonswellable natures of these microspheres, the PNIPAM hydrogel sheets exhibited out-of-plane deformation when the temperature rose above LCST.

2.2.4. Mxenes-based additives. In the past decade, a new family of 2D nanomaterials, MXenes, has received great attention owing to their unique combination of excellent mechanical strength, high metallic/ionic conductivity and tunable properties.[198–200] Thus far, MXenes have been widely used in a gamut of applications such as catalysts, biomedicines and energy storage systems.[201–203] In general, MXenes have the chemical formula $M_{n+1}X_nT_x$ (n = 1–4), where M, X and T represent the early transition metals (*e.g.*, Ti, V, *etc.*), carbon and carbon–nitrogen, and surface terminated groups (*e.g.*, OH, O, or F), respectively.[204] Such chemical formula renders high hydrophilicity and rich surface functional groups which allow the incorporation of MXenes with hydrogel systems.[205–207] Typically, MXenes can act as a crosslinker, an initiator and multifunctional additives within hydrogels. Therefore, MXene-based hydrogel can be fabricated through chemical crosslinking, physical crosslinking, MXene-activated crosslinking and post-embedment of MXene.[208]

Thanks for the excellent photothermal performance, MXenes can bring new functionalities such as 3D shape morphing to stimuli-responsive hydrogels, especially thermos-responsive hydrogels by light exposure.[209–212] Previously developed peroxide-decorated MXene (p-$Ti_3C_2T_x$) and silver nanoparticle-endowed MXene can trigger polymerization of NIPAM monomers through surface-initiated polymerization[213] and pseudo-Fenton polymerization,[214] respectively. The resulting hydrogels can undergo shape transformations through exposure to 808 nm NIR light irradiation. However, due to the limited active crosslinking sites on MXenes, they serve as photothermal additives in temperature-responsive hydrogel matrices such as PNIPAM are more reported. Ge *et al.* demonstrated a binary-layered MXene hydrogel consisting of a passive PAA-MXene layer and an active PNIPAM-MXene layer which underwent 3D deformation through NIR exposure.[215] Xue *et al.* demonstrated an MXene-containing hydrogel actuator by using an electric field during fabrication. MXenes formed a concentration gradient through the thickness of the hydrogel, thus resulting in a structural anisotropy.[216] The actuator also showed programmable shape morphing under NIR light.

2.2.5. Cellulose-based additives. As our society is increasingly demanding renewable and sustainable resources, natural cellulose-based materials with their supreme properties of biodegradation, biocompatibility and multifunctionality have been continuously used worldwide.[217,218] The family of cellulose-based materials is mainly derived as nanofibrilated cellulose (NFC) and cellulose nanocrystals (CNC). NFC particles are cellulose fibrils with a high aspect ratio (the length-width ratio is greater than 25) and contain amorphous and crystalline regions.[219–221] CNC particles are rod-like or whisker-like particles with a relatively smaller aspect ratio (the length-width ratio is greater than 10) and are highly crystalline.[222,223] Both NFC and CNC can be extracted from plants and wood which brings the advantages of abundant resources and low cost. Therefore, cellulose-based stimuli-responsive hydrogels have been the subject of research for decades. Feng *et al.* reported a cellulose hydrogel actuator with lanthanide-ligand which showed 3D deformation in response to pH.[224] Gladman *et al.* demonstrated biomimetic 4D printing utilizing NFC and NIPAM ink that the printed bilayer architectures were programmed with local swelling anisotropy which generated complex 3D shape morphing in response to temperature.[56] Similarly, Fourmann utilized CNC as rheological modifier to print CNC-PNIPAM hydrogels for shape morphing and antibacterial purposes.[225]

Owing to the unique surface chemistry of celluloses, they can be functionalized *via* different methods such as acidic degradation, oxidation and pressure-induced homogenization.[217,218,226–228] The functionalization of cellulose extends the functionalities of the cellulose-based stimuli-responsive hydrogels. Mulakkal *et al.* reported a cellulose-derived polymer that had carboxymethyl

groups bound to the hydroxyl groups of glucose.[229] This carboxymethyl cellulose was prepared to a 4D printing ink with acrylic acid and crosslinked to hydrogels by citric acid. The printed hydrogel actuators underwent reversible 3D shape morphing through the hydration–dehydration process. The cellulose-based shape morphing composite hydrogels are typically biocompatible, thus expecting future applications *in vivo*.

2.2.6. Other additives. Besides the above-mentioned classes of additives, many other additives have emerged within stimuli-responsive hydrogels to create 3D shape morphing. Some metal–organic-frameworks (MOFs) have excellent photothermal efficiency and can accelerate the water adsorption/desorption rate due to their porous structures.[230] Zhang *et al.* reported Zr–Fe MOFs-PNIPAM hydrogel actuators that can bend over 360° within 20 s in response to NIR light.[231] Similar to GO and MXenes, other 2D nanomaterials are also widely used in stimuli-responsive hydrogels. Zhong *et al.* demonstrated a bionic actuator by WS_2 nanosheets and PNIPAM for biomimetic cellular structures and steerable 3D deformations.[232] Its volume shrank ~90% within 6 s and fully recovered within 4 s upon exposure and removal of NIR light, respectively. This fast response rate allowed this actuator to mimic the motion of animals such as the swimming of jellyfish. Zhao *et al.* developed a nanoclay (NC) disk-PNIPAM composite hydrogel actuator on a polydimethylsiloxane (PDMS) layer.[233] The printed NC-PNIPAM hydrogel has confined volumetric expansion/contraction due to the rigid, non-swellable PDMS layer. By photopolymerizing NC-PNIPAM under different light intensities, the hydrogel actuator achieved 3D shape deformation in different kinetics in response to temperature. Furthermore, NC can also respond to ultrasound by converting acoustic energy to heat, thus triggering the shape deformation of PNIPAM hydrogels. Hyegyo *et al.* reported 3D-printed NC-PNIPAM ultrasound-responsive hydrogel grippers which achieved gripping motion under low-intensity ultrasonic irradiation at about 300 mW/cm^2.[234]

3. Dispersion of additives in composite hydrogels

An important consideration for high-quality composites is the uniform dispersion of additives in hydrogels. As we discussed above, some additives added into the hydrogel matrix to offer or improve stimuli-responsiveness are hydrophobic, which will aggregate in the water environment of hydrogels and impact the properties. Well-dispersed additives usually provide significant improvement in the mechanical properties and responsiveness of hydrogels. Due to the concern over dispersion, surface treatments are popular to improve the compatibility between additives and hydrogels. Here, we overview the typical surfactants and common methods of modifying additives, and evaluate their effect on additives distribution.

3.1. Surfactants

Small molecule surfactants are a type of amphiphilic molecule that have both a hydrophobic tail and a hydrophilic head. This amphiphilicity causes the surfactants to form micelles or bilayers when in an aqueous solution. The micelles that form are typically a few nanometers in diameter and consist of a hydrophobic core surrounded by a hydrophilic corona. These structures are known to help dissolve hydrophobic molecules, such as oil, by stabilizing them within the hydrophobic core.

Sodium dodecyl sulfate (SDS) is a commonly used ionic surfactant that forms nanomicelles in water-based solutions. The shape of the self-assembled SDS micelles can vary from spheres to cylinders to lamellae (vesicles), depending on factors such as the concentration of SDS, the ionic strength, and the temperature.[235–237] Liu *et al.* dissolved a hydrophobic and reactive octylphenol polyoxyethylene ether derivative (OP7-AC) in SDS micelle solutions.[238] The OP7-AC molecules within the micelle core were then initiated to copolymerize with hydrophilic acrylic acid and acrylamide monomers to create hydrogels without the need for additional crosslinkers (Fig. 5a). These hydrogels had much higher mechanical properties than those crosslinked by chemical crosslinkers, with a tensile strength of up to 120 kPa and a fracture strain of up to 1350%. The hydrophobic OP7 domains in the hydrogels underwent reversible phase transitions, becoming opaque at 40 °C and transparent when cooled to 10 °C. Surfactant micelles can host both hydrophobic and hydrophilic monomers in their core and corona, respectively. For instance, Du *et al.* dissolved hydrophobic C18 in the core and hydrophilic AMPS in an SDS solution.[239] When initiated, these monomers copolymerized to produce amphiphilic core–shell structured particles that acted as macro-crosslinkers and energy dissipation centers.

Surfactants are also widely used to improve the dispersion of hydrophobic nanoparticles in hydrogel matrices. Zhang *et al.* used an aqueous 2 wt% sodium deoxycholate (DOC) solution as the surfactant to disperse single-walled carbon nanotubes (SWNTs) in PNIPAM pregel solution to fabricate SWNT-PNIPAM hydrogels.[154] Compared to other known surfactants for SWNT dispersion, such as SDS, they found DOC to be more stable in NIPAM monomer solutions. The DOC-SWNTs and NIPAM monomer solutions formed homogeneous mixtures that exhibited stability to SWNT flocculation for several weeks. The SWNTs are uniformly dispersed in PNIPAM hydrogel during the polymerization of NIPAM monomer. Lee *et al.* embedded magnetic IONP into PNIPAM matrix (PNIPAM/IONP) to fabricate a bilayer-type photo-actuator with fast bending motion.[240] They introduced graft chains *via* polymerization of PNIPAM macromonomers (PNM) to realize fast responsiveness of hydrogel matrix due to molecule structure change. Light-responsive grafted-pNIPAM was prepared by free radical polymerization of the pre-gel solution containing macromonomer PNM, BIS as a crosslinker and magnetic IONP, thereby introducing IONP into the PNIPAM matrix after polymerization. The superparamagnetic IONP were dispersed in water by two-step addition of primary and secondary surfactants to prevent the aggregation of the nanoparticles. When IONP are trapped within a thermally responsive PNIPAm hydrogel matrix, they absorb visible light and generate heat. This heat causes the hydrogel matrix to shrink in volume (Fig. 5b).

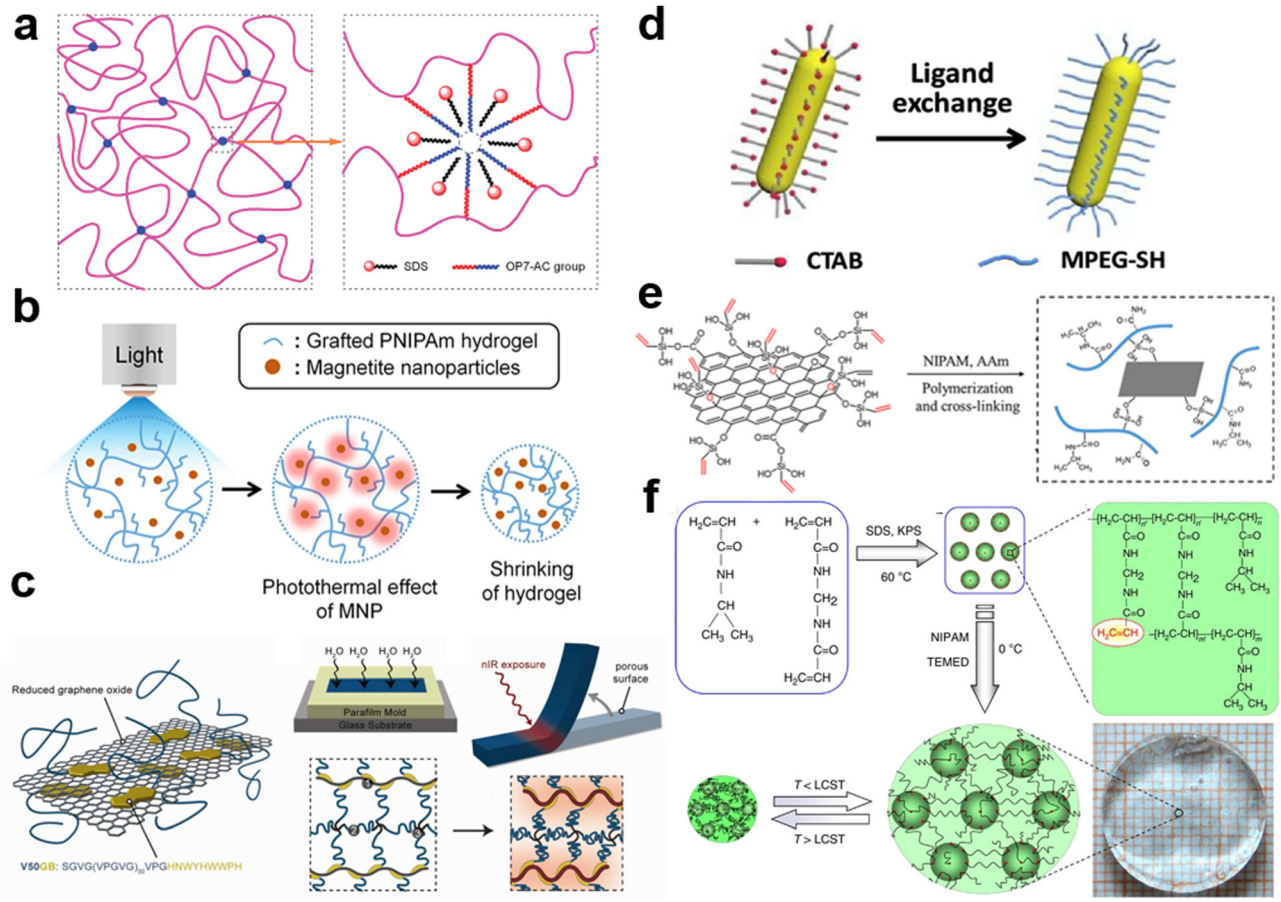

Fig. 5 (a) Schematic illustration of the proposed network model with hydrophobic associating in the gels. Reproduced with permission.[238] Copyright 2010, American Chemical Society. (b) Schematic illustration for the volume shrinking of the grafted hydrogels containing IONP under irradiation of light. Reproduced with permission.[240] Copyright 2015, Springer Nature. (c) Strategy for creating ELP-rGO composite hydrogel actuators. Reproduced with permission.[51] Copyright 2013, American Chemical Society. (d) Schematic for the ligand exchange of AuNRs. Reproduced with permission.[243] Copyright 2019, American Chemical Society. (e) Schematic of GO-VTES and the network structure of the GO composited hydrogels.[244] Reproduced with permission. Copyright 2017, Elsevier. (f) Synthesis of poly(*N*-isopropyl acrylamide) nanogels and hydrogels. Reproduced with permission.[248] Copyright 2013, Springer Nature.

3.2. Surface functionalization of additives

For rigid nanoparticles containing abundant reaction groups on the surface, it is convenient to modify their surface with functional groups.[241,242] Wang *et al.* functionalized rGO with a rationally designed elastin-like polypeptide (ELP) to create ELP-rGO composite hydrogel actuators.[51] They first created a 50 pentapeptide long ELP, V50GB to functionalize the rGO sheets to suppress rGO aggregation (Fig. 5c). V50GB displayed a short graphene-binding (GB) peptide at its C-terminus to promote anchoring to rGO surfaces and modified their surface and colloidal properties. Then they cross-linked the hybrid nanoparticles into an ELP-based network to fabricate ELP-rGO nanocomposite hydrogels with anisotropic porosity. Finally, they irradiated the hydrogels with NIR light to locally shrink the ELP-rGO hydrogels to induce bending motions. Dai *et al.* reported a shape memory hydrogel that is responsive to NIR light irradiation by incorporating gold nanorods (AuNRs) into a P(MAA-*co*-MAM) hydrogel.[243] The photothermal effect of the AuNRs caused a localized increase in temperature, which resulted in a significant reduction in Young's modulus of the pre-stretched hydrogel (from 200 to 2 MPa) and bending deformation with a controllable direction and magnitude. AuNRs were synthesized using a seed-mediated method and Cetyltrimethylammonium bromide (CTAB) as a template. However, the electrostatic interaction between CTAB ligands and a weakly charged gel matrix caused the precipitation of AuNRs in their aqueous suspension, making it unsuitable for direct use in nanocomposite hydrogel synthesis. To overcome this issue, the ligands of AuNRs were switched from CTAB to Methoxy polyethylene glycol thiol (MPEG-SH) (Fig. 5d). After adding ethanol, the suspension of modified AuNRs remained stable while the unmodified AuNRs precipitated. This was due to the desorption of CTAB ligands from the AuNRs in ethanol, whereas MPEG-SH ligands did not desorb. Therefore, the AuNRs were dispersed evenly during the hydrogel synthesis. Wang *et al.* employed vinyl double bonds modified GO to absorb potassium peroxydisulfate (KPS) as an initiator.[244] The edges and surfaces of GO nanosheets are rich in hydroxyl and

carboxylic acid groups, which are used to react with hydroxyl groups of hydrolyzed vinyltriethoxysilane (VTES). By modifying the surface of GO with vinyl double bonds, a multi-functional GO was generated that could copolymerize with thermosensitive monomers such as NIPAM (Fig. 5e). This resulted in the creation of tough and thermoresponsive hydrogels with a tunable lower critical solution temperature (LCST) by adjusting the amount of GO. Wang *et al.* synthesized graphene peroxide (GPO) with a simple radiation method from GO.[245] GO was exposed to a gamma ray with the presence of oxygen and the obtained GPO has abundant peroxides on the surface. The GPO nanosheets are employed to initiate the free radical polymerization of hydrophilic monomers and serve as polyfunctional crosslinkers. The presence of GPO significantly improves the mechanical strength and toughness of the hydrogels.

Microgels, with sizes varying from tens of nanometers to micrometers in diameter, have been employed as pliable and deformable crosslinkers to increase the toughness of hydrogels. Microgels are tiny, pliable spheres composed of crosslinked hydrophilic polymer chains.[246] The crosslink density, functionality, and dimension can be manipulated by altering the synthesis formulations. Microgels can be modified with particular functional groups that can further react or crosslink with hydrophilic polymer chains to create a flexibly crosslinked network. The deformation of microgels upon stretching enables efficient energy dissipation. When responsive components are introduced into microgels, the contraction or expansion of the small crosslinks may result in a significant synergistic effect and thus impart macroscopic responsiveness to the hydrogels.[247] Microgels can be easily modified by adding functional groups or monomers to their structure. For example, microgels with weak acid or acid groups can respond to changes in pH levels, while those with ionic groups can react to changes in ionic strength.[247] Xia *et al.* reported a simple method to synthesize smart nano-structured hydrogels (NSG) by introducing activated nanogels (ANGs) as nano-crosslinkers.[248] ANG-bearing unsaturated double bonds are synthesized by polymerization of NIPAM and BIS (Fig. 5f). Then the NSG hydrogels are fabricated from the ANG nanogels and NIPAM monomer. When the temperature changes, nanogels shrink more quickly than the larger gel. This rapid response causes a quick change in the volume of bulk PNIPAM gels that are crosslinked by microgels. It is believed that the combined response of many nanogels within the matrix leads to a fast response in the bulk gels.

4. Shape morphing mechanisms and fabrication techniques of composite hydrogels

To enable the shape morphing behavior in composite hydrogels, generating ideal "inhomogeneity" requires reasonable mechanisms. These mechanisms direct hydrogels to undergo controlled transformations in response to external stimuli such as light, heat, or pH value.[43] Hence, in this section, we focus on the basic shape morphing mechanisms of composite hydrogels and discuss the design principle for each mechanism, then explain the effect of geometry, gradient distribution, and origami/kirigami on shape morphing behavior. Moreover, since the development of composite hydrogels is closely related to their fabrication, we will summarize the advanced fabrication techniques that are critical to the production of these composite hydrogels. A comprehensive understanding of these processes will be presented.

4.1. Shape morphing mechanisms of composite hydrogels

Conventional hydrogels are characterized by homogeneous polymeric networks that exhibit isotropic volumetric changes. Herein lies the demand for the development of composite hydrogels that combine stimuli-responsive hydrogels with other materials to induce spatially nonuniform stress. This unique feature allows for the creation of composite hydrogels with fascinating shape morphing capabilities. In this section, we will explore two main mechanisms that contribute to the shape morphing behavior of composite hydrogels: heterogeneous lamella structures and spatially nonuniform distribution of additives.

4.1.1. Composite hydrogels with heterogeneous lamella structures. As the simplest approach to import "inhomogeneity", lamella composite hydrogels have been widely employed to generate out-of-plane deformation. The strain mismatch between these layers is easily obtained *via* differentiating their intrinsic properties, such as swelling ratio, thermal expansion, crosslinking density, elastic modulus, or defects.[43] Taking the uniaxial bending of bilayer composites as an example, Li *et al.* developed a bilayer composite hydrogels consisting of the PNIPAM layer with LCST of 36 °C and poly(*N*-acryloyl

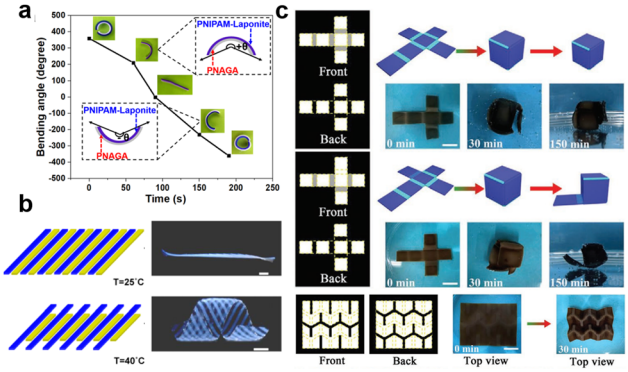

Fig. 6 The shape morphing behavior of composite hydrogels with heterogeneous lamella structures. (a) Thermoresponsive bending angle test of PNIPAM/PNAGA bilayer hydrogels as a function of time at 45 °C, where time 0 was defined when the bilayer hydrogel was rapidly transferred from 5 to 45 °C. Reproduced with permission.[124] Copyright 2020, American Chemical Society. (b) Shape transformations of the gel sheet composed of P(NIPAm-*co*-HEAM) (PG) and poly(NIPAM-*co*-HEAM)/PNIPAm (BG) stripes. The PG and BG stripes were 1 mm-wide and were oriented at 45° to the long axis of the rectangular gel sheet. Scale bars are 0.5 cm. Reproduced with permission.[251] Copyright 2013, American Chemical Society. (c) Shape transformations of GO/PDMAEMA hydrogel sheets with different initial shapes and patterned gradients in 65 °C water into different 3D structures. Scale bars are 1 cm. Reproduced with permission.[252] Copyright 2021, Wiley-VCH.

glycinamide) (PNAGA) layer with UCST of 18 °C (Fig. 6a). When the environmental temperature is lower than 18 °C, the PNAGA layer shrinks due to the phase separation, whereas the PNIPAM layer can be significantly swelled, thus the whole bilayer structure bend towards the PNAGA layer. Conversely, by heating the environmental temperature to 36 °C, the bilayer composites bend toward the PNIPAM layer.[124] Actually, this deformation of bilayer composite hydrogels is predictable. Timoshenko model provides an effective method to calculate the bending curvature of composite systems.[249] For a bilayer system, the relationship between the curvature R, strain mismatch ε_m, and geometry can be written as $R/h_N = (1 + 4\eta\xi + 6\eta^2\xi + 4\eta^3\xi + \eta^4\xi^2)/6\varepsilon_m\eta\xi(1 + \eta)$, where η is the contrast in thickness ($\eta = h_P/h_N$), ξ is the contrast in plane-strain modulus ($\xi = E_p/E_N$). According to the equation, the magnitude of bending is closely determined by the strain mismatch and relative dimensions of the constituent materials. Notably, in this model, all the constituent materials are assumed to be linearly elastic.

The geometric design of layers also plays an important role in the shape morphing behavior of composite hydrogels. Typically, the distribution of different layers includes vertical stacking, horizontal assembly, directional arrangement, or customized patterning.[27,130,250] Various shapes are generated by controlling the layer distribution. For instance, Therien-Aubin *et al.* utilized distinct designs of layer distribution to organize the PNIPAM copolymerized with 2-hydroxyethyl methacrylate (P(NIPAm-*co*-HEAM); PG) and poly(NIPAM-*co*-HEAM)/PNIPAm (BG) stripes, the resultant gel sheet exhibited various kinds of shape transformations (Fig. 6b). When PG and BG stripes were 1 mm-wide and were oriented at 45°, the sheet can transform to the helix structure.[251] Similarly, guided by origami technique, the composite hydrogel hinges enable to drive the self-folding. Yin *et al.* combined GO and poly(2(dimethylamino)ethyl methacrylate) (PDMAEMA) hydrogels with different crosslinking densities and patterns to generate a Miura folding structure (Fig. 6c). This structure can actively perform 2D–3D shape transition in H_2O at 65 °C.[252]

4.1.2. Composite hydrogels with spatially nonuniform distribution of additives. Similar to heterogeneous structural design, nonuniformly embedding functional additives is another means to fabricate composite hydrogels with shape morphing abilities. This method involves introducing functional additives in an anisotropic manner, leading to three distinct distributions: alignment, gradient, and pattern. Inspired by skeletal muscles, Gomez *et al.* reported uniaxially aligned microfibers of polycaprolactone-polyurethane (PCL-PU) copolymer on top of methacrylate hyaluronic acid (HA-MA) hydrogel layer. Such composite hydrogels can transform to scroll tube shape perpendicular to the direction of fibers.[253] Huang *et al.* utilized magnetic fields to align MNPs in a bilayer structure with poly(ethylene glycol) diacrylate (PEGDA) as the supporting layer and PNIPAM as the responsive layer, following by UV-assisted photolithography (Fig. 7a). The rigid MNPs restrict the swelling behavior of hydrogels, thus determining the final 3D shapes of the bilayer hydrogel sheets (Fig. 7b).[177]

Gradient distributions of additives often require the application of external fields. For example, Tan *et al.* used a direct current electric field (DC-EF) during the *in situ* polymerization of PNIPAM hydrogels to introduce a gradient of LAPONITE® through the thickness of the hydrogel strip (Fig. 7c).[254] LAPONITE®, known as nanoclay (NC), is a negatively charged nanosheet which migrates toward the anode. Since NC acted as physical crosslinkers, PNIPAM hydrogels with a gradient concentration of NC led to a gradient deswelling behavior across the thickness of hydrogel sheets. As a result, the composite hydrogel bent toward the NC-free surface at the equilibrium state when the temperature was above the LCST (Fig. 7d). Similarly, Chen *et al.* reported the gradient distribution of MNPs within PNIPAM hydrogels under a magnetic field.[255] The composite hydrogels demonstrate bending deformation under increasing temperature.

When the external field source is smaller than the size of the hydrogel, the gradient becomes localized, giving rise to patterns in the hydrogel matrices. These localized patterns often lead to deformations beyond simple bending, such as folding and wrinkling. Chen *et al.* demonstrated the fabrication of asymmetric P(AA-*co*-AM) hydrogels with complex shape deformations by patterning IONP with multiple magnets onto a mold.[176] By placing the magnets alternatively on each side of the mold, the composite hydrogels deformed in multiple directions in an acidic solution. Another innovative approach is the stamping method, which allows for the direct introduction of additives into hydrogels through diffusion. For example, Guo *et al.* utilized stamping to pattern iron ions onto PNIPAM hydrogels and subsequently sprayed NaOH to synthesize IONP *in situ* at the ion pattern positions (Fig. 7e).[183] These patterns can be easily erased by applying an HCl solution and can be rewritten for new designs. Such patterns of IONP can generate complex 3D deformation of the composite hydrogel upon NIR light exposure (Fig. 7f). For additives that are not responsive to external fields, appropriate chemical modification can address this limitation. Lin *et al.* synthesized tunicate cellulose nanocrystals (TCNC) and introduced a gradient of negatively charged TCNC in PNIPAM-based hydrogels through an electric field.[256] These composite hydrogels underwent reversible shape deformation upon temperature changes.

Traditional particle alignments using external fields typically rely on the responsiveness of particles to magnetic or electric fields. However, the approach utilizing the acoustic field for particle distribution offers an alternative method, where the distribution of particles is exclusively dependent on the acoustic impedance between the particles and the fluid.[257] This unique characteristic allows for the patterning of particles without requiring their responsiveness to magnetic or electric fields. Li *et al.* reported a novel technique ''acousto-photolithography'', which combines surface acoustic waves and photolithography to precisely control the distribution of photothermal particles in the pregel solution (Fig. 7g).[258] This approach enables the assembly of particles into arranged chain patterns with controllable spacing. This approach allows the assembly of particles into arranged chain patterns with adjustable spacing. After photocrosslinking to immobilize the particles within the PNIPAM hydrogel matrix, the resulting composite hydrogel sheet

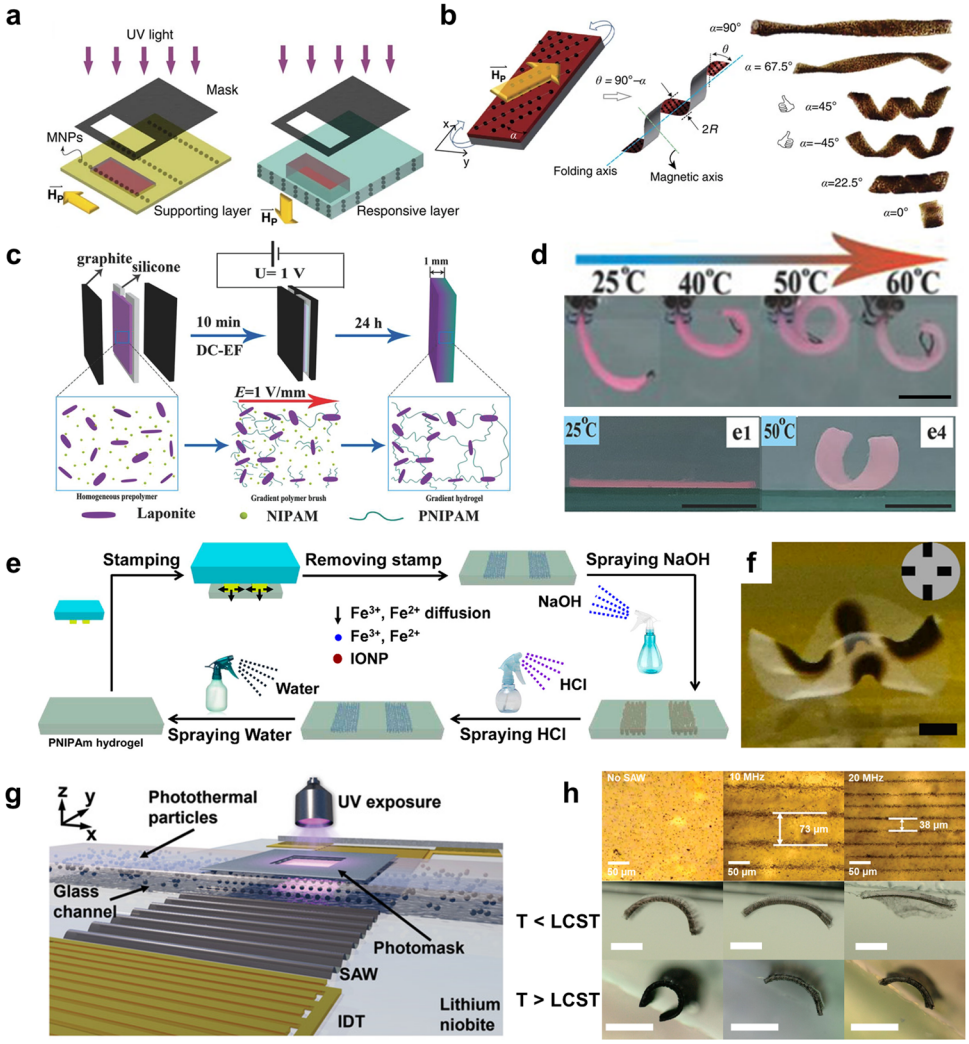

Fig. 7 Shape morphing of stimuli-responsive composite hydrogel with spatially nonuniform distribution of additives. (a) Schematic illustration for the preparation of programmable bilayer hydrogel sheet with alignments of MNPs under magnetic field. (b) The 3D shape deformation of bilayer hydrogel sheets with different orientations of MNPs alignment. Reproduced with permission.[177] Copyright 2016, Springer Nature. (c) Schematic illustration of the preparation of the gradient NC hydrogels in an electric field. (d) Shape morphing of composite hydrogels with gradient of NC below and above LCST. Scale bar is 1 cm. Reproduced with permission.[254] Copyright 2018, Wiley-VCH. (e) Schematic illustration of the patterning, erasing, and rewriting IONPs in a thermoresponsive PNIPAm hydrogel matrix. (f) The optical image of shape morphing of PNIPAM hydrogel with IONP patterns. Scale bar is 2 mm. Reproduced with permission.[183] Copyright 2019, American Chemical Society. (g) Illustration of the acousto-photolithography preparation for alignment of photothermal particles in PNIPAM hydrogels. (h) The pattern spacing is determined by the input frequency of surface acoustic waves, which results in different bending behavior for temperature below and above LCST. Scale bar is 500 μm. Reproduced with permission.[258] Copyright 2022, Wiley-VCH.

demonstrates programmable deformation based on the spacing between the patterns (Fig. 7h). This unique feature opens up new possibilities for precise and versatile manipulation of particles within the hydrogel matrix.

4.2. Fabrication techniques for shape transformation systems using composite hydrogels

Generally, stimuli-responsive composite hydrogels undergo a fabrication process consisting of two essential steps (1) generating the composite hydrogel and (2) crosslinking the composite hydrogel.[259] A common strategy employed to generate a composite hydrogel is generating a bilayer structure, where two materials are overlaid upon one another. There are several fabrication techniques which can be utilized to achieve a bilayer hydrogel system including coating.[155] casting,[260] 3D printing,[261] injection,[262] origami,[263] and kirigami.[264] To generate these composite hydrogel systems, a single fabrication technique or a combination of multiple fabrication techniques can be utilized. Once the composite hydrogel has been generated using one or more of the aforementioned fabrication techniques, the composite hydrogel can undergo crosslinking, thereby finishing the fabrication process.[259]

When the composite bilayer structure is employed on a material system composed of one or more stimuli-responsive materials, it results in a stimuli-responsive composite hydrogel capable of undergoing shape transformation. The bilayer structure is crucial in inducing shape transformation, the strain

mismatch of the two different materials causes a shape change upon exposure to an external stimulus (*i.e.*, temperature,[233] pH,[59] light,[265] *etc.*). Frequently utilized stimuli-responsive materials in these stimuli-responsive composite hydrogel systems include PNIPAM,[266] chitosan,[267] metallic nanoparticles, GO[7] and CNT.[155] For instance, double-network PNIPAM/PVA hydrogels when casted into sheets and adhered to polyimide tape formed a temperature-responsive actuator capable of undergoing a shape transformation.[266]

Each fabrication technique has its own set of unique advantages and disadvantages, which lend to their preferred usage in different applications. Additionally, different fabrication techniques are more favorable in particular applications based upon the desired shape transformation of the stimuli-responsive composite hydrogel. For example, injection is typically used for biomedical applications due to its ability to form vascular-like structures with relative ease,[262] however, this technique is not as frequently used in the fabrication of soft robotics. In this section, fabrication techniques used to generate the composite bilayer structure are discussed.

4.2.1. Coating and casting. There are two common fabrication techniques utilized for developing thin films for stimuli-responsive composite hydrogels: coating and casting. Coating gives the ability to deposit ultra-thin coatings by either spraying,[268] spinning,[269] or dipping[270] a hydrogel precursor solution onto an existing surface. Whereas casting allows for the fabrication of both thin and thicker hydrogel films alike, with the added benefit of casting hydrogels into customizable 2-dimensional structures.

Spray coating is a widely applicable processing technique used inside and outside of polymer chemistry because of its scalability and economic favorability.[155] While, broadly applicable in large-scale manufacturing, in developing stimuli-responsive composite hydrogels, the spray coating fabrication technique is not the most common. Typically, the spray coating fabrication technique involves pneumatically dispensing a hydrogel precursor solution from a syringe.[271] The hydrogel precursor solution exits the syringe nozzle in small droplets covering the surface. Upon spraying the hydrogel precursor solution on the surface, it can be crosslinked. Devices used for spray coating include custom-built spray coaters and commercial nebulizers repurposed as spray coaters.[272] The thickness of the coating that is sprayed is dependent on the pressurization of the syringe, the distance between the surface and the nozzle, spraying time, and viscosity of the precursor solution. In a recent study, a hygromorphic actuator was developed with a liquid crystal (LCN) spray coated onto films of hydrogel polyamide 6 (PA6) as demonstrated in Fig. 8a.[268] The LCN/PA6 hygromorphic actuator undergoes a curvature change as the humidity of the environment changes.

Spin coating is a commonly used fabrication technique in laboratories due to its efficiency in generating thin homogeneous films.[273] In spin coating, typically the hydrogel precursor solution is placed in the center of a target surface in excess and then rotated at a very high speed. Centrifugal acceleration on the hydrogel precursor solution in the center causes it to spread in a thin uniform layer on the target surface. Once the hydrogel precursor solution has been thinly spread onto the target surface, it can then be crosslinked. The thickness of the coating *via* spin coating can be controlled by the speed of spinning and the viscosity of the precursor solution. Recently, Nam *et al.* demonstrated spin-coating both layers of the bilayer composite hydrogel, copolymerized *N*(isopropylacrylamide) and acrylic acid denoted as P(AA-*co*-NIPAAm) and silicone elastomer Ecoflex, before adhering the two layers together using silicone adhesive as seen in Fig. 8b.[269] When placing a thin film of

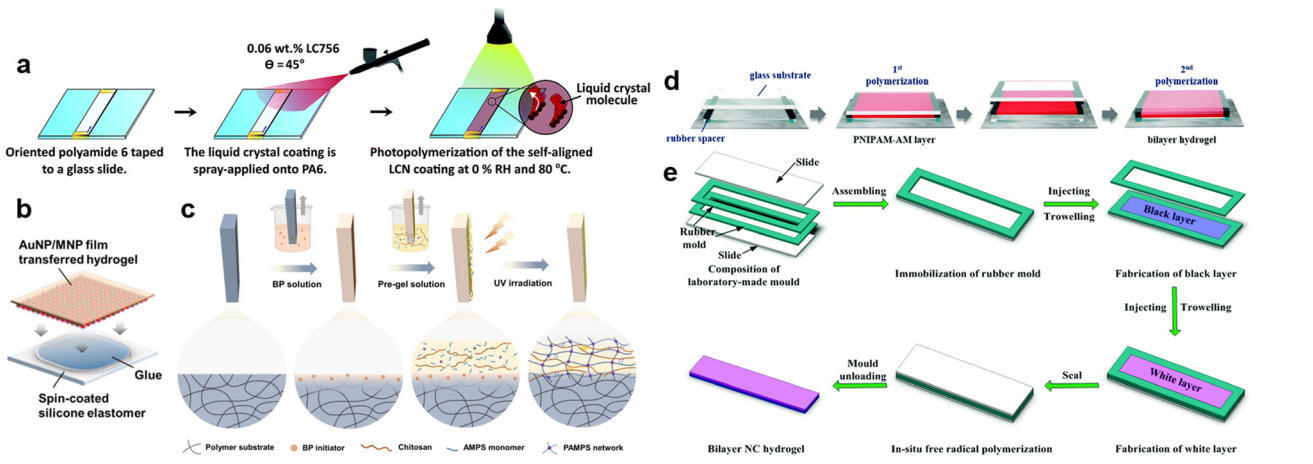

Fig. 8 Fabrication of composite bilayer hydrogel structures using different coating techniques: (a) spray coating of liquid crystal elastomer (LCN) onto the surface of polyamide 6 (PA6) using a spray gun. Reproduced with permission.[268] Copyrights 2018, Royal Society of Chemistry. (b) AuNP/MNP film transferred onto spin-coated temperature-responsive hydrogel attached to spin-coated silicon elastomer; reproduced with permission.[269] Copyrights 2021, American Chemical Society. (c) Dip coating fabrication technique used for double-network hydrogels. Reproduced with permission.[274] Copyrights 2022, American Chemical Society Publications. Casting fabrication process for composite bilayer hydrogel systems: (d) casting bilayer hydrogels with rubber spacers where the precursor solution is injected in between two glass slides; reproduced with permission.[277] Copyrights 2018, Royal Society of Chemistry. (e) Casting bilayer hydrogels inside customized laboratory made molds. Reproduced with permission.[279] Copyrights 2018, Royal Society of Chemistry.

AuNP on P(AAc-*co*-NIPAAm)/Ecoflex, the actuator has the capability bending when exposed both magnetic and light stimuli.[269]

In developing stimuli-responsive composite hydrogels, dip coating is not as common compared with spray coating and spin coating. Dip coating involves a substrate dipped into a hydrogel precursor solution followed by crosslinking as seen in Fig. 8c.[274] A study conducted by Stoychev *et al.* employed dip coating to produce the bilayer structure in the composite hydrogel.[270] The co-polymerized hydrogel consisting of PNIPAM, PAA, and benzophenone-acrylate, denotated as P(NIPAM-*co*-AA-*co*-BPA), was fabricated onto a silicon wafer using dip-coating. This was followed by dip-coating a co-polymerized poly(methyl methacryate) and benzophenone-acrylate, denoted as P(MMA-*co*-BPA) onto the surface of P(NIPAM-*co*-AA-*co*-BPA). Once prepared, it was patterned with UV light, and when exposed to temperature it demonstrated folding in half.

Casting, also referred to as molding, is one of the most ubiquitous fabrication techniques for developing stimuli-responsive composite hydrogels due to its simplicity and its application versatility. Casting is an alternative fabrication technique that can not only create thin and thick films, but also create more customizable shapes using a mold. To cast thin and thicker films, typically a precursor solution can be injected in between two glass slides separated by non-reactive spacers on either side as demonstrated in Fig. 8d (*i.e.*, Kapton film,[7] PTFE,[275] silicone spacers[263] and rubber[276]).[277] The capillary forces cause the injected solution to flood the space in between the glass slides forming uniform sheets of hydrogels which can be later on layered to create the bilayer composite structure. Zhang *et al.* demonstrated this fabrication technique with a stimuli-responsive composite hydrogel composed of PNIPAM and PVA.[278] First the PVA was injected in between two quartz glass slides separated by a thin silica rubber spacer and cured, then the PNIPAM was injected over that layer using a slightly thicker silica spacer.

To cast more complex 2-dimensional structures, a mold can be constructed as seen in Fig. 8e.[279] Once the mold is created, the hydrogel precursor solution can be injected or poured into the mold and subsequently crosslinked. A study conducted by Zhang *et al.* used custom molds including a flower and a hand to demonstrate more complex shape transformations of their stimuli-responsive composite hydrogel PNIPAM and spiropyran.[275]

By using both the coating and casting fabrication techniques, both simple and complex shape morphing mechanisms can be developed making this a highly versatile fabrication technique. In a study conducted by Li *et al.* both casting and spray coating fabrication techniques were used to develop a stimuli-responsive composite hydrogel used as a light switch.[155] First, CNT were synthesized into thin films using ethanol and Ecoflex. Ecoflex was then spray coated on the CNT thin films creating the CNT–Ecoflex layer. PNIPAM was then casted on the surface of the CNT/Ecoflex layer using benzophenone to improve adhesion between the two layers to finish fabricating the stimuli-responsive composite hydrogel CNT–Ecoflex/PNIPAM. Due to CNTs photothermal properties, NIR irradiation[123] was used to generate heat in the CNT causing an overall temperature increase, thereby actuating the stimuli-responsive composite hydrogel system to turn on and off a light switch.

4.2.2. 3D printing. 3D printing, also known as additive manufacturing, is a fabrication technique that can rapidly construct customized 3D architectures (*e.g.*, birds,[263] flowers,[280] *etc.*) through the layer-by-layer accumulation of printing materials (or inks).[281] The difference between 3D printing and traditional fabrication methods is that the essence of 3D printing is rapid and accurate molding, which can better and faster meet the customized requirements of enterprises and individuals for products, and minimize the processing cycle and processing loss of complex molds. In 1986, 3D printing technology was first proposed by Chuck Hull, who employed layer-by-layer lithographic manufacturing of solid objects.[282] With the continuous development of printing equipment and materials science, a variety of printing technologies have gradually emerged.[283] These 3D printing techniques have different resolutions and printing speeds, and can quickly obtain three-dimensional block parts from raw materials with different dimensions, like liquid resins, particles, or filaments. Even different kinds of materials ranging from hydrogels to metals to ceramics can be printed out.[284–288] Notably, when employing the 3D printing fabrication technique on stimuli-responsive inks, the shapes, structures, or properties of printed products enable to evolve with time upon exposure to an external stimulus, which introduces the additional fourth dimension, also called 4D printing.[289] Thus, to fabricate shape morphable composite hydrogels, two typical methods are utilizing 3D printing to controllably distribute the additives inside composite hydrogels and multi-material 3D printing of different hydrogel inks. By integrating the computer aided design (CAD), 3D printers, and stimuli-responsive hydrogel inks, composite hydrogels can be printed and undergo a preprogrammed shape transformation over time yielding a highly complex 3D structure.[290] Actually, there are numerous processes that have been utilized in 3D printing of shape morphing composite hydrogels, such as Direct Ink Writing (DIW),[280,291] Fused Deposit Molding (FDM),[292] Digital Light Processing (DLP),[293] and Stereolithography (SLA).[294,295]

DIW is commonly used in the fabrication of stimuli-responsive composite hydrogels due to its ability to print a wide variety of materials using different nozzles.[296] Its printing versatility can be attributed the prerequisites for the precursor solution. While other techniques require specific classes of materials, DIW can be used for any precursor solution that has a low enough viscosity for printing and a high enough storage modulus to retain shape upon extrusion.[296] Owing to its ability to print a wide variety of materials, DIW is frequently used in fabricating stimuli-responsive composite hydrogels. However, while a wide variety of materials can be printed using DIW, the resolution of printing is not as high as other techniques such as Digital Light Processing and Stereolithography. DIW operates based on pneumatic or mechanical extrusion where it deposits the hydrogel precursor ink directly onto the printing substrate as seen in Fig. 9a.[297] A study conducted by Li and co-works demonstrates DIW 3Dprinting of poly *N*(isopropylacrylamide)-*co*-dimethyl aminopropyl methacrylamide-clay (PNIPAM-*co*-DMAPMA/clay) stimuli-responsive

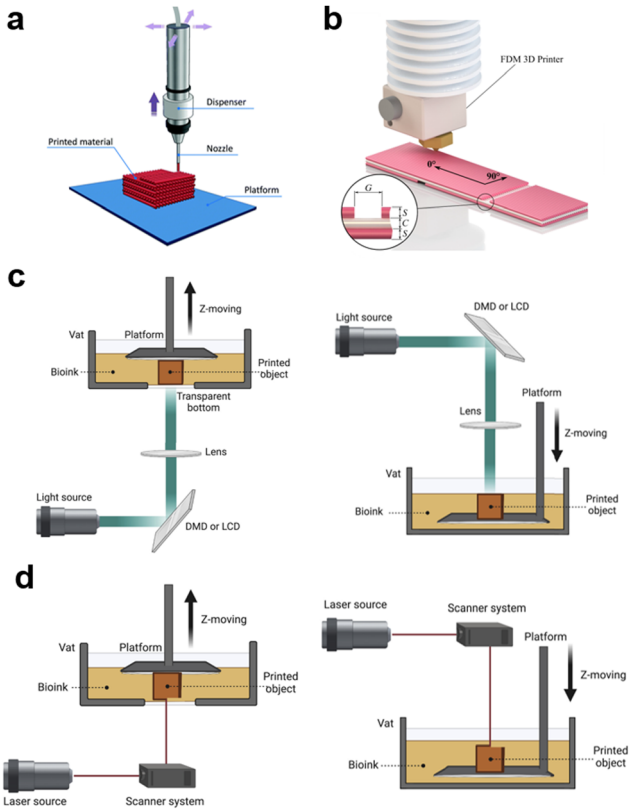

Fig. 9 3D printing fabrication strategies. (a) Schematic of Direct Ink Writing (DIW) printing where the hydrogel exits from a syringe and its nozzle using pressure or mechanical extrusion. Reproduced with permission.[297] Copyrights 2016, Royal Society of Chemistry. (b) Schematic of Fused Filament Fabrication (FFF) where thermoset plastics are heated through a nozzle and extruded. Reproduced with permission.[292] Copyrights 2019, Elsevier. (c) Bottom-down approach and top-down approach Digital Light Processing (DLP) printing. Bottom-down DLP has the light source projected by a digital mirror device (DMD) or a liquid crystal display (LCN) from the bottom into the vat of precursor solution, whereas top-down DLP has the light source projected from the top of the vat. (d) Schematics of both the bottom-down and top-down approach of stereolithography (SLA) printing. Bottom-down SLA where a laser directed toward the bottom of the vat and top-down SLA where a laser is directed at the top of the vat. Reproduced with permission.[299] Copyrights 2023, Elsevier.

composite hydrogel ink.[280] PNIPAM-*co*-DMAPMA/clay was copolymerized using varying monomer concentrations to create the bilayer system for the stimuli-responsive composite hydrogel system.[280] The bottom layer was copolymerized using high NIPAM and low DMAPMA concentration, whereas the top layer was copolymerized using low NIPAM and high DMAPMA concentration. These two inks of varied monomer concentrations were used to print a bilayer structure in the shape of a 2D flower. Upon exposure to 80 °C water, the 2D flower structure underwent a rapid pre-programmed shape deformation response changing into a 3D flower within 65 seconds.

While FDM, also known as fused filament fabrication (FFF), is popular fabrication technique for 3D printing used by both researchers and hobbyists alike, its usage in the fabrication of shape morphing composite hydrogels is much less common due to its pre-requisites in the material.[261] FDM requires thermoplastic polymers as the filament, which narrows the number of materials that can be printed, hence their lower usage amongst researchers studying shape morphing composite hydrogel systems. In FDM 3D printing, a long and continuous thermoplastic filament is heated by an extruder and deposited onto a platform where the filament cools down into the designed structure.[298] As seen in Fig. 9b, Baker *et al.* were able to demonstrate FDM printing to achieve a trilayer hydrogel structure composed of polyurethane and Tecophilic TPU capable of undergoing shape transformation from humidity actuation.[292]

An alternative to DIW and FDM 3D printing is using a vat polymerization printing technique. There are two methods of vat polymerization printing used to produce shape morphing composite hydrogels including DLP and SLA. DLP is a fabrication technique which yields high fidelity printing and requires photocurable precursor solution. In essence, DLP photopolymerizes entire layers within a vat of a hydrogel precursor solution using ultraviolet light projected with either a digital mirror device (DMD) or liquid crystal display as demonstrated in Fig. 9c.[299] There are two different approaches to DLP, a top-down approach and a bottom-up approach which are in accordance with the direction the 3D object is built. In a top-down approach, the ultraviolet light source comes from the top and shines down and cures the hydrogel precursor solution on the liquid-air interface.[299,300] The platform where the 3D object is printed on moves downward to reveal more of the hydrogel precursor solution ready to be photopolymerized. Whereas in a bottom-up approach, the ultraviolet light source originates from the bottom and shines upward into a bath of hydrogel precursor solution and cures it at the bottom of this bath. The platform where the 3D object is printed on moves upwards. DLP has been harnessed in fabricating shape transforming composite hydrogels. In a study by Ge *et al.*, bottom-up DLP 3D printing is utilized to fabricate a soft pneumatic actuator with acrylamide monomer and polyethylene glycol diacrylate (PEG) and elastomer base.[293]

Similar to DLP, SLA harnesses vat polymerization to print. Functionally, it operates very similarly to DLP, however in SLA, the UV light is sourced from raster laser scattering instead of using a DMD as seen in Fig. 9d.[299] Since DLP mirrors light, it is able to photopolymerize entire layers. However, SLA is able to direct UV light to draw and therefore photopolymerize in specific patterns. There are two different configurations to SLA, similar to DLP, a bottom-up and top-down approach as drawn in Fig. 9d. In the top-down approach, the ultraviolet light is drawn on the surface of liquid–air interface and cures the top layer, and the platform with the structure moves downward revealing more precursor to photopolymerize.[301] Conversely, in the bottom-up approach, the ultraviolet light is directed upward to the bottom of the vat and draws the pattern causing the precursor to photopolymerize and then the platform with the structure moves upwards revealing addition precursor to photopolymerize. Ji *et al.* demonstrated a temperature and humidity responsive hydrogel composed of PEG, HEMA, 3-sulfopropyl methacrylate potassium salt (SPMA), aliphatic urethane diacrylate (AUD), and 2-(2-methoxyethoxy) ethyl methacrylate (MEO_2MA) printed using bottom-up SLA.[294]

4.2.3. Injection. Injection is a widely used in the fabrication of hydrogel and polymer microfibers and microtubes, long tubes both solid and hollow, respectively, that have micron-ordered and nano-ordered diameters.[302] These microfibers and microtubes have potential applications in biomedical devices and biomimetic structures. By utilizing an injection fabrication technique for microfibers and microtubes, it can create vascular-like structures.[262] While the utility in the injection fabrication technique lies primarily with biomedical engineering, there have been several studies that have utilized injection-based fabrication for shape transforming hydrogels. Electrospinning,[303] wet-spinning,[304] microcapillary injection[262] are among those injection-based methods utilized in fabricating shape transforming composite hydrogels.

Microcapillary injection can be utilized to fabricate microfibers and microtubes. This can be achieved by attaching two different outer diameter sized glass capillary tubes to one another as demonstrated in Fig. 10a.[262] A hydrogel precursor solution is injected through the first smaller outer diameter glass capillary tube where it enters the second smaller outer diameter tube where the precursor is crosslinked through a variety of methods (*i.e.*, ionic crosslinking *via* aqueous solution and UV crosslinking). A study conducted by Lim *et al.* utilized injection to synthesize microfibers and microtubes of the stimuli-responsive hydrogel PNIPAM with IONP.[262] This was achieved by injecting a monomer precursor solution containing PNIPAM/IONP and calcium alginate into the channel of a microfluidic device. The monomer precursor solution was crosslinked using calcium ions and UV curing. Once polymerized, the calcium alginate was removed using ethylenediaminetetraacetic acid (EDTA), leaving behind microfibers and microtubes of PNIPAM/IONP. These PNIPAM/IONP microfibers and microtubes were stimulated with 380 mW cm^{-2} of light to induce a volume phase transition and shape change.

Unlike microcapillary injection, both electrospinning and wet-spinning are not typically used independently to fabricate shape morphing composite hydrogels. Due to the resulting nano-scale fibers formed by both electrospinning,[302] they are used in tandem with other fabrication techniques such as 4D printing and casting to develop shape-morphing composite hydrogels.[253] Often times, these fibers produced from electrospinning and wet-spinning are used as fillers or for patterning alignment.[305] While fabrication techniques of both electrospinning and wet-spinning are primarily employed in shape morphing hydrogels as additive fillers, there are several studies that utilize only electrospinning or wet-spinning to fabricate a shape-morphing composite hydrogel.

In an electrospinning set-up, a syringe pump with a polymer precursor is electrified using a high-power supply allowing for the polymer precursor to be stretched into long fibers to be deposited onto a ground collector, followed by crosslinking as seen in Fig. 10b.[302] Liu *et al.* demonstrated electrospinning of P(NIPAM-ABP) into fibers agglomerated together into large mats in a 0-, 45-, 90-degree, or randomized configuration.[303] When aligned P(NIPAM-ABP) and randomized P(NIPAM-ABP) were layered on one-another it caused shape change when actuated using temperature.[303]

Wet-spinning is a fabrication technique that has long been used in material processing. In a wet-spinning set-up, a polymer precursor is extruded by a syringe apparatus directly into a coagulation bath where the fibers take their shape.[304] Once the fibers have taken their form, typically these fibers are rolled for storage. Additionally, these fibers can undergo additional processing (*i.e.*, washing and drying). Zheng *et al.* demonstrated wet-spinning of both SA and SA/GO into fibers as demonstrated in Fig. 10c.[306] The fibers of SA and SA/GO were twisted together show shape-morphing when actuated with light and humidity.

4.2.4. Origami and kirigami. Unlike the previously discussed fabrication techniques, both origami and kirigami utilize the aforementioned fabrication techniques to achieve an origami- or kirigami-inspired structures. Both origami and

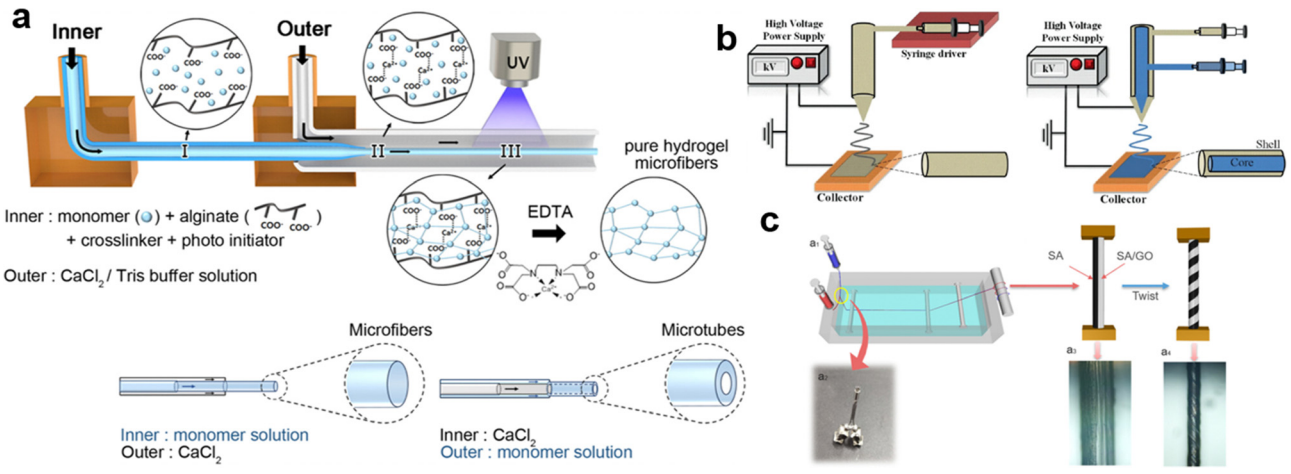

Fig. 10 Injection fabrication strategies. (a) Injecting hydrogel precursor solution through glass capillary tubes followed by crosslinking to achieve microfibers or microtubes. Reproduced with permission.[262] Copyrights 2018, American Chemical Society. (b) Electrospinning where hydrogel precursor solution is extruded from a syringe pump onto the surface which is electrically charged. Reproduced with permission.[302] Copyrights 2022, Springer. (c) Wet-spinning where hydrogel precursor solution is extruded from a syringe pump directly into a coagulation bath. Reproduced with permission.[306] Copyrights 2021, American Chemical Society.

kirigami fabrication approaches receive their namesake from the Japanese art forms origami and kirigami that can transform a single sheet of paper into 3D structures using simple folding and a combination of folding and cutting, respectively.[307] In stimuli-responsive composite hydrogels, both the origami and kirigami fabrication techniques can be used to trigger localized bending or folding from strategically placed hinges to self-assemble a 2D hydrogel sheet into a complex 3D structure.[308] The hinges for origami/kirigami rely on anisotropic swelling which can be patterned using 3D printing and photolithography.[307]

3D printing is frequently utilized to fabricate origami and kirigami inspired structures due to its versatility, simplicity, and ability to accommodate a wide range of materials. In 3D printing, the hinges are printed onto an existing 2D structure, where they can later on be actuated using a stimulus as seen in Fig. 11a.[233] Zhao *et al.* demonstrated folding of polydimethylsiloxane (PDMS) by 4D printing a hinge consisting of temperature responsive hydrogel NC-PNIPAM. Upon exposure to room temperature water, the composite hydrogel demonstrates folding into an origami-inspired box.

Photolithography is especially useful in fabricating origami and kirigami inspired structures on the micro- and nano-scale due to its precision.[307] Typically, photomasks are placed on the surface of the hydrogel, then exposed to ultraviolet light.[309] The UV irradiation can be utilized in patterning composite hydrogels to induce origami-inspired folding as seen in Fig. 11b.[249] Direct exposure to UV light can cause a higher crosslinking density and differing swelling ratios allowing for anisotropic swelling and folding.[310] Patterning using photolithography is widely used for inorganic systems, however, many studies employ photolithography for designing origami and kirigami inspired composite hydrogels. Na *et al.* successfully fabricated complex origami structures from poly(*p*-methylstyrene) (PpMS) and PNIPAM.[249] The trilayered PpMS/PNIPAM/PpMS was patterned using UV light. When exposed to room temperature water, these preprogrammed PpMS/PNIPAM/PpMS trilayer were able to fold into a Randlett's bird, conversely, when exposed to hot water the PpMS/PNIPAM/PpMS trilayer unfolded into a nearly flat sheet.

Kirigami is a variation of origami and utilizes a combination of folding and cutting to create highly intricate 3D structures (*i.e.*, building models, snowflakes, *etc.*). The kirigami technique for stimuli-responsive composite hydrogel fabrication utilizes cuts in addition to the existing folding origami technique to create highly complex 3D structures.[308] To achieve cut-outs in kirigami-inspired structures, both laser cutting and photolithography have been employed. Laser cutting is employed to attain the cut-outs in kirigami-inspired structures by cutting the composite hydrogel similarly. Laser cutting, widely used in materials manufacturing, allows for clean and precise slices into the target material with no contact.[311] When employed for slicing hydrogels, it allows for the fabrication of kirigami-inspired structures as seen in Fig. 11c.[264] Liu *et al.* demonstrated laser cutting in wearable sensors.[264]

While kirigami traditionally involves cutting paper to attain the cut-outs, non-cutting techniques have been employed in fabricating the cut-outs in kirigami-inspired structures such as multi-stage photolithographic polymerization.[312] Multi-stage photolithographic polymerization can be employed in fabricating kirigami inspired structures by curing the precursor solution in specific areas with a photomask generating the cut-outs. Hao *et al.* demonstrated multi-stage photolithographic polymerization by polymerizing poly(acrylamide-*co*-2-acrylamido-2-methylpropanesulfonic acid) [P(AM-*co*-AMPS)], PAM, and poly(methacrylamide-*co*-methacrylic acid) [P(MAM-*co*-MAA)] as seen in Fig. 11d.[313]

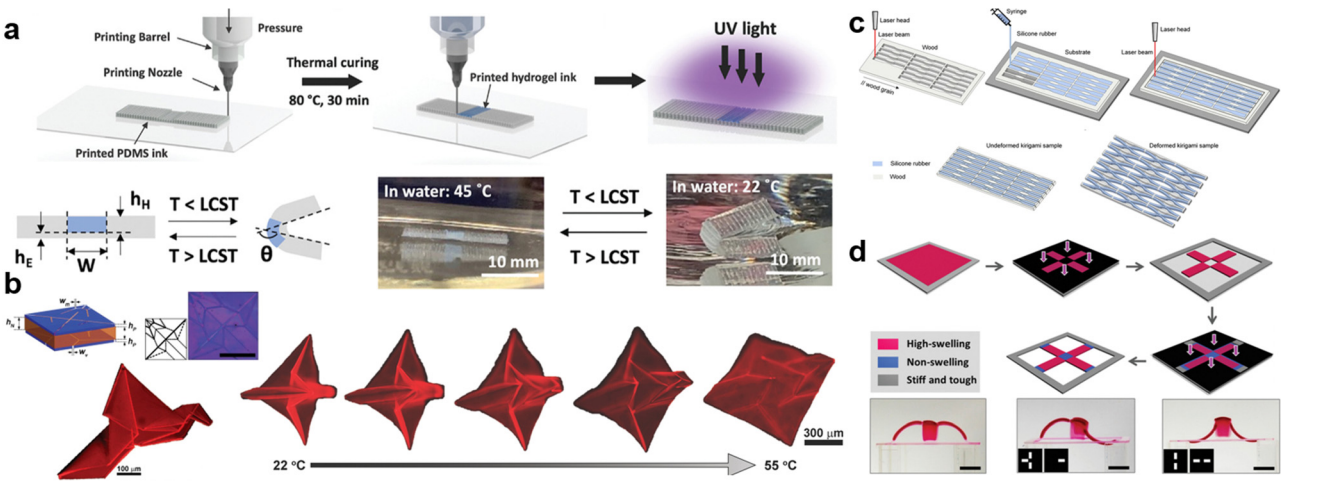

Fig. 11 Strategies for fabricating hinges and cutouts in origami and kirigami, respectively. (a) Schematic depicting Direct Ink Writing (DIW) 4D printing fabrication technique utilized for printing hinges that allow for origami-inspired folding. Reproduced with permission.[233] Copyrights 2022, Wiley-VCH. (b) Photolithography used to pattern hydrogel sheet with UV light which creates the hinges on the hydrogel sheet which exhibits reversible folding and unfolding of a Randlett's bird when exposed to different temperatures. Reproduced with permission.[249] Copyrights 2015, Wiley-VCH. (c) Cured hydrogel sliced into a kirigami-inspired structure using a laser cutter. Reproduced with permission.[264] Copyrights 2019, Springer Nature. (d) Photolithography mask used during the hydrogel curing process to create kirigami-inspired cut outs. Reproduced with permission.[313] Copyrights 2020, Wiley-VCH.

5. Shape morphing behaviors of composite hydrogels controlled by external stimuli

Living biological systems continuously and autonomously respond and transform to adapt to their surrounding environments. To mimic these adaptive behaviors in shape morphing composite hydrogels, it is critical to design hydrogels that can response to a wide range of stimuli. Here, we survey the major classes of external stimuli to control the shape morphing of composite hydrogels. The non-invasive stimuli including temperature, light and magnetic field. Additionally, researchers have developed composite hydrogels in response to invasive stimuli such as electricity, pH changes and solvent variations. Other stimuli such as mechanical force and chemicals are briefly discussed lastly.

5.1. Temperature

Temperature serves as a well-known stimulus for inducing deformation in hydrogels.[314] Typically, hydrogel polymers are relatively soluble and hydrophilic, but they undergo a transition to become insoluble and hydrophobic at a certain temperature.[315] This reversible transformation is known as the coil-globule transition. Some polymers exhibit this phase transition at the LCST, remaining soluble below the LCST but turning hydrophobic above it.[316] Conversely, the other group undergoes the coil-globule transition at the UCST, where the polymers become insoluble and aggregate below the UCST.[317] The occurrence of this transition is generally influenced by the formation or deformation of bonding within the polymers and interactions between the polymers and surrounding water. However, the specific intra and intermolecular interactions, LCST, and UCST values depend on the nature of the polymers.[318]

PNIPAm-based hydrogel stands out as the most extensively studied LCST-type thermoresponsive hydrogel, particularly in the context of shape morphing applications.[319,320] Above its LCST of 32–33 °C, the PNIPAm hydrogel undergoes deswelling, resulting in the release of water and causing the hydrogel to collapse and shrink (Fig. 12a).[321] Conversely, upon lowering the temperature below the LCST, the hydrogel reswells, absorbing water and increasing in volume. This swelling and deswelling processes mainly stem from the hydrogen bonds of PNIPAm interacting with water molecules, with an exothermic formation enthalpy below the LCST and deformation of the hydrogen bonds beyond it.[322] However, The LCST of NIPAM can be adjusted through copolymerization with hydrophilic or hydrophobic materials. Copolymerization with hydrophobic monomers lowers the LCST temperature, while incorporation of hydrophilic monomers elevates it.[323] For instance, Kim *et al.* reported an increase in LCST when PNIPAM was copolymerized with 2,2′-hydroxyethyl methacrylate, with the LCST reaching up to 68.2 °C depending on the molar ratio between the copolymers.[324] This LCST can raise up to 68.2 °C depending on the molar ratio between copolymers. Interestingly, PNIPAM can also exhibit UCST behavior in ionic liquids, and this behavior can be tuned through copolymerization. So *et al.* demonstrated the UCST variation of PNIPAM by incorporating comonomers such as acrylic acid (AA), methyl acrylate (MA), and photocrosslinkable comonomer acrylamidobenzophenone (BP).[325] The UCST increased with copolymerization of AA and decreased with MA (Fig. 12b). Capitalizing on this behavior, a PNIPAM-based hydrogel sheet was developed with the ability of sequential folding (Fig. 12c). As the temperature reached 60 °C, 90 °C, and 170 °C, the arms of the hydrogel sheet folded sequentially (Fig. 12d).

Furthermore, for stimuli-responsive hydrogels, the crosslinking density significantly influences their swelling/deswelling behaviors. A higher crosslinking density restricts the deformation of the polymeric networks, thereby limiting water adsorption/extraction and volumetric expansion/contraction, respectively.[326] Leveraging this phenomenon, Yoon *et al.* devised a method to create hydrogel strips with distinct panels and hinges featuring varying degrees of crosslinking density. This was achieved by

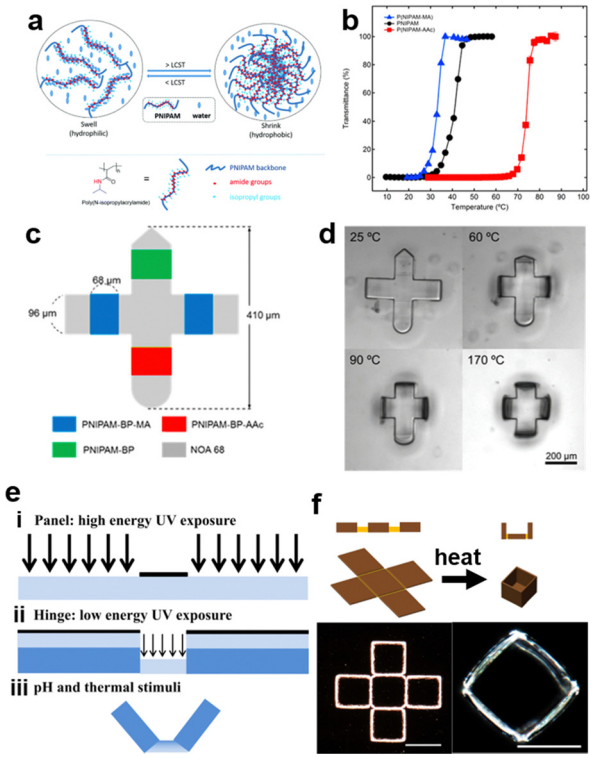

Fig. 12 (a) Schematic illustration of thermos-responsive LCST behavior of PNIPAM. Reproduced with permission.[321] Copyrights 2020, Royal Society of Chemistry. (b) Temperature dependence of transmittance at 515 nm for PNIPAM copolymer solutions in ionic liquid at a heating rate of 1 °C min^{-1} (c) Schematic illustration of the design for a sequential self-folding PNIPAM-based hydrogel sheet in the plan view (d) Optical images of a self-folding micropatterned PNIPAM-based hydrogel sheet in ionic liquid at different temperatures throughout heating. Reproduced with permission.[325] Copyright 2017, American Chemical Society. (e) Schematic of P(NIPAM-AAc) hydrogel strip with (i) thick, fully crosslinked panel and (ii) thin, gradient crosslinked hinge. (iii) Schematic deformation of hydrogel strip under Ph and thermal stimuli (f) Schematic and optical images of temperature responsive self-folding. Reproduced with permission.[327] Copyright 2014, IOP Publishing.

adjusting the total UV energy during photopolymerization (Fig. 12e).[327] The resulting P(NIPAM-*co*-AA) hydrogels exhibit responsiveness to pH and other stimuli. Upon temperature changes, the hydrogel sheets undergo complex shape deformation due to the mismatch in deswelling between the hinges and panels (Fig. 12f). This unique behavior adds further versatility to the design and applications of stimuli-responsive hydrogel systems.

5.2. Light

Direct illumination of light onto photoresponsive composite hydrogels provides a remote and non-invasive method to stimulate shape deformation.[328] This approach takes advantage of the wide range of wavelengths in the electromagnetic spectrum, enabling the use of various light sources, from sunlight to excimer lasers.[149,329] To achieve shape morphing upon light exposure, the composite hydrogels are developed to respond to light through chemical reactions including molecular switching, bond dissociation or formation, otherwise through physical reactions such as the photothermal effect.

Hydrogel networks can be rendered photo-responsive through the incorporation of photoactive moieties like azobenzene[330] or spiropyran,[331] which undergo reversible photochemical reactions upon light absorption. For instance, azobenzene is a well-studied example that exhibits a transition from *cis* to *trans* configurations. Si *et al.* introduced tetra caboxylic azobenzene into polyacrylic acid-based hydrogel sheets, into PAA-based hydrogel sheets, resulting in thin sheets that exhibited reversible bending under UV light and a 532 nm green laser.[332] The bending behavior was attributed to the length difference between *cis* and *trans* isomerization of the azobenzene (5.5 and 9.0 Å, respectively), which causes the expansion of the hydrogel network. Similarly, spiropyrans demonstrate ring opening and closing processes upon exposure to light.[16] Li *et al.* reported the bending behavior of PNIPAM-based hydrogels with a spiropyran-based complex under visible light (Fig. 13a).[333] The photoisomerization of the spiropyran-based complex led to an increase in the net charge density, which in turn promoted water diffusion into the hydrogel and caused its expansion. Such bending direction can be alternated by modifying the functional groups on the complex. Thereby, combining photoexpanding and photocontracting

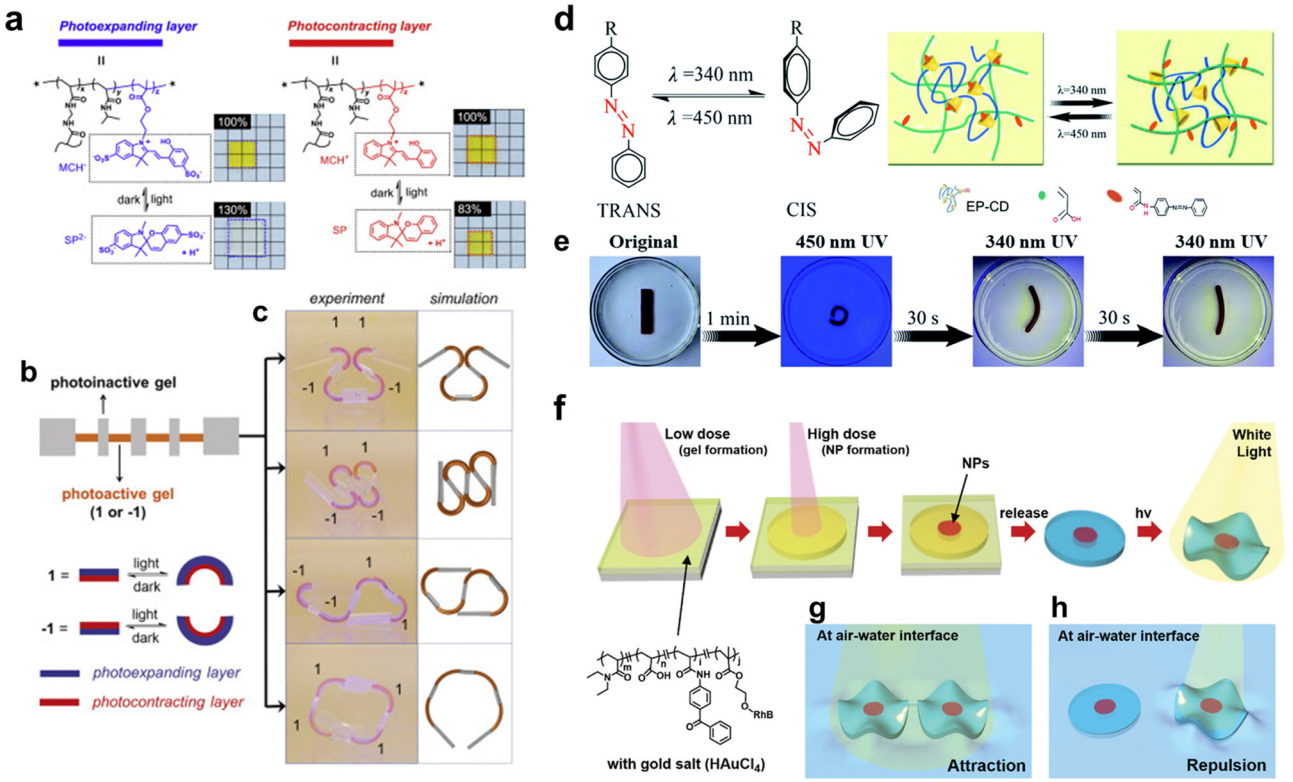

Fig. 13 The light-responsive shape morphing behavior of composite hydrogels. (a) Light driven hydrogel actuator with origami-like shape change. Molecular structure of the photoexpanding and photocontracting hydrogels and photographs depicting the light-triggered expansion and contraction of the gels. (b) Schematic representation of bilayer objects exhibiting different bending behaviors upon irradiation which are defined as 1 and −1. (c) Photographs of shapes from four different designing geometries and their corresponding snapshots from finite element simulations. Reproduced with permission.[333] Copyright 2021, Elsvier. (d) UV-driven shape morphing hydrogels. Light-driven *cis*–*trans* isomerization of 4-AcrylamideAzobenzene. Schematics of light-driven swelling behavior change that trans-structure formed under 450 nm light enhances host–guest effect and crosslinking density. (e) Light-responsive shape morphing of composite hydrogels. Reproduced with permission.[340] Copyright 2022, Royal Society of Chemistry. (f) Schematic illustration of a hydrogel nanocomposite actuator prepared by two-step photopatterning, to first crosslink the polymer film, and then produce the NPs. Chemical structure of the photo-crosslinkable copolymer, RhB = rhodamine B. (g), (h) illustration of light-induced wrinkling causing attraction or repulsion at the air/water interface. Reproduced with permission.[344] Copyright 2018, Wiley-VCH.

hydrogels with opposite bending directions resulted in complex out-of-plane deformation (Fig. 13b and c).

Another approach to impart photo-responsiveness to hydrogels is through photo-driven bond formation/dissociation of supramolecular assemblies including triphenylmethane leuco (TPML), cyclodextrin (CD) and their derivatives.[334–337] Chen *et al.* developed photo-responsive PAM hydrogels by incorporating TPML derivatives and 2-nitrobenzaldehyde, enabling out-of-plane shape deformation upon light exposure.[338] Under light exposure, the TPML derivatives and 2-nitrobenzaldehyde dissociated, generating immobile ions and establishing a local unbalanced osmotic field.[339] This resulted in solvent uptake and localized volumetric expansion, leading to swelling of the hydrogel. Li *et al.* introduced 4-acrylamideazobenzene and polycyclodextrin to PAA hydrogels, enabling complex 3D shape morphing through a host–guest reaction triggered by light.[240] Upon exposure of visible light (λ = 450 nm), the host–guest complexes formed between 4-acrylamideazobenzene and polycyclodextrin molecules (Fig. 13d), thus increasing the effective crosslinking density of hydrogel networks and leading to size shrinkage (*i.e.*, deswelling). The host–guest complexes could be reversibly dissociated upon irradiation with 365 nm UV light, causing water uptake and subsequent volumetric expansion (*i.e.*, reswelling). This volumetric expansion or shrinkage allows the composite hydrogels to bend out-of-plane in response to light with different wavelengths (Fig. 13e).

Aside from photochemical reactions, the photothermal effect is another prominent method employed in photo-responsive composite hydrogels. Upon light exposure, photothermal materials convert light to heat, this eventually leads to volumetric changes of the composite hydrogels, which results in shape transformation. Over the years, a wide range of photothermal materials has been developed and integrated into thermos-responsive hydrogel matrices, including carbon-based materials, metal nanoparticles, inorganic compounds and more. For example, several researchers have reported thermo- and photo-responsive composite hydrogels by loading GO into the PNIPAM matrix.[156,159,165,276,341] The out-of-plane deformation can be achieved by local light irradiation[7,163] assemblies of GO-PNIPAM active layer with a non-thermo-responsive passive layer[342,343] or by introducing a gradient distribution of GO within the matrix.[160,161] Other photothermal additives such as AuNP and WS_2 inorganic compounds can cooperate with PNIPAM hydrogel matrices using similar methods. For example, Kim *et al.* demonstrated light-induced wrinkling of AuNP/PNIPAM hydrogel disks at the air–water interface, which resulted from localized patterning of AuNP in the center of PNIPAM hydrogel disks (Fig. 13f).[344] The wrinkling deformation was generated due to the different swelling ratios between the AuNP-loaded inner disk and AuNPs-free outer disk. Such hydrogel disks can demonstrate attraction or repulsion at the air–water interface under light depending on their shape and position of light (Fig. 13g and h).

5.3. Electricity

Electric-responsive hydrogels can undergo conformational changes such as expanding (*e.g.*, swelling) and shrinking (*e.g.*, deswelling) in response to the external electric field. The mechanism of electrical field-induced shape morphing is due to the movement of free ions within the hydrogel matrix under an electric field.[345] As the movement of free ions creates the change of local distribution of ion concentrations, the osmotic pressure is created within hydrogels, thus leading to the swelling or deswelling of the hydrogels. Current electric-responsive hydrogels can obtain actuation within electric fields with a frequency of 1 Hz.[333] Such fast response provides promising aspects on applications of drug delivery, artificial muscles and soft robotics. For example, Choi *et al.* reported 3D shape morphing of electric-responsive hydrogels composed of sodium 4-vinylbenzene sulfonate, 2-hydroxyethyl methacrylate and acrylamide (VBS/HEMA/AAm) in NaCl solution (Fig. 14a(i)).[346] The electric-responsive hydrogel swelled asymmetrically due to the dispersion of ions under different directions of electric fields (Fig. 14a(ii)). Ko *et al.* developed an electric-responsive hydrogel actuator by *in situ* assembly of AuNP on a bare PAA-*co*-AM hydrogel surface.[347] As shown in Fig. 14b(i), when the electric potential is generated between the surfaces of the hydrogel actuator, the osmotic pressure is driven toward the negative potential, thus resulting in swelling of hydrogels on the negative electrode and deswelling of hydrogels on the positive electrode. Such shape morphing behavior is dependent on the thickness of the hydrogel (Fig. 14a(ii)).

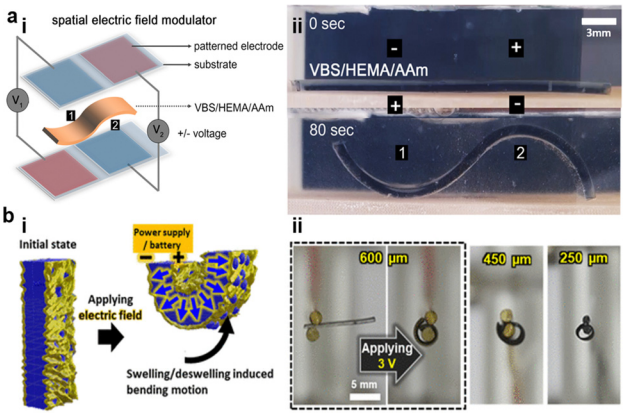

Fig. 14 The electric-responsive shape morphing behavior of composite hydrogels. (a) Electroactive hydrogel actuator. (i) Schematic diagram of the positive and negative curvatures bending for hydrogel as a function of the separated electric field with a vertical electrode configuration. (ii) Sequential images of hydrogel having bidirectional bending. Reproduced with permission.[346] Copyrights 2020, Springer Nature. (b) Electrified hydrogel actuators based on wrinkled nanomembrane electrodes. (i) Schematic illustration of the WNE actuator showing its working mechanism and operation with a power supply or on-board battery. (ii) Photographic images of hydrogel actuators with different thicknesses operating at 3 V. Reproduced with permission.[347] Copyrights 2022, American Association for the Advancement of Science.

5.4. Magnetic fields

Magnetic fields are among a class of external stimuli that can be applied to a stimuli-responsive composite hydrogel to induce shape transformation actuation. Stimuli-responsive composite hydrogels that can respond to a magnetic field stimulus are

considered to be magnetic-responsive. By utilizing magnetic fields as the external stimulus, it gives the ability to actuate specific regions of the stimuli-responsive composite hydrogel remotely using either an alternating or static magnetic field.[189] Additionally, studies have shown actuation *via* magnetic-fields can be harnessed in biological applications due to its biocompatibility.[348] While magnetic field actuation has its advantages, the disadvantages of magnetic field actuation include poor responsiveness.[349] Often magnetic-responsive hydrogels are coupled with additional stimuli (*i.e.*, temperature, light, and heat) which broadens the applicability of the material system.[281]

The composition of magnetic-responsive composite hydrogels includes a base of a hydrogel with some type of magnetic fillers (*e.g.*, IONP) embedded. Among the hydrogels selected for the magnetic-responsive composite hydrogel material system include both non-stimuli-responsive hydrogels and stimuli-responsive hydrogels. Some non-stimuli-responsive hydrogels utilized in magnetic-responsive composite hydrogels include alginate,[306] gelatin,[275] and collagen.[350] Stimuli-responsive hydrogels are commonly used in the composition of magnetic-responsive composite hydrogels because they provide an additional stimuli-responsive quality. Well-studied temperature-responsive hydrogel PNIPAM is frequently used in magnetic-responsive composite hydrogels.[189,351]

Magnetic fillers in magnetic-responsive composite hydrogels include both soft-magnetic particles and hard-magnetic particles. Soft-magnetic particles are typically characterized as having a low coercivity resulting in particles which are easily magnetized and demagnetize.[352] Additionally, soft-magnetic particles are actuated using an alternating magnetic field, which is a magnetic field that changes its amplitude with time. Commonly utilized soft-magnetic particles, which are able to demonstrate shape transformation under alternating magnetic fields, include ferromagnetic nanoparticles such as magnetic IONP[189] and maghemite gamma-Fe_2O_3.[353] Conversely, hard-magnetic particles are difficult to magnetize and demagnetize having a high coercivity.[352] Hard-magnetic particles are capable of response to static magnetic fields (*i.e.*, permanent magnet[354]), and have recently garnered more interest for its ability to be re-programmed and observe large shape deformations.[355] Frequently studied hard-magnetic particles include neodymium–iron–boron (NdFeB) and Ni nanowires (NiNW). Li *et al.* demonstrated a walking and steering robot by NiNW-PNIPAM composite hydrogels under a magnetic field and light (Fig. 15a).[356] This soft robot showed a fast walking and steering motion of 0.3 body length per second and 45° per second, respectively. This walking speed is comparable to the biologically relevant system (1 body length per second).

Simple magnetic-responsive composite hydrogels can undergo shape transformation when exposed to only a magnetic field. Sun *et al.* demonstrated magnetic-responsive hydrogel composed of 2-acrylamido-2-methyl-1-propanesulfonic acid sodium salt (NaAMPS) and NdFeB hard-magnetic particles.[354] PNaAMPS/NdFeB was first 3D printed then magnetized using a uniform magnetic field. Once magnetized, PNaAMPS/NdFeB was actuated using a permanent NdFeB magnet causing the initial 2D structure to bend or twist into a final 3D structure as demonstrated in Fig. 15b.

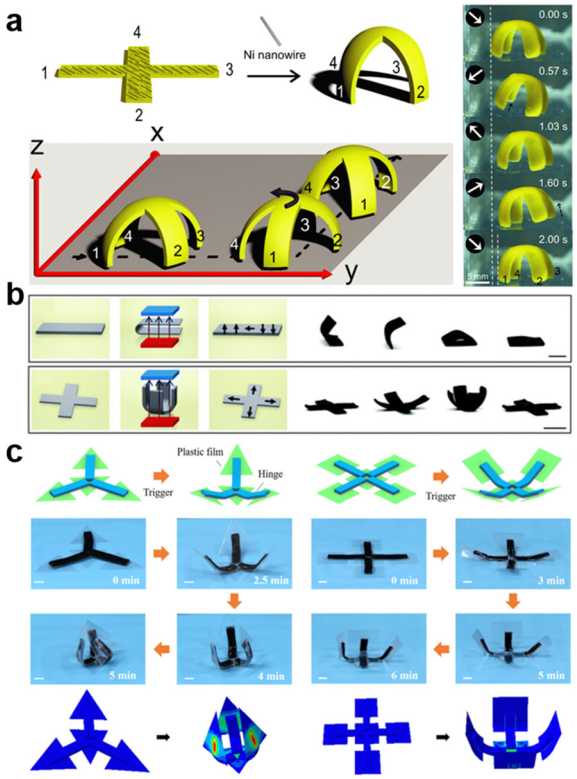

Fig. 15 The magnetic-responsive shape morphing behavior of composite hydrogels. (a) Schematic representation of the hydrogel robotics rotating its body 90° counterclockwise when the rotation direction of the magnetic field changes due to the addition of Ni nanowire from the *y*–*z* plane to the *x*–*z* plane. Reproduced with permission.[356] Copyrights 2020, American Association for the Advancement of Science. (b) PNaAMPS/NdFeB composite hydrogel is programmed with a NDFeB magnet and actuated using a static magnetic field in the form of a permanent magnet inducing a shape change. Scale bars are 10 mm.[354] Reproduced with permission. Copyrights 2021, Royal Society of Chemistry. (c) Fe_3O_4/PNIPAM is actuated with an alternating magnetic field causing a shape change. Scale bars are 5 mm. Reproduced with permission.[189] Copyrights 2019, American Chemical Society.

While magnetic-responsive composite hydrogels can stand alone as the only external stimulus applied to the material system, often magnetic-responsive composite hydrogels are coupled with additional stimuli such as temperature, light, and heat to produce a multi-stimuli-responsive composite hydrogel capable of responding to more than one stimulus. Typically, magnetic nanoparticles are embedded within a stimuli-responsive hydrogel, whereby the magnetic nanoparticles endow the stimuli-responsive hydrogel with a magnetic-responsive quality. For example, Tang *et al.* fabricated a magnetic-responsive composite hydrogel comprising of soft-magnetic IONP and well-studied temperature-responsive IONP/PNIPAM.[189] IONP/PNIPAM was fixed to an elastomer, VHB 4905, to form a bilayer structure capable of magnetic actuation. The stimuli-responsive composite hydrogel was actuated using an alternating magnetic field into complex structures such as an origami-inspired pyramid and an uncovered box depicted in Fig. 15c. When the composite hydrogel was exposed to an alternating magnetic field, it caused an effect known as photothermal heating, where magnetic particles generate heat and

cause the temperature-responsive hydrogel PNIPAM to de-swell and change shape.

5.5. pH value

The shape morphing behavior of pH-responsive composite hydrogels mostly relies on the pH-sensitive swelling/deswelling of the hydrogel matrix containing weak acidic or basic groups.[139] These ionic species can generate ionic concentration differences inside and outside hydrogels, thus forming the osmosis force that promotes to the uptake of surrounding H_2O molecules. Additionally, the ionic repulsion contributes to creating a larger space between polymer chains, allowing for more H_2O penetration. As a result, if more ionizable groups connect with polymer chains, the hydrogel network will exhibit a higher swelling ratio.[117] Notably, the mechanism of pH responsiveness for these ionic hydrogels is based on the protonation and de-protonation of ionic groups. Taking carboxyl groups as an example, when the pH value is higher than pK_a of –COOH, carboxyl groups deprotonate and exist in an anionic form. However, decreasing the pH value below to pK_a of –COOH gives rise to the protonation of $-COO^-$, the carboxyl groups exist as –COOH form. By controlling the pH value, the amount of the carboxyl anion can be reversibly regulated, thereby switching the expansion or shrinkage of hydrogels.[357] Since pH-responsive swelling/deswelling behaviors of ionic hydrogels are isotropic, composite hydrogels, especially bilayer structures consisting of the active layer and the passive layer are most common, provides a promising approach to generating anisotropic 3D deformation. For instance, Xiang *et al.* synthesized a pH-responsive peptide (MA-FIID) and copolymerized it with the PNIPAM, then they utilized PNIPAM/peptide copolymer and pure PNIPAM to successfully create a bilayer actuator with the ability to generate the pH-responsive shape morphing (Fig. 16a). Notably, the assembly and disassembly of peptide molecules can be controlled by acidic and basic environments, respectively. In the acidic condition, assembled peptide molecules lead to the shrinkage of the copolymer network, which drives the bending of bilayer structure. In addition, this bending can be recovered in basic environments, the high pH value results in the disassembly of peptide molecules and the deprotonation of carboxyl groups inside the peptide. The ionic copolymer layer can gradually reswell and attain to a greater expansion compare to the swelling of the pure PNIPAM layer, which means the bilayer structure can be flat and even oppositely bend.[358] Moreover, to realize the complicate shape morphing and multifunctionalities, integrating hydrogels with different responsiveness or various functions is attractive. Inspired by the metamorphosis development of bioluminescent octopuses, Wang *et al.* combined the temperature-responsive hydrogel, the pH-responsive hydrogel, and the redlight-emitting Eu^{3+} coordinated hydrogel (Eu-gel) to construct a hydrogel actuator enabling to execute origami-like 3D shape morphing and information encryptions (Fig. 16b). Temperature-responsive and pH-responsive hydrogels are capable of growing onto the surface of the Eu-gel, their swelling behaviors endow bilayer samples with the structure editing. Since the information written by red fluorescent carbon dots (CDs) is easily encrypted and decrypted through the wavelength-dependent redlight/non-fluorescence transition of Eu-gel, various shape morphing and corresponding visual information can be conveyed by employing different environmental stimuli.[359] Furthermore, due to the contrary pH-responsiveness of cationic hydrogels and anionic hydrogels, two-way shape-morphable bilayer structures can be realized. Kumar *et al.* constructed a bilayer structure consisting of the cationic CS hydrogel and the

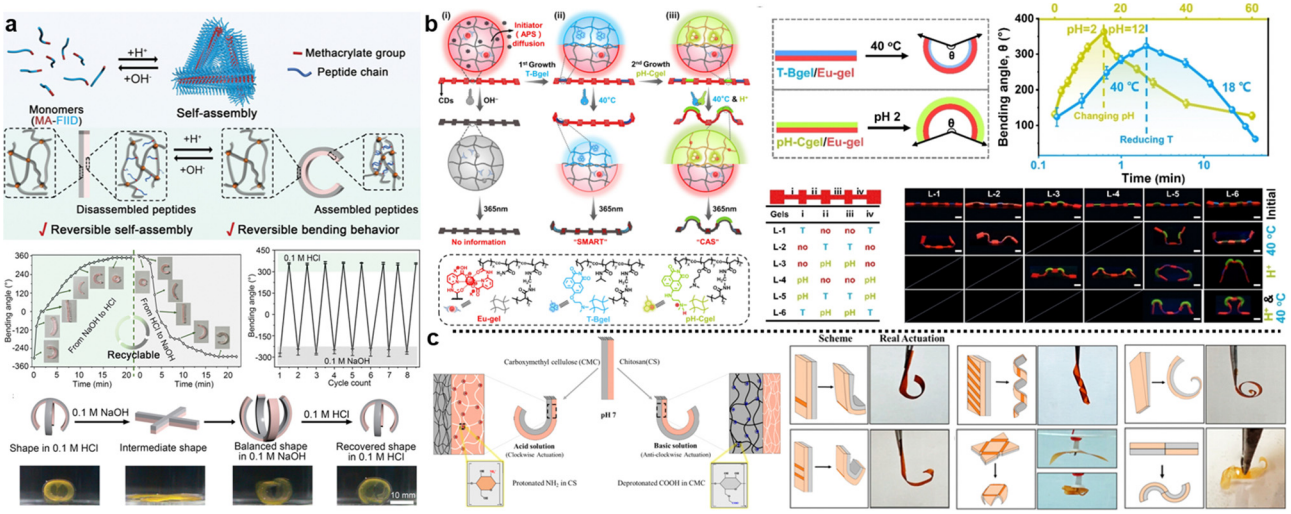

Fig. 16 The pH-responsive shape morphing behavior of composite hydrogels. (a) The pH-responsive assembly/disassembly of synthesized peptides (MA-FIID) determines the pH-responsive bending behavior of the bilayer composite hydrogel, which is composed by the PNIPAM layer and the PNIPAM/MA-FIID copolymer layer. Reproduced with permission.[358] Copyrights 2023, Wiley-VCH. (b) The composite hydrogel consisting of the redlight-emitting Eu^{3+} coordinated hydrogel (Eu-gel), the temperature-responsive hydrogel (T-Bgel), and the pH-responsive hydrogel (pH-Cgel) exhibits the shape editing function and the programmable fluorescence. The scale bar in photographs is 1cm. Reproduced with permission.[359] Copyrights 2023, Wiley-VCH. (c) The pH-tunable two-way bending behavior of composite hydrogel is realized *via* integrating the anionic carboxymethyl cellulose (CMC) layer and the cationic chitosan layer. Reproduced with permission.[53] Copyright 2022, American Chemical Society.

anionic carboxymethyl cellulose (CMC) (Fig. 16c). When the bilayer was submerged in an acidic medium, the amino groups in the CS layer become protonated (NH_3^+). Simultaneously, carboxyl groups in the CMC layer performed as COOH form after the protonation, which means the swelling ratio of the CMC layer is much smaller than that of the CS layer. This swelling mismatch caused a clockwise actuation of the bilayer. Conversely, the basic environment contributes to the inverted ionization (NH_2 in the CS layer, COO^- in CMC layers), thus acquiring an anti-clockwise actuation. In their standard system, CS/CMC bilayer films required roughly 40 s to fully fold in a clockwise direction when placed in 0.1 M HCl, whereas they took approximately 78 s to fully fold in an anticlockwise direction in a 0.1 M NaOH solution.[53]

5.6. Solvents

Similar to pH-responsiveness, the solvent-responsive shape morphing of composite hydrogel is typically determined by the intrinsic properties of hydrogel matrices. Generally, different solvents enable to create various chemical environments for polymer chains. Their polarity, solubility, composition, and concentration are crucial to determine the chains' conformation and the stability of hydrogel networks. Actually, the swelling behavior of hydrogels in H_2O can be regarded as the simplest source to generate the solvent-responsive shape morphing by controlling their structural parameters. For example, Gladman *et al.* used a soft acrylamide ink embedded with stiff cellulose fibrils, which mimics the composition of plant cell walls, to print shape morphable structures (Fig. 17a). Since the localized and anisotropic swelling behavior of printed hydrogel filaments is tuned by the orientation of cellulose fills, some plant-inspired architectures can be programmably fabricated. These printed structures yield complex three-dimensional morphologies on immersion in H_2O.[56] Additionally, the wettability difference between solvents and polymers introduces the heterogeneous factor into shape morphing hydrogels. Li *et al.* employed the Fe^{3+}/SA and the acrylamide to fabricate a SA/PAM composite hydrogel with light-responsive and solvent-responsive shape morphing (Fig. 17b). They found that the UV irradiation can dissociate coordination between Fe^{3+} and SA due to the reduction of Fe^{3+} to Fe^{2+}. The irradiated surficial network has a looser crosslinking density with the inner network, which contributes to the swelling mismatch and shape morphing in an aqueous environment. Once the sample is moved to ethanol, the deformed shape will recover to its initial state. This is attributed to the poor wettability of ethanol to SA/PAM hydrogels, which means both surficial and inner networks have similar swelling behaviors in ethanol environment.[54] Moreover, the cosolvency and cononsolvency effects also play important roles in achieving solvents-responsive deformation of composite hydrogels. Wang *et al.* printed a PNIPAM-PEG bilayer hydrogels with solvent-responsiveness by applying the cononsolvency effect of H_2O/ethanol (Fig. 17c). For PNIPAM layer in this system, the PNIPAM polymer chains is hard to dissolve into the H_2O/ethanol mixture that the concentration of ethanol is from 20 to 40 mol%. In other words, the swelled PNIPAM hydrogel inclines to deswell in this mixed solvent. Thus, the bilayer structure can transform in the opposite direction in the solvent within the above concentration.[360] Indeed, the difference between the protic and aprotic solvents can lead to the shape deformation of hydrogels. Zhang *et al.* prepared a starfish-like bilayer actuator made of (2-(dimethylamino)ethyl methacrylate) (PDMAE) and gelatin hydrogels, this actuator can move through alternative swelling/deswelling transition (Fig. 17d). This transition is achieved *via* continuously switching the H_2O and acetonitrile (ACN). When bilayer hydrogels are introduced from a water solution into an acetonitrile solution, it promotes the water to transfer from the gelatin layer to the PDMAE layer. This transition also boosts the swelling of the PDMAE layer.[361] Overall, solvent-responsive shape morphing in hydrogels represents a vibrant research area with significant potential for practical applications.

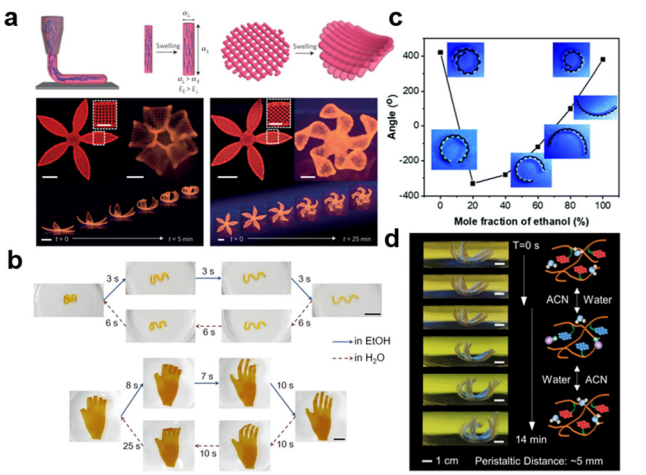

Fig. 17 The solvent-responsive shape morphing behavior of composite hydrogels. (a) Biomimetic 4D printed composite hydrogel (cellulose reinforced PAM) flowers with the H_2O-induced shape morphing, which can attribute to the anisotropic swelling of composite hydrogels and reasonable structural designs. The scale bar in photographs is 5 mm. Reproduced with permission.[56] Copyrights 2016, Springer Nature. (b) Solvents (H_2O/EtOH) driven actuation of SA/PAM hydrogels. The scale bar in photographs is 1 cm. Reproduced with permission.[54] Copyright 2020, American Chemical Society. (c) The cononsolvency effect of H_2O/ethanol contributes to the deformation of PNIPAM/PEGDA bilayer composite hydrogels.[360] (d) A starfish-like bilayer actuator consisting of (2-(dimethylamino)ethyl methacrylate) (PDMAE) and gelatin hydrogels, its movement is driven by H_2O/ACN switching. Reproduced with permission.[361] Copyright 2023, Elsvier.

6. Emerging applications of deformable composite hydrogels

Since the shape morphing behavior, including bending, twisting, folding, curling, swelling, and shrinking, of stimuli-responsive composite hydrogels renders them highly adaptable, movements and changes to their physical shape provide great promise that allows for precise and programmable responses in various applications, such as in healthcare, energy, and the environment to name a few. From the gripping of tumor cells and cargo transportation at the nanoscale to the unfolding of encrypted

information and self-locomotion at the macroscale, the ability to respond to environmental cues on demand provides the foundation for new emerging applications, many of which imitate the structure, function, and reversible behaviors of humans, plants, and animals. Here, we summarize some of the recent progress in the use of shape morphing composite hydrogels in the context of actuation applications as well as provide recent examples in the developments of soft robotics, information encryption, biomedical applications, flexible electronics, and engineered living materials.

6.1. Soft robotics

Deformable composite hydrogels have opened up new avenues in actuation applications, giving rise to a novel class of smart soft robotics capable of unique programming to navigate and respond to specific environmental conditions.[362–364] Unlike traditional hard robotics with rigid, limited adaptability, these smart soft robotics exhibit greater flexibility, enabling a broader range of programmable responses.[69,365,366] Hydrogel-based soft grippers can be designed to gently pick up and manipulate delicate objects without causing damage. They can be used in food handling, medical applications, or handling biological samples. Jian *et al.* designed a bilayer hydrogel sponge actuator comprising thermoresponsive PNIPAm and temperature-insensitive pan paper (Fig. 18a).[367] The hydrogel sponge's large-pore structure facilitates rapid swelling and de-swell responses within seconds, while retaining its capacity to deform significantly. This rapid adaptability enables the actuator to capture moving objects, showcasing its potential in the rescue of living creatures (Fig. 18b). Notably, they demonstrated its effectiveness by capturing live crabs that had fallen into dangerously high-temperature waters.

The hydrogel-based robotics can also harvest energy from environmental stimuli to achieve locomotion such as swimming and walking. Zhao *et al.* developed a phototactic swimmer based on a self-sustained hydrogel oscillator.[368] The hydrogel pillar composed of PNIPAM and AuNP folded toward the light source. When the folding angle surpassed 90°, the near-end of the hinge facing the light source began obstructing the light from reaching the far-end of the hinge, resulting in what is commonly known as the self-shadowing effect. This shadowed region experienced a persistent cooling below the lower critical solution temperature (LCST), causing rapid reswelling until the previously blocked area was once again exposed to light (Fig. 18c). Therefore, the hydrogel pillar oscillated around a folding angle of 90°, thus propelling water backward to provide force to swim away from the light source (Fig. 18d and e). Furthermore, hydrogels which actuated walking motion have been studied over decades. For instance, GO was locally infiltrated into the PNIPAM hydrogel matrix with a pore size gradient along the thickness direction (Fig. 18f).[159] When exposed to NIR light, the GO-PNIPAM hydrogel folded towards the surface with a larger pore size. As a result of this asymmetric deformation, unbalanced frictions were generated, causing the hydrogel sheets to move towards the end with larger frictions (Fig. 18g). Such movement is similar to the locomotion of an inchworm (Fig. 18h).

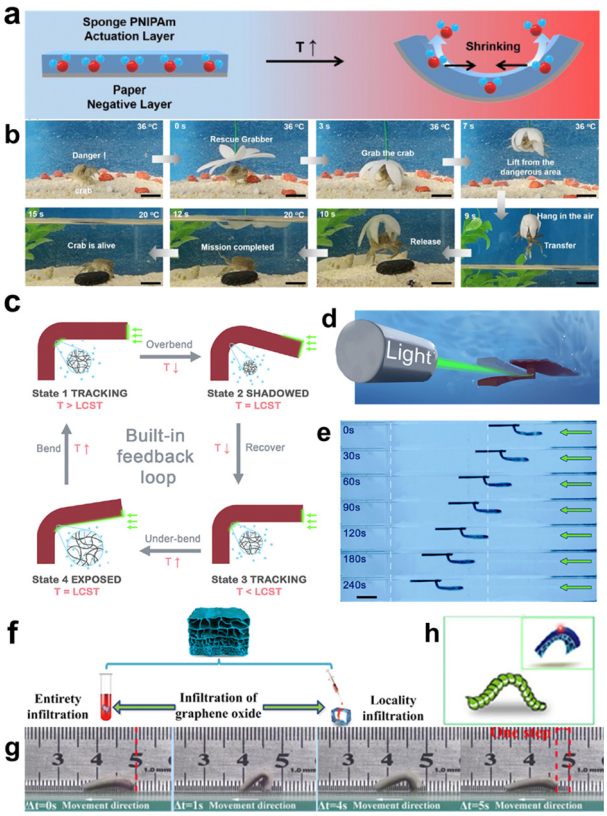

Fig. 18 Hydrogel-based soft robotics. (a) Schematic of the structure and bending mechanism of actuator based on the hydrogel-based bilayer with active PNIPAM layer and negative paper layer. (b) Gripper demonstration by grabbing crab and moving in a fast fashion. Reproduced with permission.[367] Copyright 2022, Elsevier. (c) Mechanism of the oscillation based on self-shadowing effect. (d) Scheme of the soft swimmer and (e) the optical images a flagellum-inspired swimmer. Reproduced with permission.[368] Copyright 2019, American Association for the Advancement of Science. (f) Bionic hydrogel soft robotics based on infiltration method. (g) Bionic hydrogel walking robot inspired by inchworm under NIR light exposure. (h) Movement of inchworm. Reproduced with permission.[159] Copyright 2018, Elsevier. Scale bar: (b) and (e) 1 cm.

Overall, the use of deformable composite hydrogels has given rise to a new class of soft robotics and actuators, addressing the limitations of conventional rigid robotics that struggle to fit or adapt to tight spaces. These innovative advancements hold significant promise for a wide array of applications, from underwater exploration to rescue missions, and demonstrate the potential of smart soft robotics to revolutionize various industries.

6.2. Information encryption and decryption

Information technology has been an increasingly popular field as technologies continue to evolve to improve lives; however, many new problems have emerged as well, such as breaches in security that impact the transfer and storage of information. Therefore, there is a great interest for an efficient, stable, and safe way to handle sensitive information in a timely manner. Deformable composite hydrogels have been proposed as a potential solution by using these materials to encrypt and

decrypt information on demand, thus improving security levels where concealed information only unlock after certain conditions are met.[369] In addition to typical fluorescence protection, the shape-morphing behavior of hydrogels can conceal whole patterned fluorescence inside the deformation, thus forming secondary protection. For example, Zhu *et al.* synthesized a poly(1-vinylimidazole-*co*-methacrylic acid) (P(VI-*co*-MAA)) hydrogel, which incorporated by VPTP chromophores (Fig. 19a). Interestingly, upon the irradiation of UV light with 370 nm wavelength, (P(VI-*co*-MAA)) hydrogel exhibited the blue fluorescence with 415 nm emission wavelength. If the excitation wavelength changed to 365 nm, the blue fluorescence gradually became to green (the emission wavelength is 415 nm) with the irradiation time extended to 30 min. By harnessing this phenomenon and shape memory effect, this (P(VI-*co*-MAA)) hydrogel can realize dual encryption/decryption. The correct information is only readable after both sequential shape recovery and UV light irradiation.

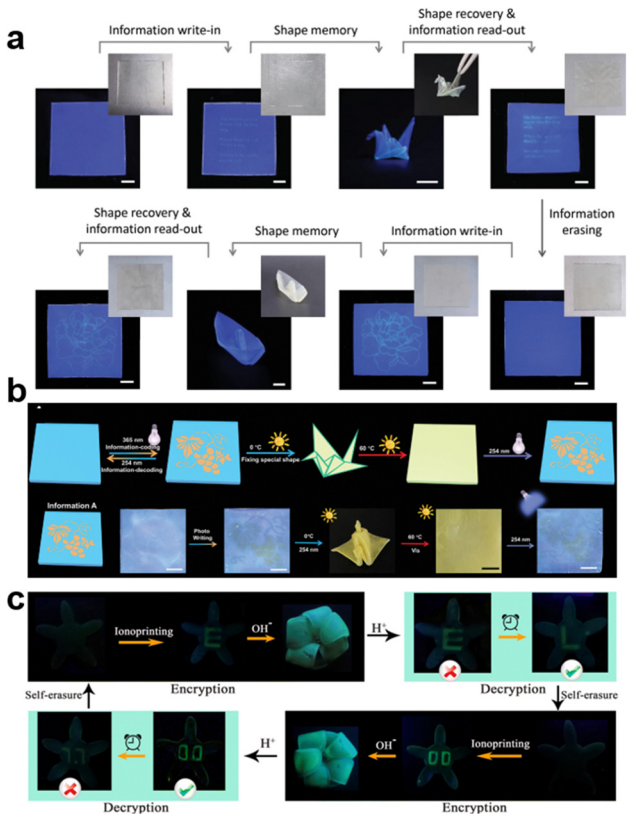

Fig. 19 The application of deformable composite hydrogels into Information encryption and decryption. (a) The dual encryption/decryption of fluorescent poly(1-vinylimidazole-*co*-methacrylic acid) P(VI-*co*-MAAc) hydrogels is based on its shape memory effect and VPTP chromophores. The scale bar is 1 cm. Reproduced with permission.[57] Copyrights 202, Wiley-VCH. (b) The dual encryption/decryption of fluorescent P(DMA-DEAN)/P(SMA-9-ANA) organohydrogels. The scale bar is 0.5 cm. Reproduced with permission.[134] Copyrights 2022, Wiley-VCH. (c) The multistage information encryption/decryption of the bilayer hydrogel composed of the AIE-active fluorescence layer containing amino-functionalized tetraphenylethene ($TPE3N^{3+}$) and active shape deformation layer containing PAA. Reproduced with permission.[370] Copyright 2023, Royal Society of Chemistry.

Notably, all green fluorescence information can be erased *via* irradiating 370 nm UV light.[57] Similarly, Shang *et al.* prepared an organohydrogel enabling to dual encrypt/decrypt information (Fig. 19b). Within this organohydrogel, naphthalimide moieties are introduced into the hydrophilic poly(N,N-dimethylacrylamide) (PDMA) hydrogel, resulting in a green-yellow emission fluorescence. Simultaneously, anthracene (ANA) units are copolymerized into the hydrophobic polystearate methacrylate (PSMA) organogel, producing a blue emission fluorescence. Since the dimerization of ANA moieties can be reversibly tuned by the wavelength of UV light, the blue light emission can eliminate with dimerizing ANA, which means the green-yellow light is dominant. In virtue of the photolithography and crystallization-induced shape memory performance, the information can be protected by its fluorescence and deformation.[134]

Yang *et al.* construct a sophisticated AIE fluorescence-based multilevel information security system using the shape modification and patterned fluorescence alteration of the $TPE3N^{3+}$-hydrogel/PAA hydrogel bilayer hydrogel (Fig. 19c). When the $TPE3N^{3+}$-hydrogel submerged into basic solution, the deprotonated TPE aggregated and emitted green fluorescence. These TPE aggregates dissociated when placing it into acidic solution with eliminating green fluorescence. Notably, $TPE3N^{3+}$ units can reversibly interact with PSS or HCHO *via* electrostatic interaction and dynamic imine bonds, respectively. These interactions slow down the dissociation of TPE aggregates, creating the time difference of eliminating fluorescence in the treated region and the untreated region. This enables the generation of encoded fluorescence patterns. In addition, in virtue of pH-responsive bending of bilayer composite hydrogel, they achieved 3D multistage information encryption through a synergistic deformation and fluorescence color shift.[370]

6.3. Biomedical applications

Unlike traditional biomaterials that maintain a consistent function, composite hydrogels exhibiting shape-changing behavior have opened a broad spectrum of opportunities in bioengineering and medical applications. Owing to their high biocompatibility and stimuli-responsive shape deformability, these hydrogels are frequently utilized as therapeutic tools, such as targeted drug delivery and localized eradication of cancer cells. Xin *et al.* developed shape morphing microrobots (SMMRs) that consist of pH-responsive hydrogels, which allows them to adapt to their surrounding environmental conditions for localized cancer cell treatment that requires targeted drug delivery, such as DOX (Fig. 20a).[59] These SMMRs are able to clamp and unclamp in order to encapsulate, transport, and release in a controllable manner at specific desired locations. Shape morphing microcrabs (SMMC) and shape morphing microfish (SMMF) have also been designed, highlighting the ease of printability and the complexity of structures that can be precisely created.

In addition to therapeutic drug delivery, shape morphable composite hydrogels can be applied to remotely controlled foreign body removal. Liu *et al.* developed magnetic arthropod millirobots *via* designing structures with joint and 3D printing of PAM hydrogels incorporated with NdFeB magnetic nanoparticles

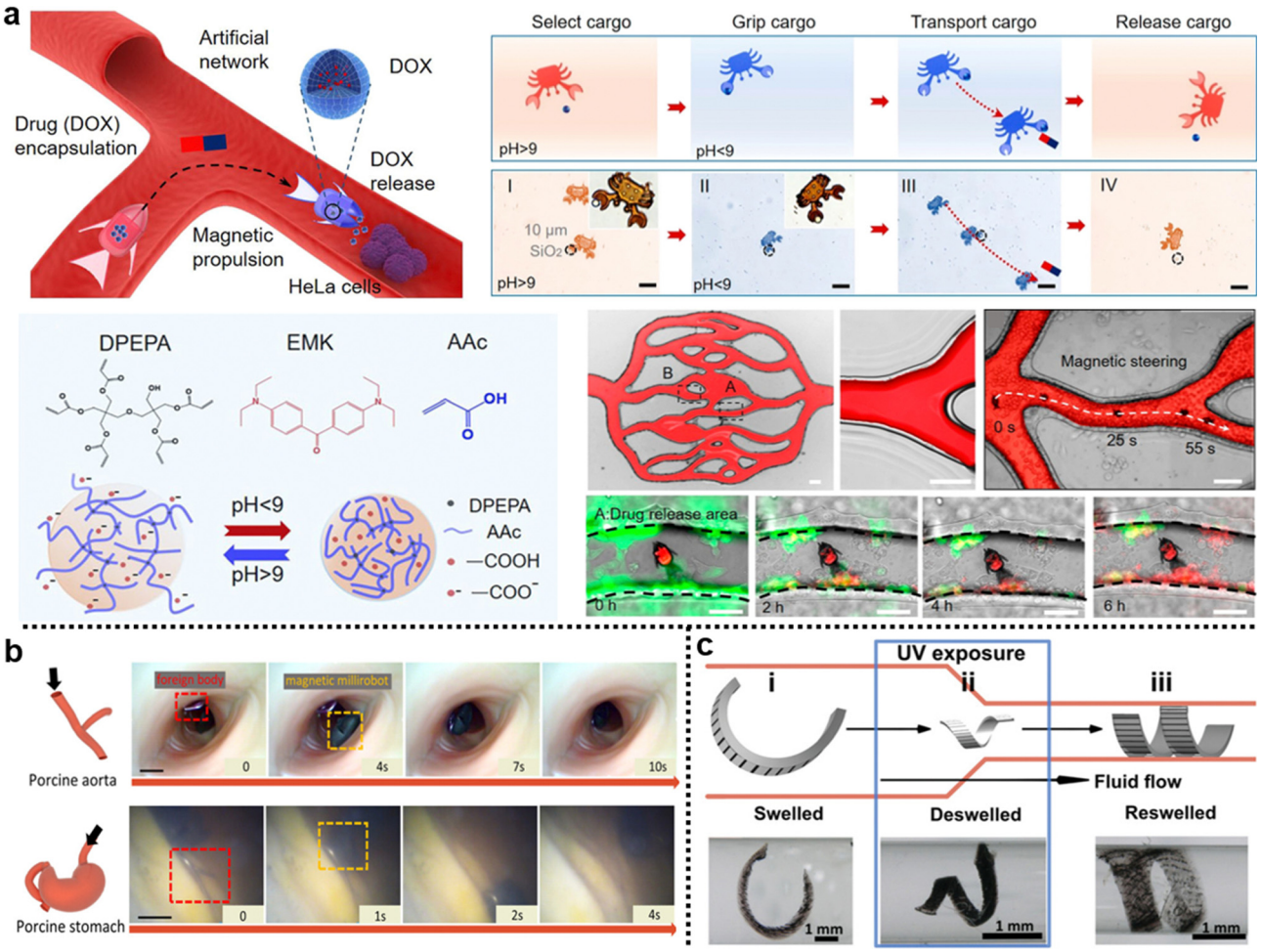

Fig. 20 The biomedical application of deformable composite hydrogels. (a) The environmentally adaptive shape-morphing microrobots (SMMRs) for targeted DOX release to treat cancer cells by shape morphing. The movement of hydrogel microrobots is based on incorporated magnetic particles inside, while cargo gripping and releasing are based on pH-responsive swelling/deswelling of the hydrogel matrix. The scale bar in photographs of crab robotics is 50 μm, scale bars in photographs of fish moving and drug releasing are 100 and 50 μm, respectively. Reproduced with permission.[59] Copyrights 2021, American Chemical Society. (b) Foreign body removal in porcine aorta and stomach using the magnetic-responsive shape morphing of composite hydrogels. The scale bar is 10 mm. Reproduced with permission.[188] Copyrights 2022, Wiley-VCH. (c) Illustration of rGO/AuNP-PNIPAM hydrogel sheet as a stent. Its swelling/deswelling behavior can be controlled by UV lights. Reproduced with permission.[258] Copyrights 2022, Wiley-VCH.

(Fig. 20b).[188] Within printed products, a six-armed arthropod microrobot enables multiple modes of movement, including free-standing, moving, folding, and unfolding, by controlling the magnetic field. This contributes to the realization of foreign body removal in the porcine aorta and stomach.[361]

Stents are small expandable metal tubes traditionally implanted by inflation from a balloon within narrowed or blocked blood vessels to restore proper blood flow. However, the implantation of traditional stents through the blood vessels can potentially cause damage to healthy vessel walls. To address this concern, researchers are exploring alternative solutions, such as utilizing stimuli-responsive hydrogels that can travel through blood vessels without causing harm. Li *et al.* presented a remarkable approach using a GO/AuNP-PNIPAM hydrogel sheet that exhibits unique shape morphing capabilities (Fig. 20c). This hydrogel sheet can shrink and traverse from a capillary channel with a larger diameter to a narrower channel with a diameter. Subsequently, it reswells to expand within the smaller channel, mimicking the function and behavior of traditional stents. This innovative use of stimuli-responsive hydrogels shows great promise for safer and more effective medical interventions, offering a potential breakthrough in the field of cardiovascular treatments.[258]

6.4. Flexible electronics

Shape morphing abilities have also opened many opportunities for flexible electronics that can extend and contract in various configurations as well as act as supercapacitors and conductors. Flexible electronics have been an area of high interest as they are particularly useful for wearable devices and sensors because of their non-toxicity and high biocompatibility. Du *et al.* reported a method for creating shape-adaptable 3D flexible electronics (Fig. 21a). This approach combines photothermally responsive AuNR-PNIPAM composite hydrogels with

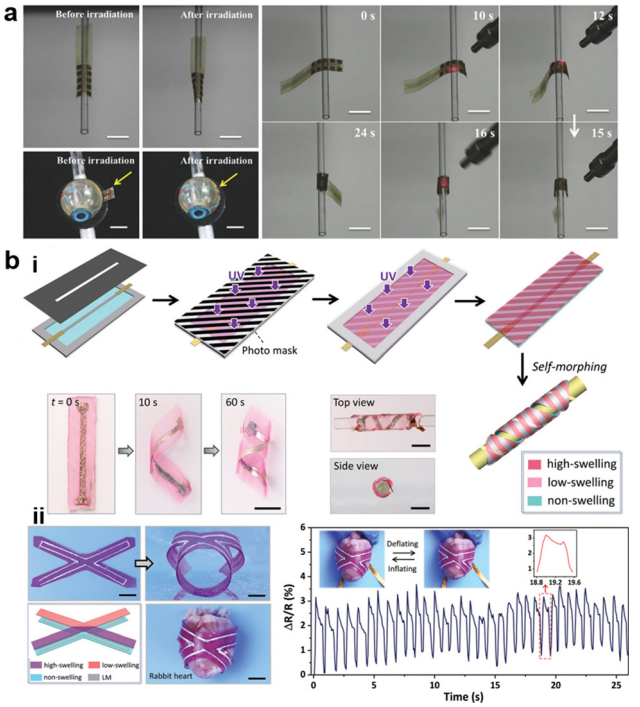

Fig. 21 The application of deformable composite hydrogels into flexible electronics. (a) Conforming behavior of the AuNR-PNIPAM hydrogel-based flexible microelectrode arrays (fMEA) before and after irradiation with NIR light. Scale bar is 10 mm. Reproduced with permission.[371] Copyrights 2017, Wiley-VCH. (b) (i) Schematic for the fabrication and photos to show the morphing process and shape fixation of the hydrogel-based soft electronics (HSE) on a glass rod. Scale bar: 1 cm. (ii) Monitoring the motions of a rabbit heart by self-shaping HSE. Scale bar: 1 cm. Reproduced with permission.[58] Copyrights 2021, Wiley-VCH.

traditional flexible microelectrode arrays (fMEAs). The fMEAs-enhanced composite hydrogels are adaptable and can fit various surface geometries. When triggered remotely by NIR light at a wavelength of 808 nm, the composite hydrogel layer, grafted on the rear side of the fMEAs, shrinks to initiate a desirable shape transformation in the fMEAs. Through patterning the responsive hydrogel layer, the fMEAs can demonstrate planar-to-twisted structural transformations in response to external stimuli, driven by differential shrinkage and their elastic moduli. This strategy allows fMEAs to modify their shape remotely and fit unpredictable shapes of different surfaces through NIR irradiation.[371]

Hao *et al.* studied hydrogel-based soft electronics that dynamically deform to grab onto objects, where they created a gradient structure in the hydrogel substrate by stencil-printing liquid metals in order to integrate multiple sensing units in the hydrogel and allow for active, 3-dimensional deformations in the presence of external stimuli (Fig. 21b). The versatility and flexibility of these soft electronics can give rise to many emerging technologies, such as electronics that can monitor the beating heart of a rabbit and electronics that can mimic the motions of an electric eel.[58]

6.5. Engineered living materials

Engineered living materials (ELMs), which consist of living biological systems that are incorporated into non-living polymeric matrices, have been an area of growing interest in recent years. Combining recent advances in synthetic biology and in materials science, this new emerging class of materials enables even more unique functionalities and properties as it incorporates biological aspects into synthetic materials.[39,372,373] Examining the shape morphing behavior of plant-based ELMs, Zhao *et al.* developed plant cyborgs, where 3D printed composite hydrogels that contain NC and GO were embedded onto the surfaces of spinach leaves to control their shape in response to temperature and UV light (Fig. 22a and b).[61] Due to the strain mismatch between the composite hydrogel and the leaf, the morphology of the leaf can change, enabling reversible folding and bending capabilities. This idea of integrating actuation capabilities and living plants opens up a new class of plant-based materials that are able to adapt and respond to environmental conditions, such as plant-based tissue engineering scaffolds and plant-based biosensors that can monitor the health of

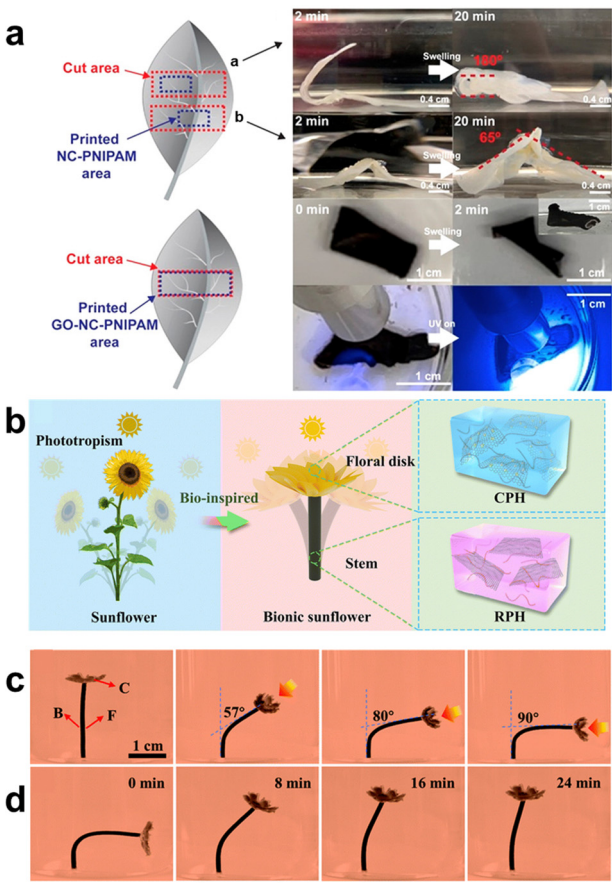

Fig. 22 The application of deformable composite hydrogels into engineered living materials. (a) Hydrogels incorporated onto plant tissues enable programmable shape control. Schematic of the top view of the cut area of the decellularized leaf (red) and NC-PNIPAM (blue) and photographs of actuation process by temperature increasing and light exposure. Reproduced with permission.[61] Copyright 2022, American Chemical Society. (b) Bionic sunflower based on stimuli-responsive hydrogels. Schematic illustration of a natural sunflower and the bionic sunflower. (c) Photographs of a bionic sunflower at different angles of incident light. (d) Photographs for the shape recovery process of a bended bionic sunflower. Reproduced with permission.[374] Copyright 2021, The Royal Society of Chemistry.

plants to improve precision farming and reduce food insecurity. Besides integrating hydrogels with plants, using hydrogel-based photocatalytic systems to mimic the plant, thus harvesting energy from nature is another attraction. For instance, Qin *et al.* developed a bionic sunflower capable of spontaneously tracking and orienting itself directionally towards a light source, emulating the phototropism observed in real plants (Fig. 22b).[374] This bionic sunflower consists of two components: rGO-PNIPAM hydrogels (RPH) acting as phototropic stems to facilitate the light tracking process, and CdS/rGO-PNIPAM hydrogels (CPH) serving as photoreactors for conducting various photocatalytic reactions, including the generation of H_2O_2. Under illumination, the bionic sunflower bends toward the light source due to temperature differences between the backside (B), the frontside (F), and the surface of CPH (C) (Fig. 22c). When the light source is removed, the bionic sunflower gradually recovers its original shape within 30 minutes, resembling the behavior of a real sunflower during the night (Fig. 22d). The mechanism behind the light tracking process is further supported by simulated thermal distribution within the bionic sunflower under light exposure. This confirms the effectiveness of the phototropism exhibited by the sunflower, achieved through the coordinated actions of RPH and CPH components in response to light. Furthermore, demonstrating that soft robotics and actuators are no longer primarily restricted to abiotic applications that typically require harsh physiochemical conditions to induce shape morphing, Ding *et al.* highlighted the high cell viability of their cell-laden trilayer hydrogel actuators that consists of two outer oxidized methacrylated alginate (OMA) layers and one inner methacrylated gelatin (GelMA) layer in between.[375] With high integrity and repeatability, their cytocompatible cell-laden hydrogel actuator can be controlled to transition between multiple configurations without using harsh stimuli, such as low pH, high temperatures, and toxic chemicals or solvents. Through the synergy between the properties of the hydrogels and the interactions between the cells and living organisms, this allows for complex shape transformations that can be controlled for biomimicry of living tissue morphogenesis and for living tissue regeneration applications.

7. Conclusions and perspectives

In this review, we have compiled the main material systems of stimuli-responsive composite hydrogels, focusing on their role in achieving complex 3D shape morphing. These hydrogels represent a promising class of soft materials that exhibit remarkable changes in shape and function in response to various external controls and stimuli. By incorporating diverse types of additives, these hydrogel matrices gain extra functionalities, broadening their range of applications. The spatiotemporal control of functional additive dispersion, along with the ability to assemble stimuli-responsive hydrogels with other materials, empowers the creation of programmable shape morphing in the resulting composite hydrogel systems. As a result, these shape morphing stimuli-responsive composite hydrogels find widespread applications in soft robotics, information security, biomedical fields, flexible electronics, and even in engineering living materials.

Currently, several challenges hinder the practical applications of stimuli-responsive composite hydrogels. A prominent issue is their slow response speed, primarily dictated by the mass transport of water or ions within the hydrogels. To address this challenge, it becomes crucial to focus on factors like size scale and porosity when designing these hydrogels. Miniaturization and enhancing porosity emerge as potential solutions to expedite their responses. For applications requiring large-scale hydrogels, such as smart windows and cargo transport systems, fabricating them with uniformity, without cracks, while maintaining rapid response times, presents a less explored area in recent research.

Furthermore, incorporating stimuli-responsive composite hydrogels into the realm of biomaterials raises uncertainties. On one hand, achieving successful cell growth and cultivation within hydrogels necessitates meticulous control of living conditions, which keeps most biological applications at a distance from commercialization and mass production. On the other hand, certain stimuli-responsive hydrogels and additives, like PDMAEMA and GO, respectively, exhibit cytotoxicity and non-biodegradability. These limitations hinder the integration of stimuli-responsive composite hydrogels into clinical systems, such as drug delivery, medical device implantation, and cell growth scaffolds. Addressing these issues is crucial for the broader adoption of these promising materials in biomedical applications.

In order to enable parallel functions and extend the operational capabilities of stimuli-responsive hydrogels, it is essential to explore and develop novel fabrication techniques and material systems. Achieving high stimuli sensitivity and rapid response speed demands a concerted effort involving the incorporation of multiple materials, miniaturization, and mechanical design of the hydrogel-based systems. To enhance the response speed, considerable effort should be devoted to scaling down the design of hydrogel matrices. By reducing the dimensions, the time required for stimuli recognition and response can be significantly shortened, leading to more efficient and dynamic behavior in various applications. Moreover, the miniaturization of hydrogel-based systems offers the potential for enhanced portability and versatility in various fields. Miniaturized hydrogel devices can be more easily integrated into wearable electronics, implantable medical devices, and soft robotics, opening up new possibilities for responsive and adaptive systems. Simultaneously, the development of advanced techniques to fabricate complex designs of stimuli-responsive composite hydrogels at the micro- or nanometer scale is crucial. These techniques will enable the integration of different functional additives and materials with precise control, resulting in hydrogel systems with tailored and multifunctional properties.

Overall, stimuli-responsive hydrogels hold significant prospects for the development of dynamic, smart, and multifunctional materials, adaptive structures, and autonomous devices. With further advancements, stimuli-responsive hydrogels have the potential to revolutionize diverse fields and unlock new possibilities for responsive and adaptive systems.

Author contributions

All authors performed the literature search and prepared the initial draft. X. Li, M. Li and J. Bae revised the draft and wrote the final version. All authors read and approved the manuscript.

Conflicts of interest

There are no conflicts to declare.

Acknowledgements

This work was supported by the National Science Foundation (CBET-2224740) and the National Science Foundation through the UC San Diego Materials Research Science and Engineering Center (UCSD MRSEC), grant number DMR-2011924, with additional support from the ACS Petroleum Research Fund, grant number PRF# 62570-DNI5.

Notes and references

1 T. Graham, X. Liquid diffusion applied to analysis, *Philos. Trans. R. Soc. London*, 1861, **151**, 183–224.
2 S. C. Lee, I. K. Kwon and K. Park, Hydrogels for delivery of bioactive agents: a historical perspective, *Adv. Drug Delivery Rev.*, 2013, **65**, 17–20.
3 J. Jose, V. P. Athira, H. Michel, A. R. Hafeela, S. G. Bhat, S. Thomas and L. Pereira, Maria, Hydrogels: An overview of the history, classification, principles, applications, and kinetics, *Sustainable Hydrogels*, 2023, 1–22.
4 F. Ullah, M. B. Othman, F. Javed, Z. Ahmad and H. Md, Akil, Classification, processing and application of hydrogels: A review, *Mater. Sci. Eng., C*, 2015, **57**, 414–433.
5 M. M. Khansari, L. V. Sorokina, P. Mukherjee, F. Mukhtar, M. R. Shirdar, M. Shahidi and T. Shokuhfar, Classification of Hydrogels Based on Their Source: A Review and Application in Stem Cell Regulation, *JOM*, 2017, **69**, 1340–1347.
6 Z. J. Wang, C. Y. Li, X. Y. Zhao, Z. L. Wu and Q. Zheng, Thermo- and photo-responsive composite hydrogels with programmed deformations, *J. Mater. Chem. B*, 2019, **7**, 1674–1678.
7 M. Li and J. Bae, Tunable swelling and deswelling of temperature- and light-responsive graphene oxide-poly(N-isopropylacrylamide) composite hydrogels, *Polym. Chem.*, 2020, **11**, 2332–2338.
8 C. Yu, Z. Duan, P. Yuan, Y. Li, Y. Su, X. Zhang, Y. Pan, L. L. Dai, R. G. Nuzzo, Y. Huang, H. Jiang and J. A. Rogers, Electronically programmable, reversible shape change in two- and three-dimensional hydrogel structures, *Adv. Mater.*, 2013, **25**, 1541–1546.
9 N. N. Reddy, Y. M. Mohan, K. Varaprasad, S. Ravindra, P. A. Joy and K. M. Raju, Magnetic and electric responsive hydrogel-magnetic nanocomposites for drug-delivery application, *J. Appl. Polym. Sci.*, 2011, **122**, 1364–1375.
10 J. Odent, S. Vanderstappen, A. Toncheva, E. Pichon, T. J. Wallin, K. Wang, R. F. Shepherd, P. Dubois and J.-M. Raquez, Hierarchical chemomechanical encoding of multi-responsive hydrogel actuators via 3D printing, *J. Mater. Chem. A*, 2019, **7**, 15395–15403.
11 Z. Wang, X. Zheng, T. Ouchi, T. B. Kouznetsova, H. K. Beech, S. Av-Ron, T. Matsuda, B. H. Bowser, S. Wang, J. A. Johnson, J. A. Kalow, B. D. Olsen, J. Ping Gong, M. Rubinstein and S. L. Craig, Toughening hydrogels through force-triggeredchemical reactions that lengthen polymer strands, *Science*, 2021, **374**, 193–196.
12 C. Lv, X.-C. Sun, H. Xia, Y.-H. Yu, G. Wang, X.-W. Cao, S.-X. Li, Y.-S. Wang, Q.-D. Chen, Y.-D. Yu and H.-B. Sun, Humidity-responsive actuation of programmable hydrogel microstructures based on 3D printing, *Sens. Actuators, B*, 2018, **259**, 736–744.
13 M. Santhamoorthy, T. T. Vy Phan, V. Ramkumar, C. J. Raorane, K. Thirupathi and S. C. Kim, Thermo-Sensitive Poly(*N*-isopropylacrylamide-*co*-polyacrylamide) Hydrogel for pH-Responsive Therapeutic Delivery, *Polymers*, 2022, **14**, 4128.
14 C. Yu, H. Guo, K. Cui, X. Li, Y. N. Ye, T. Kurokawa and J. P. Gong, Hydrogels as dynamic memory with forgetting ability, *Proc. Natl. Acad. Sci. U. S. A.*, 2020, **117**, 18962–18968.
15 F. Wu, Y. Pang and J. Liu, Swelling-strengthening hydrogels by embedding with deformable nanobarriers, *Nat. Commun.*, 2020, **11**, 4502.
16 H. Ding, B. Li, Z. Liu, G. Liu, S. Pu, Y. Feng, D. Jia and Y. Zhou, Decoupled pH- and Thermo-Responsive Injectable Chitosan/PNIPAM Hydrogel via Thiol-Ene Click Chemistry for Potential Applications in Tissue Engineering, *Adv. Healthcare Mater.*, 2020, **9**, e2000454.
17 Z. Wang, L. Guo, H. Xiao, H. Cong and S. Wang, A reversible underwater glue based on photo- and thermo-responsive dynamic covalent bonds, *Mater. Horiz.*, 2020, **7**, 282–288.
18 H. H. Tonnesen and J. Karlsen, Alginate in drug delivery systems, *Drug Dev. Ind. Pharm.*, 2002, **28**, 621–630.
19 J. Li, Q. Ding, H. Wang, Z. Wu, X. Gui, C. Li, N. Hu, K. Tao and J. Wu, Engineering Smart Composite Hydrogels for Wearable Disease Monitoring, *Nano-Micro Lett.*, 2023, **15**, 105.
20 E. M. Bressler, S. Adams, R. Liu, Y. L. Colson, W. W. Wong and M. W. Grinstaff, Boolean logic in synthetic biology and biomaterials: Towards living materials in mammalian cell therapeutics, *Clin. Transl. Med.*, 2023, **13**, e1244.
21 M. M. El Sayed, Production of Polymer Hydrogel Composites and Their Applications, *J. Polym. Environ.*, 2023, **31**, 2855–2879.
22 G. Cui, X. Guo, P. Su, T. Zhang, J. Guan and C. Wang, Mussel-inspired nanoparticle composite hydrogels for hemostasis and wound healing, *Front. Chem.*, 2023, **11**, 1154788.
23 M. Sun, H. Li, Y. Hou, N. Huang, X. Xia, H. Zhu, Q. Xu, Y. Lin and L. Xu, Multifunctional tendon-mimetic hydrogels, *Sci. Adv.*, 2023, **9**, eade6973.
24 G. Tozzi, A. De Mori, A. Oliveira and M. Roldo, Composite Hydrogels for Bone Regeneration, *Materials*, 2016, **9**, 267.
25 W. Zulaikha, M. Zaki Hassan and S. A. Abdul Aziz, Nanoparticle-embedded hydrogels as a functional polymeric

composite for biomedical applications, *Mater. Today: Proc.*, 2023, DOI: 10.1016/j.matpr.2023.05.668.
26 Z. Li, Y. Li, C. Chen and Y. Cheng, Magnetic-responsive hydrogels: From strategic design to biomedical applications, *J. Controlled Release*, 2021, **335**, 541–556.
27 Y. Chen, J. Yang, X. Zhang, Y. Feng, H. Zeng, L. Wang and W. Feng, Light-driven bimorph soft actuators: design, fabrication, and properties, *Mater. Horiz.*, 2021, **8**, 728–757.
28 P. He, J. Wu, X. Pan, L. Chen, K. Liu, H. Gao, H. Wu, S. Cao, L. Huang and Y. Ni, Anti-freezing and moisturizing conductive hydrogels for strain sensing and moist-electric generation applications, *J. Mater. Chem. A*, 2020, **8**, 3109–3118.
29 L. Zhang, S. R. Jean, S. Ahmed, P. M. Aldridge, X. Li, F. Fan, E. H. Sargent and S. O. Kelley, Multifunctional quantum dot DNA hydrogels, *Nat. Commun.*, 2017, **8**, 381.
30 P. Zhang, I. M. Lei, G. Chen, J. Lin, X. Chen, J. Zhang, C. Cai, X. Liang and J. Liu, Integrated 3D printing of flexible electroluminescent devices and soft robots, *Nat. Commun.*, 2022, **13**, 4775.
31 C. Li, Q. He, Y. Wang, Z. Wang, Z. Wang, R. Annapooranan, M. I. Latz and S. Cai, Highly robust and soft biohybrid mechanoluminescence for optical signaling and illumination, *Nat. Commun.*, 2022, **13**, 3914.
32 X. Li, Q. Sun, Q. Li, N. Kawazoe and G. Chen, Functional Hydrogels With Tunable Structures and Properties for Tissue Engineering Applications, *Front. Chem.*, 2018, **6**, 499.
33 K. J. De France, F. Xu and T. Hoare, Structured Macroporous Hydrogels: Progress, Challenges, and Opportunities, *Adv. Healthcare Mater.*, 2018, **7**, 1700927.
34 O. Erol, A. Pantula, W. Liu and D. H. Gracias, Transformer Hydrogels: A Review, *Adv. Mater. Technol.*, 2019, **4**, 1900043.
35 X. Yao, H. Chen, H. Qin and H. P. Cong, Nanocomposite Hydrogel Actuators with Ordered Structures: From Nanoscale Control to Macroscale Deformations, *Small Methods*, 2023, e2300414.
36 S. Huang, X. Hong, M. Zhao, N. Liu, H. Liu, J. Zhao, L. Shao, W. Xue, H. Zhang, P. Zhu and R. Guo, Nanocomposite hydrogels for biomedical applications, *Bioeng. Transl. Med.*, 2022, **7**, e10315.
37 H. Kim, S.-k Ahn, D. M. Mackie, J. Kwon, S. H. Kim, C. Choi, Y. H. Moon, H. B. Lee and S. H. Ko, Shape morphing smart 3D actuator materials for micro soft robot, *Mater. Today*, 2020, **41**, 243–269.
38 W. Wang, L. Yao, C. Cheng, T. Zhang, H. Atsumi, L. Wang, G. Wang, O. Anilionyte, H. Steiner, J. Ou, K. Zhou, C. Wawrousek, K. Petrecca, A. M. Belcher, R. Karnik, X. Zhao, D. I. C. Wang and H. Ishii, Harnessing the hygroscopic and biofluorescent behaviors of genetically tractable microbial cells to design biohybrid wearables, *Sci. Adv.*, 2017, **3**, e1601984.
39 L. K. Rivera-Tarazona, Z. T. Campbell and T. H. Ware, Stimuli-responsive engineered living materials, *Soft Matter*, 2021, **17**, 785–809.
40 D. Buenger, F. Topuz and J. Groll, Hydrogels in sensing applications, *Prog. Polym. Sci.*, 2012, **37**, 1678–1719.
41 H. Wang and S. Cai, Drying-induced cavitation in a constrained hydrogel, *Soft Matter*, 2015, **11**, 1058–1061.
42 J.-F. Louf, N. B. Lu, M. G. O'Connell, H. Jeremy Cho and S. S. Datta, Under pressure: Hydrogel swelling in a granular medium, *Sci. Adv.*, 2021, **7**, eabd2711.
43 J. Liu, Y. Gao, Y.-J. Lee and S. Yang, Responsive and Foldable Soft Materials, *Trends Chem.*, 2020, **2**, 107–122.
44 M. D. Hager, S. Bode, C. Weber and U. S. Schubert, Shape memory polymers: Past, present and future developments, *Prog. Polym. Sci.*, 2015, **49–50**, 3–33.
45 Z. Guan, L. Wang and J. Bae, Advances in 4D printing of liquid crystalline elastomers: materials, techniques, and applications, *Mater. Horiz.*, 2022, **9**, 1825–1849.
46 L. Tang, L. Wang, X. Yang, Y. Feng, Y. Li and W. Feng, Poly(N-isopropylacrylamide)-based smart hydrogels: Design, properties and applications, *Prog. Mater. Sci.*, 2021, **115**, 100702.
47 X. Yang, C. Valenzuela, X. Zhang, Y. Chen, Y. Yang, L. Wang and W. Feng, *Matter*, 2023, **6**, 1278–1294.
48 Y. Chen, C. Valenzuela, X. Zhang, X. Yang, L. Wang and W. Feng, *Nat. Commun.*, 2023, **14**, 3036.
49 J. Ma, Y. Yang, C. Valenzuela, X. Zhang, L. Wang and W. Feng, *Angew. Chem., Int. Ed.*, 2022, **61**, e202116219.
50 K. Malachowski, J. Breger, H. R. Kwag, M. O. Wang, J. P. Fisher, F. M. Selaru and D. H. Gracias, Stimuli-responsive theragrippers for chemomechanical controlled release, *Angew. Chem., Int. Ed.*, 2014, **53**, 8045–8049.
51 E. Wang, M. S. Desai and S. W. Lee, Light-controlled graphene-elastin composite hydrogel actuators, *Nano Lett.*, 2013, **13**, 2826–2830.
52 M. Sun, C. Tian, L. Mao, X. Meng, X. Shen, B. Hao, X. Wang, H. Xie and L. Zhang, Reconfigurable Magnetic Slime Robot: Deformation, Adaptability, and Multifunction, *Adv. Funct. Mater.*, 2022, **32**, 2112508.
53 A. Kumar, R. Rajamanickam, J. Hazra, N. R. Mahapatra and P. Ghosh, Engineering the Nonmorphing Point of Actuation for Controlled Drug Release by Hydrogel Bilayer across the pH Spectrum, *ACS Appl. Mater. Interfaces*, 2022, **14**, 56321–56330.
54 G. Li, T. Gao, G. Fan, Z. Liu, Z. Liu, J. Jiang and Y. Zhao, Photoresponsive Shape Memory Hydrogels for Complex Deformation and Solvent-Driven Actuation, *ACS Appl. Mater. Interfaces*, 2020, **12**, 6407–6418.
55 J. Wei, R. Li, L. Li, W. Wang and T. Chen, Touch-Responsive Hydrogel for Biomimetic Flytrap-Like Soft Actuator, *Nano-Micro Lett.*, 2022, **14**, 182.
56 A. S. Gladman, E. A. Matsumoto, R. G. Nuzzo, L. Mahadevan and J. A. Lewis, Biomimetic 4D printing, *Nat. Mater.*, 2016, **15**, 413–418.
57 C. N. Zhu, T. Bai, H. Wang, J. Ling, F. Huang, W. Hong, Q. Zheng and Z. L. Wu, Dual-Encryption in a Shape-Memory Hydrogel with Tunable Fluorescence and Reconfigurable Architecture, *Adv. Mater.*, 2021, **33**, 2102023.
58 X. P. Hao, C. Y. Li, C. W. Zhang, M. Du, Z. Ying, Q. Zheng and Z. L. Wu, Self-Shaping Soft Electronics Based on Patterned Hydrogel with Stencil-Printed Liquid Metal, *Adv. Funct. Mater.*, 2021, **31**, 2105481.

59 C. Xin, D. Jin, Y. Hu, L. Yang, R. Li, L. Wang, Z. Ren, D. Wang, S. Ji, K. Hu, D. Pan, H. Wu, W. Zhu, Z. Shen, Y. Wang, J. Li, L. Zhang, D. Wu and J. Chu, Environmentally Adaptive Shape-Morphing Microrobots for Localized Cancer Cell Treatment, *ACS Nano*, 2021, **15**, 18048–18059.
60 J. Cui, J. Chen, Z. Ni, W. Dong, M. Chen and D. Shi, High-Sensitivity Flexible Sensor Based on Biomimetic Strain-Stiffening Hydrogel, *ACS Appl. Mater. Interfaces*, 2022, **14**, 47148–47156.
61 J. Zhao, Y. Ma, N. F. Steinmetz and J. Bae, Toward Plant Cyborgs: Hydrogels Incorporated onto Plant Tissues Enable Programmable Shape Control, *ACS Macro Lett.*, 2022, **11**, 961–966.
62 R. Hsissou, R. Seghiri, Z. Benzekri, M. Hilali, M. Rafik and A. Elharfi, Polymer composite materials: A comprehensive review, *Compos. Struct.*, 2021, **262**, 113640.
63 P. Thoniyot, M. J. Tan, A. A. Karim, D. J. Young and X. J. Loh, Nanoparticle-Hydrogel Composites: Concept, Design, and Applications of These Promising, Multi-Functional Materials, *Adv. Sci*, 2015, **2**, 1400010.
64 E. Howard, M. Li, M. Kozma, J. Zhao and J. Bae, Self-strengthening stimuli-responsive nanocomposite hydrogels, *Nanoscale*, 2022, **14**, 17887–17894.
65 M. Chau, K. J. De France, B. Kopera, V. R. Machado, S. Rosenfeldt, L. Reyes, K. J. W. Chan, S. Förster, E. D. Cranston, T. Hoare and E. Kumacheva, Composite Hydrogels with Tunable Anisotropic Morphologies and Mechanical Properties, *Chem. Mater.*, 2016, **28**, 3406–3415.
66 S. Gantenbein, E. Colucci, J. Kach, E. Trachsel, F. B. Coulter, P. A. Ruhs, K. Masania and A. R. Studart, Three-dimensional printing of mycelium hydrogels into living complex materials, *Nat. Mater.*, 2023, **22**, 128–134.
67 S. Utech and A. R. Boccaccini, A review of hydrogel-based composites for biomedical applications: enhancement of hydrogel properties by addition of rigid inorganic fillers, *J. Mater. Sci.*, 2015, **51**, 271–310.
68 F. Urushizaki, H. Yamaguchi, K. Nakamura, S. Numajiri, K. Sugibayashi and Y. Morimoto, Swelling and mechanical properties of poly(vinyl alcohol) hydrogels, *Int. J. Pharm.*, 1990, **58**, 135–142.
69 S. J. Jeon, A. W. Hauser and R. C. Hayward, Shape-Morphing Materials from Stimuli-Responsive Hydrogel Hybrids, *Acc. Chem. Res.*, 2017, **50**, 161–169.
70 M. C. Catoira, L. Fusaro, D. Di Francesco, M. Ramella and F. Boccafoschi, Overview of natural hydrogels for regenerative medicine applications, *J. Mater. Sci.: Mater. Med.*, 2019, **30**, 115.
71 D. A. Gyles, L. D. Castro, J. O. C. Silva and R. M. Ribeiro-Costa, A review of the designs and prominent biomedical advances of natural and synthetic hydrogel formulations, *Eur. Polym. J.*, 2017, **88**, 373–392.
72 C. Liu, Z. Zhang, X. Liu, X. Ni and J. Li, Gelatin-based hydrogels with β-cyclodextrin as a dual functional component for enhanced drug loading and controlled release, *RSC Adv.*, 2013, **3**, 25041–25049.
73 K. Y. Lee and D. J. Mooney, Alginate: properties and biomedical applications, *Prog. Polym. Sci.*, 2012, **37**, 106–126.
74 A. Hurtado, A. A. A. Aljabali, V. Mishra, M. M. Tambuwala and A. Serrano-Aroca, Alginate: Enhancement Strategies for Advanced Applications, *Int. J. Mol. Sci.*, 2022, **23**, 4486.
75 C. Hu, W. Lu, A. Mata, K. Nishinari and Y. Fang, Ions-induced gelation of alginate: Mechanisms and applications, *Int. J. Biol. Macromol.*, 2021, **177**, 578–588.
76 Y. Zhao, W. Shen, Z. Chen and T. Wu, Freeze-thaw induced gelation of alginates, *Carbohydr. Polym.*, 2016, **148**, 45–51.
77 V. A. Petrova, V. Y. Elokhovskiy, S. V. Raik, D. N. Poshina, D. P. Romanov and Y. A. Skorik, Alginate Gel Reinforcement with Chitin Nanowhiskers Modulates Rheological Properties and Drug Release Profile, *Biomolecules*, 2019, **9**, 291.
78 G. T. Grant, E. R. Morris, D. A. Rees, P. J. C. Smith and D. Thom, Biological interactions between polysacchartdes and divalent cations: the egg-box model, *FEBS Lett.*, 1973, **32**, 195–198.
79 P. Eiselt, K. Y. Lee and D. J. Mooney, Rigidity of Two-Component Hydrogels Prepared from Alginate and Poly(ethylene glycol)−Diamines, *Macromolecules*, 1999, **32**, 5561–5566.
80 D. Ji, J. M. Park, M. S. Oh, T. L. Nguyen, H. Shin, J. S. Kim, D. Kim, H. S. Park and J. Kim, Superstrong, superstiff, and conductive alginate hydrogels, *Nat. Commun.*, 2022, **13**, 3019.
81 J. Y. Sun, X. Zhao, W. R. Illeperuma, O. Chaudhuri, K. H. Oh, D. J. Mooney, J. J. Vlassak and Z. Suo, Highly stretchable and tough hydrogels, *Nature*, 2012, **489**, 133–136.
82 N. Kaushal and M. Singh, Fabrication and characterization of a bilayered system enabling sustained release of bioflavonoids derived from mandarin biomass, *Food Hydrocolloids Health*, 2023, **3**, 100114.
83 O. Smidsrød, Solution properties of alginate, *Carbohydr. Res.*, 1970, **13**, 359–372.
84 X. Liu, M. E. Inda, Y. Lai, T. K. Lu and X. Zhao, Engineered Living Hydrogels, *Adv. Mater.*, 2022, **34**, e2201326.
85 S. Xie, Y. Chen, Z. Guo, Y. Luo, H. Tan, L. Xu, J. Xu and J. Zheng, Agar/carbon dot crosslinked polyacrylamide double-network hydrogels with robustness, self-healing, and stimulus-response fluorescence for smart anti-counterfeiting, *Mater. Chem. Front.*, 2021, **5**, 5418–5428.
86 Y. Chen, Y. Liu, Q. Dong, C. Xu, S. Deng, Y. Kang, M. Fan and L. Li, Application of functionalized chitosan in food: A review, *Int. J. Biol. Macromol.*, 2023, **235**, 123716.
87 S. Liu, D. Li, Y. Wang, G. Zhou, K. Ge and L. Jiang, Adhesive, antibacterial and double crosslinked carboxylated polyvinyl alcohol/chitosan hydrogel to enhance dynamic skin wound healing, *Int. J. Biol. Macromol.*, 2023, **228**, 744–753.
88 G. Huang, Z. Tang, S. Peng, P. Zhang, T. Sun, W. Wei, L. Zeng, H. Guo, H. Guo and G. Meng, Modification of Hydrophobic Hydrogels into a Strongly Adhesive and Tough Hydrogel by Electrostatic Interaction, *Macromolecules*, 2021, **55**, 156–165.
89 K. Chen, Z. Wu, Y. Liu, Y. Yuan and C. Liu, Injectable Double-Crosslinked Adhesive Hydrogels with High Mechanical Resilience and Effective Energy Dissipation for Joint Wound Treatment, *Adv. Funct. Mater.*, 2021, **32**, 2109687.

90 V. K. Mourya and N. N. Inamdar, Chitosan-modifications and applications: Opportunities galore, *React. Funct. Polym.*, 2008, **68**, 1013–1051.
91 R. Andreazza, A. Morales, S. Pieniz and J. Labidi, Gelatin-Based Hydrogels: Potential Biomaterials for Remediation, *Polymers*, 2023, **15**, 1026.
92 S. Thakur, P. P. Govender, M. A. Mamo, S. Tamulevicius and V. K. Thakur, Recent progress in gelatin hydrogel nanocomposites for water purification and beyond, *Vacuum*, 2017, **146**, 396–408.
93 C. Liu, H. J. Zhang, X. You, K. Cui and X. Wang, Electrically Conductive Tough Gelatin Hydrogel, *Adv. Electron. Mater.*, 2020, **6**, 2000040.
94 N. S. Said and N. M. Sarbon, Physical and Mechanical Characteristics of Gelatin-Based Films as a Potential Food Packaging Material: A Review, *Membranes*, 2022, **12**, 442.
95 J. Chen, J. Huang and Y. Hu, 3D Printing of Biocompatible Shape-Memory Double Network Hydrogels, *ACS Appl. Mater. Interfaces*, 2021, **13**, 12726–12734.
96 X. Zhao, Q. Lang, L. Yildirimer, Z. Y. Lin, W. Cui, N. Annabi, K. W. Ng, M. R. Dokmeci, A. M. Ghaemmaghami and A. Khademhosseini, Photocrosslinkable Gelatin Hydrogel for Epidermal Tissue Engineering, *Adv. Healthcare Mater.*, 2016, **5**, 108–118.
97 E. Karadağ and S. Kundakcı, Application of highly swollen novel biosorbent hydrogels in uptake of uranyl ions from aqueous solutions, *Fibers Polym.*, 2015, **16**, 2165–2176.
98 U. S. K. Madduma-Bandarage and S. V. Madihally, Synthetic hydrogels: Synthesis, novel trends, and applications, *J. Appl. Polym. Sci.*, 2020, **138**, 50376.
99 M. F. Akhtar, M. Hanif and N. M. Ranjha, Methods of synthesis of hydrogels … A review, *Saudi. Pharm. J.*, 2016, **24**, 554–559.
100 M. Wang, J. Bai, K. Shao, W. Tang, X. Zhao, D. Lin, S. Huang, C. Chen, Z. Ding, J. Ye and C. Vasile, Poly(vinyl alcohol) Hydrogels: The Old and New Functional Materials, *Int. J. Polym. Sci.*, 2021, **2021**, 1–16.
101 M. Zhang, Y. Yang, M. Li, Q. Shang, R. Xie, J. Yu, K. Shen, Y. Zhang and Y. Cheng, Toughening Double-Network Hydrogels by Polyelectrolytes, *Adv. Mater.*, 2023, e2301551.
102 L. Xu, S. Gao, Q. Guo, C. Wang, Y. Qiao and D. Qiu, A Solvent-Exchange Strategy to Regulate Noncovalent Interactions for Strong and Antiswelling Hydrogels, *Adv. Mater.*, 2020, **32**, e2004579.
103 Y. Chen, J. Li, J. Lu, M. Ding and Y. Chen, Synthesis and properties of Poly(vinyl alcohol) hydrogels with high strength and toughness, *Polym. Test.*, 2022, **108**, 107516.
104 H. Adelnia, R. Ensandoost, S. Shebbrin Moonshi, J. N. Gavgani, E. I. Vasafi and H. T. Ta, Freeze/thawed polyvinyl alcohol hydrogels: Present, past and future, *Eur. Polym. J.*, 2022, **164**, 110974.
105 Y. Yan, S. Duan, B. Liu, S. Wu, Y. Alsaid, B. Yao, S. Nandi, Y. Du, T. W. Wang, Y. Li and X. He, Tough Hydrogel Electrolytes for Anti-Freezing Zinc-Ion Batteries, *Adv. Mater.*, 2023, **35**, e2211673.
106 L. Xu, Y. Qiao and D. Qiu, Coordinatively Stiffen and Toughen Hydrogels with Adaptable Crystal-Domain Cross-Linking, *Adv. Mater.*, 2023, **35**, e2209913.
107 W. Ma, P. Zhang, B. Zhao, S. Wang, J. Zhong, Z. Cao, C. Liu, F. Gong and H. Matsuyama, Swelling Resistance and Mechanical Performance of Physical Crosslink-Based Poly(Vinyl Alcohol) Hydrogel Film with Various Molecular Weight, *J. Polym. Sci., Part B: Polym. Phys.*, 2019, **57**, 1673–1683.
108 N. Wen, B. Jiang, X. Wang, Z. Shang, D. Jiang, L. Zhang, C. Sun, Z. Wu, H. Yan, C. Liu and Z. Guo, Overview of Polyvinyl Alcohol Nanocomposite Hydrogels for Electro-Skin, Actuator, Supercapacitor and Fuel Cell, *Chem. Rec.*, 2020, **20**, 773–792.
109 Y. Zhan, W. Fu, Y. Xing, X. Ma and C. Chen, Advances in versatile anti-swelling polymer hydrogels, *Mater. Sci. Eng., C*, 2021, **127**, 112208.
110 W. Zhang, H. Wang, H. Wang, J. Y. E. Chan, H. Liu, B. Zhang, Y.-F. Zhang, K. Agarwal, X. Yang, A. S. Ranganath, H. Y. Low, Q. Ge and J. K. W. Yang, Structural multi-colour invisible inks with submicron 4D printing of shape memory polymers, *Nat. Commun.*, 2021, **12**, 112.
111 G. Sennakesavan, M. Mostakhdemin, L. K. Dkhar, A. Seyfoddin and S. J. Fatihhi, Acrylic acid/acrylamide based hydrogels and its properties - A review, *Polym. Degrad. Stab.*, 2020, **180**, 109308.
112 S. K. Patra and S. K. Swain, Swelling study of superabsorbent PAA-*co*-PAM/clay nanohydrogel, *J. Appl. Polym. Sci.*, 2011, **120**, 1533–1538.
113 N. Tang, Z. Peng, R. Guo, M. An, X. Chen, X. Li, N. Yang and J. Zang, Thermal Transport in Soft PAAm Hydrogels, *Polymers*, 2017, **9**, 688.
114 J. Kim, G. Zhang, M. Shi and Z. Suo, Fracture, fatigue, and friction of polymers in which entanglements greatly outnumber cross-links, *Science*, 2021, **374**, 212–216.
115 J. Rosiak and K. Burozak, and W. Pekala, Polyacrylamide hydrogels as sustained release drug delivery dressing materials, *Radiat. Phys. Chem.*, 1983, **22**, 907–915.
116 K. Elkhoury, C. S. Russell, L. Sanchez-Gonzalez, A. Mostafavi, T. J. Williams, C. Kahn, N. A. Peppas, E. Arab-Tehrany and A. Tamayol, Soft-Nanoparticle Functionalization of Natural Hydrogels for Tissue Engineering Applications, *Adv. Healthcare Mater.*, 2019, **8**, e1900506.
117 A. Saha, S. Sekharan and U. Manna, Superabsorbent hydrogel (SAH) as a soil amendment for drought management: A review, *Soil Tillage Res.*, 2020, **204**, 104736.
118 C. C. Lin and K. S. Anseth, PEG hydrogels for the controlled release of biomolecules in regenerative medicine, *Pharm. Res.*, 2009, **26**, 631–643.
119 Z. Wang, Q. Ye, S. Yu and B. Akhavan, Poly Ethylene Glycol (PEG)-Based Hydrogels for Drug Delivery in Cancer Therapy: A Comprehensive Review, *Adv. Healthcare Mater.*, 2023, **12**, e2300105.
120 L. H. Chen, N. W. Liang, W. Y. Huang, Y. C. Liu, C. Y. Ho, C. H. Kuan, Y. F. Huang and T. W. Wang, Supramolecular hydrogel for programmable delivery of therapeutics to

cancer multidrug resistance, *Biomater. Adv.*, 2023, **146**, 213282.

121 A. P. Dhand, J. H. Galarraga and J. A. Burdick, Enhancing Biopolymer Hydrogel Functionality through Interpenetrating Networks, *Trends Biotechnol.*, 2021, **39**, 519–538.

122 J. P. Gong, Y. Katsuyama, T. Kurokawa and Y. Osada, Double-Network Hydrogels with Extremely High Mechanical Strength, *Adv. Mater.*, 2003, **15**, 1155–1158.

123 M. A. Mohamed, A. Fallahi, A. M. A. El-Sokkary, S. Salehi, M. A. Akl, A. Jafari, A. Tamayol, H. Fenniri, A. Khademhosseini, S. T. Andreadis and C. Cheng, Stimuli-responsive hydrogels for manipulation of cell microenvironment: From chemistry to biofabrication technology, *Prog. Polym. Sci.*, 2019, **98**, 101147.

124 J. Li, Q. Ma, Y. Xu, M. Yang, Q. Wu, F. Wang and P. Sun, Highly Bidirectional Bendable Actuator Engineered by LCST-UCST Bilayer Hydrogel with Enhanced Interface, *ACS Appl. Mater. Interfaces*, 2020, **12**, 55290–55298.

125 S. Hu, Y. Fang, C. Liang, M. Turunen, O. Ikkala and H. Zhang, Thermally trainable dual network hydrogels, *Nat. Commun.*, 2023, **14**, 3717.

126 Y. Alsaid, S. Wu, D. Wu, Y. Du, L. Shi, R. Khodambashi, R. Rico, M. Hua, Y. Yan, Y. Zhao, D. Aukes and X. He, Tunable Sponge-Like Hierarchically Porous Hydrogels with Simultaneously Enhanced Diffusivity and Mechanical Properties, *Adv. Mater.*, 2021, **33**, e2008235.

127 A. Halperin, M. Kroger and F. M. Winnik, Poly(N-isopropylacrylamide) Phase Diagrams: Fifty Years of Research, *Angew. Chem., Int. Ed.*, 2015, **54**, 15342–15367.

128 I. Juurinen, S. Galambosi, A. G. Anghelescu-Hakala, J. Koskelo, V. Honkimaki, K. Hamalainen, S. Huotari and M. Hakala, Molecular-level changes of aqueous poly(N-isopropylacrylamide) in phase transition, *J. Phys. Chem. B*, 2014, **118**, 5518–5523.

129 Y. Shi, C. Ma, L. Peng and G. Yu, Conductive ''Smart'' Hybrid Hydrogels with PNIPAM and Nanostructured Conductive Polymers, *Adv. Funct. Mater.*, 2015, **25**, 1219–1225.

130 L. Hua, M. Xie, Y. Jian, B. Wu, C. Chen and C. Zhao, Multiple-Responsive and Amphibious Hydrogel Actuator Based on Asymmetric UCST-Type Volume Phase Transition, *ACS Appl. Mater. Interfaces*, 2019, **11**, 43641–43648.

131 C. Zhao, Z. Ma and X. X. Zhu, Rational design of thermoresponsive polymers in aqueous solutions: A thermodynamics map, *Prog. Polym. Sci.*, 2019, **90**, 269–291.

132 D. Lou, Y. Sun, J. Li, Y. Zheng, Z. Zhou, J. Yang, C. Pan, Z. Zheng, X. Chen and W. Liu, Double Lock Label Based on Thermosensitive Polymer Hydrogels for Information Camouflage and Multi-level Encryption, *Angew. Chem., Int. Ed.*, 2022, **61**, e202117066.

133 X. Lin, H. Zhang, Y. Qin and X. Hu, Design and Fabrication of Photo-Responsive Hydrogel for the Application of Functional Contact Lens, *Front. Mater.*, 2021, **8**, 680359.

134 H. Shang, X. Le, Y. Sun, F. Shan, S. Wu, Y. Zheng, D. Li, D. Guo, Q. Liu and T. Chen, Integrating Photorewritable Fluorescent Information in Shape-Memory Organohydrogel Toward Dual Encryption, *Adv. Opt. Mater.*, 2022, **10**, 2200608.

135 J. Liu, C. Xie, A. Kretzschmann, K. Koynov, H. J. Butt and S. Wu, Metallopolymer Organohydrogels with Photo-Controlled Coordination Crosslinks Work Properly Below 0 degrees C, *Adv. Mater.*, 2020, **32**, 1908324.

136 H. Zhou, C. Xue, P. Weis, Y. Suzuki, S. Huang, K. Koynov, G. K. Auernhammer, R. Berger, H. J. Butt and S. Wu, Photoswitching of glass transition temperatures of azobenzene-containing polymers induces reversible solid-to-liquid transitions, *Nat. Chem.*, 2017, **9**, 145–151.

137 Y. Guan, H.-B. Zhao, L.-X. Yu, S.-C. Chen and Y.-Z. Wang, Multi-stimuli sensitive supramolecular hydrogel formed by host–guest interaction between PNIPAM-Azo and cyclodextrin dimers, *RSC Adv.*, 2014, **4**, 4955–4959.

138 S. Tamesue, Y. Takashima, H. Yamaguchi, S. Shinkai and A. Harada, Photoswitchable supramolecular hydrogels formed by cyclodextrins and azobenzene polymers, *Angew. Chem., Int. Ed.*, 2010, **49**, 7461–7464.

139 G. Kocak, C. Tuncer and V. Bütün, pH-Responsive polymers, *Polym. Chem.*, 2017, **8**, 144–176.

140 G. Li, G. Zhang, R. Sun and C.-P. Wong, Dually pH-responsive polyelectrolyte complex hydrogel composed of polyacrylic acid and poly(2-(dimthylamino) ethyl methacrylate), *Polymer*, 2016, **107**, 332–340.

141 R. Kempaiah and Z. Nie, From nature to synthetic systems: shape transformation in soft materials, *J. Mater. Chem. B*, 2014, **2**, 2357–2368.

142 T. Matsuda, R. Kawakami, R. Namba, T. Nakajima and J. P. Gong, Mechanoresponsive self-growing hydrogels inspired by muscle training, *Science*, 2019, **363**, 504–508.

143 Q. Mu, K. Cui, Z. J. Wang, T. Matsuda, W. Cui, H. Kato, S. Namiki, T. Yamazaki, M. Frauenlob, T. Nonoyama, M. Tsuda, S. Tanaka, T. Nakajima and J. P. Gong, Force-triggered rapid microstructure growth on hydrogel surface for on-demand functions, *Nat. Commun.*, 2022, **13**, 6213.

144 J. Zhang, X. Jiang, X. Wen, Q. Xu, H. Zeng, Y. Zhao, M. Liu, Z. Wang, X. Hu and Y. Wang, Bio-responsive smart polymers and biomedical applications, *JPhys Mater.*, 2019, **2**, 032004.

145 M. F. Maitz, U. Freudenberg, M. V. Tsurkan, M. Fischer, T. Beyrich and C. Werner, Bio-responsive polymer hydrogels homeostatically regulate blood coagulation, *Nat. Commun.*, 2013, **4**, 2168.

146 K. Ariga, K. Minami and L. K. Shrestha, Nanoarchitectonics for carbon-material-based sensors, *Analyst*, 2016, **141**, 2629–2638.

147 W. Sheehan, Periodic table of elements with emphasis, *Chemistry*, 1976, **49**, 17–18.

148 K. P. Gopinath, D.-V. N. Vo, D. Gnana Prakash, A. Adithya Joseph, S. Viswanathan and J. Arun, Environmental applications of carbon-based materials: a review, *Environ. Chem. Lett.*, 2021, **19**, 557–582.

149 Y. Yang and Y. Shen, Light-Driven Carbon-Based Soft Materials: Principle, Robotization, and Application, *Adv. Opt. Mater.*, 2021, **9**, 2100035.

150 B. Han, Y. L. Zhang, Q. D. Chen and H. B. Sun, Carbon-based photothermal actuators, *Adv. Funct. Mater.*, 2018, **28**, 1802235.

151 Y. Jin, Y. Shen, J. Yin, J. Qian and Y. Huang, Nanoclay-Based Self-Supporting Responsive Nanocomposite Hydrogels for Printing Applications, *ACS Appl. Mater. Interfaces*, 2018, **10**, 10461–10470.

152 L. Zhang, X. Zhang, L. Li, Y. Liu, D. Wang, L. Xu, J. Bao and A. Zhang, Fabrication of Photothermally Responsive Nanocomposite Hydrogel through 3D Printing, *Macromol. Mater. Eng.*, 2019, **305**, 1900718.

153 M. Li and J. Bae, Programmable Dual-Responsive Actuation of Single-Hydrogel-Based Bilayer Actuators by Photothermal and Skin Layer Effects with Graphene Oxides, *Adv. Mater. Interfaces*, 2023, 2300169.

154 X. Zhang, C. L. Pint, M. H. Lee, B. E. Schubert, A. Jamshidi, K. Takei, H. Ko, A. Gillies, R. Bardhan, J. J. Urban, M. Wu, R. Fearing and A. Javey, Optically- and thermally-responsive programmable materials based on carbon nanotube-hydrogel polymer composites, *Nano Lett.*, 2011, **11**, 3239–3244.

155 H. Li, Y. Liang, G. Gao, S. Wei, Y. Jian, X. Le, W. Lu, Q. Liu, J. Zhang and T. Chen, Asymmetric bilayer CNTs-elastomer/hydrogel composite as soft actuators with sensing performance, *Chem. Eng. J.*, 2021, **415**, 128988.

156 C. Ma, X. Le, X. Tang, J. He, P. Xiao, J. Zheng, H. Xiao, W. Lu, J. Zhang, Y. Huang and T. Chen, A Multiresponsive Anisotropic Hydrogel with Macroscopic 3D Complex Deformations, *Adv. Funct. Mater.*, 2016, **26**, 8670–8676.

157 J.-C. Kuo, H.-W. Huang, S.-W. Tung and Y.-J. Yang, A hydrogel-based intravascular microgripper manipulated using magnetic fields, *Sens. Actuators, A*, 2014, **211**, 121–130.

158 H. Shang, X. Le, M. Si, S. Wu, Y. Peng, F. Shan, S. Wu and T. Chen, Biomimetic organohydrogel actuator with high response speed and synergistic fluorescent variation, *Chem. Eng. J.*, 2022, **429**, 132290.

159 Q. Zhao, Y. Liang, L. Ren, Z. Yu, Z. Zhang and L. Ren, Bionic intelligent hydrogel actuators with multimodal deformation and locomotion, *Nano Energy*, 2018, **51**, 621–631.

160 X. Peng, C. Jiao, Y. Zhao, N. Chen, Y. Wu, T. Liu and H. Wang, Thermoresponsive Deformable Actuators Prepared by Local Electrochemical Reduction of Poly(N-isopropylacrylamide)/Graphene Oxide Hydrogels, *ACS Appl. Nano Mater.*, 2018, **1**, 1522–1530.

161 Y. Yang, Y. Tan, X. Wang, W. An, S. Xu, W. Liao and Y. Wang, Photothermal Nanocomposite Hydrogel Actuator with Electric-Field-Induced Gradient and Oriented Structure, *ACS Appl. Mater. Interfaces*, 2018, **10**, 7688–7692.

162 L. Guo, Y.-W. Hao, P. Yang, P.-L. Li, N. Sun, X.-W. Feng, J. Zhao, C.-A. Chen and J.-F. Song, Fast fabrication of graphene oxide/reduced graphene oxide hybrid hydrogels for thermosensitive smart actuator utilizing laser irradiation, *Mater. Lett.*, 2019, **237**, 245–248.

163 X. Peng, T. Liu, C. Jiao, Y. Wu, N. Chen and H. Wang, Complex shape deformations of homogeneous poly-(N-isopropylacrylamide)/graphene oxide hydrogels programmed by local NIR irradiation, *J. Mater. Chem. B*, 2017, **5**, 7997–8003.

164 Q. Wang, L. Zhu, D. Wei, H. Sun, C. Tang, Z. Liu, K. Li, J. Yang, G. Qin and G. Sun, Near-infrared responsive shape memory hydrogels with programmable and complex shape-morphing, *Sci. China: Technol. Sci.*, 2021, **64**, 1752–1764.

165 O. Czakkel, B. Berke and K. László, Effect of graphene-derivatives on the responsivity of PNIPAM-based thermosensitive nanocomposites – A review, *Eur. Polym. J.*, 2019, **116**, 106–116.

166 K. Shi, Z. Liu, Y. Y. Wei, W. Wang, X. J. Ju, R. Xie and L. Y. Chu, Near-Infrared Light-Responsive Poly(N-isopropylacrylamide)/Graphene Oxide Nanocomposite Hydrogels with Ultrahigh Tensibility, *ACS Appl. Mater. Interfaces*, 2015, **7**, 27289–27298.

167 X. Ma, Y. Li, W. Wang, Q. Ji and Y. Xia, Temperature-sensitive poly(N-isopropylacrylamide)/graphene oxide nanocomposite hydrogels by in situ polymerization with improved swelling capability and mechanical behavior, *Eur. Polym. J.*, 2013, **49**, 389–396.

168 Z. Li, J. Shen, H. Ma, X. Lu, M. Shi, N. Li and M. Ye, Preparation and characterization of pH- and temperature-responsive hydrogels with surface-functionalized graphene oxide as the crosslinker, *Soft Matter*, 2012, **8**, 3139–3145.

169 M. Zhang, Y. Wang, M. Jian, C. Wang, X. Liang, J. Niu and Y. Zhang, Spontaneous alignment of graphene oxide in hydrogel during 3D printing for multistimuli-responsive actuation, *Adv. Sci.*, 2020, **7**, 1903048.

170 A. Gregg, M. F. De Volder and J. J. Baumberg, Light-actuated anisotropic microactuators from CNT/hydrogel nanocomposites, *Adv. Opt. Mater.*, 2022, **10**, 2200180.

171 Z. Ying, Q. Wang, J. Xie, B. Li, X. Lin and S. Hui, Novel electrically-conductive electro-responsive hydrogels for smart actuators with a carbon-nanotube-enriched three-dimensional conductive network and a physical-phase-type three-dimensional interpenetrating network, *J. Mater. Chem. C*, 2020, **8**, 4192–4205.

172 X. Liu, J. Liu, S. Lin and X. Zhao, Hydrogel machines, *Mater. Today*, 2020, **36**, 102–124.

173 E. Palleau, D. Morales, M. D. Dickey and O. D. Velev, Reversible patterning and actuation of hydrogels by electrically assisted ionoprinting, *Nat. Commun.*, 2013, **4**, 2257.

174 Z. Xu and J. Fu, Programmable and reversible 3D-/4D-shape-morphing hydrogels with precisely defined ion coordination, *ACS Appl. Mater. Interfaces*, 2020, **12**, 26476–26484.

175 B. P. Lee and S. Konst, Novel hydrogel actuator inspired by reversible mussel adhesive protein chemistry, *Adv. Mater.*, 2014, **26**, 3415–3419.

176 C. Gong, Y. Zhai, J. Zhou, Y. Wang and C. Chang, Magnetic field assisted fabrication of asymmetric hydrogels for complex shape deformable actuators, *J. Mater. Chem. C*, 2022, **10**, 549–556.

177 H. W. Huang, M. S. Sakar, A. J. Petruska, S. Pane and B. J. Nelson, Soft micromachines with programmable motility and morphology, *Nat. Commun.*, 2016, **7**, 12263.

178 Y. Gao, X. Zhao, X. Han, P. Wang and W. J. Zheng, Soft actuator based on metal/hydrogel nanocomposites with anisotropic structure, *Macromol. Chem. Phys.*, 2022, **223**, 2100117.

179 D. Jaque, L. M. Maestro, B. del Rosal, P. Haro-Gonzalez, A. Benayas, J. Plaza, E. M. Rodríguez and J. G. Solé, Nanoparticles for photothermal therapies, *Nanoscale*, 2014, **6**, 9494–9530.

180 X. Huang, S. Neretina and M. A. El-Sayed, Gold nanorods: from synthesis and properties to biological and biomedical applications, *Adv. Mater.*, 2009, **21**, 4880–4910.

181 Y. Chen, Y. Gao, Y. Chen, L. Liu, A. Mo and Q. Peng, Nanomaterials-based photothermal therapy and its potentials in antibacterial treatment, *J. Controlled Release*, 2020, **328**, 251–262.

182 Y. Zhou, A. W. Hauser, N. P. Bende, M. G. Kuzyk and R. C. Hayward, Waveguiding Microactuators Based on a Photothermally Responsive Nanocomposite Hydrogel, *Adv. Funct. Mater.*, 2016, **26**, 5447–5452.

183 H. Guo, J. Cheng, K. Yang, K. Demella, T. Li, S. R. Raghavan and Z. Nie, Programming the Shape Transformation of a Composite Hydrogel Sheet via Erasable and Rewritable Nanoparticle Patterns, *ACS Appl. Mater. Interfaces*, 2019, **11**, 42654–42660.

184 S. Watanabe, H. Era and M. Kunitake, Two-wavelength infrared responsive hydrogel actuators containing rare-earth photothermal conversion particles, *Sci. Rep.*, 2018, **8**, 13528.

185 M. Kim, J. H. Lee and J. M. Nam, Plasmonic photothermal nanoparticles for biomedical applications, *Adv. Sci.*, 2019, **6**, 1900471.

186 X. Huang and M. A. El-Sayed, Plasmonic photo-thermal therapy (PPTT), *Alexandria J. Med.*, 2011, **47**, 1–9.

187 A. F. Zedan, S. Moussa, J. Terner, G. Atkinson and M. S. El-Shall, Ultrasmall gold nanoparticles anchored to graphene and enhanced photothermal effects by laser irradiation of gold nanostructures in graphene oxide solutions, *ACS Nano*, 2013, **7**, 627–636.

188 B. Sun, R. Jia, H. Yang, X. Chen, K. Tan, Q. Deng and J. Tang, Magnetic Arthropod Millirobots Fabricated by 3D-Printed Hydrogels, *Adv. Intell. Syst.*, 2022, **4**, 2100139.

189 J. Tang, Q. Yin, Y. Qiao and T. Wang, Shape morphing of hydrogels in alternating magnetic field, *ACS Appl. Mater. Interfaces*, 2019, **11**, 21194–21200.

190 J. Hu, K. Hiwatashi, T. Kurokawa, S. M. Liang, Z. L. Wu and J. P. Gong, Microgel-reinforced hydrogel films with high mechanical strength and their visible mesoscale fracture structure, *Macromolecules*, 2011, **44**, 7775–7781.

191 M. Yao, Z. Wei, J. Li, Z. Guo, Z. Yan, X. Sun, Q. Yu, X. Wu, C. Yu and F. Yao, Microgel reinforced zwitterionic hydrogel coating for blood-contacting biomedical devices, *Nat. Commun.*, 2022, **13**, 5339.

192 C. Li, X. Zhou, L. Zhu, Z. Xu, P. Tan, H. Wang, G. Chen and X. Zhou, Tough hybrid microgel-reinforced hydrogels dependent on the size and modulus of the microgels, *Soft Matter*, 2021, **17**, 1566–1573.

193 V. P. Anju, R. Pratoori, D. K. Gupta, R. Joshi, R. K. Annabattula and P. Ghosh, Controlled shape morphing of solvent free thermoresponsive soft actuators, *Soft Matter*, 2020, **16**, 4162–4172.

194 C.-Y. Lo, Y. Zhao, C. Kim, Y. Alsaid, R. Khodambashi, M. Peet, R. Fisher, H. Marvi, S. Berman and D. Aukes, Highly stretchable self-sensing actuator based on conductive photothermally-responsive hydrogel, *Mater. Today*, 2021, **50**, 35–43.

195 H. J. Sim, J. H. Noh and C. Choi, Bio-inspired shape-morphing actuator with a large stroke at low temperatures, *Sens. Actuators, B*, 2023, **378**, 133185.

196 K. Depa, A. Strachota, M. Šlouf and J. Brus, Poly(*N*-isopropylacrylamide)-SiO_2 nanocomposites interpenetrated by starch: Stimuli-responsive hydrogels with attractive tensile properties, *Eur. Polym. J.*, 2017, **88**, 349–372.

197 D. Morales, B. Bharti, M. D. Dickey and O. D. Velev, Bending of Responsive Hydrogel Sheets Guided by Field-Assembled Microparticle Endoskeleton Structures, *Small*, 2016, **12**, 2283–2290.

198 B. Anasori, M. R. Lukatskaya and Y. Gogotsi, 2D metal carbides and nitrides (MXenes) for energy storage, *Nat. Rev. Mater.*, 2017, **2**, 1–17.

199 Z. Fu, N. Wang, D. Legut, C. Si, Q. Zhang, S. Du, T. C. Germann, J. S. Francisco and R. Zhang, Rational design of flexible two-dimensional MXenes with multiple functionalities, *Chem. Rev.*, 2019, **119**, 11980–12031.

200 M. Carey and M. Barsoum, MXene polymer nanocomposites: a review, *Mater. Today Adv.*, 2021, **9**, 100120.

201 K. Hantanasirisakul and Y. Gogotsi, Electronic and optical properties of 2D transition metal carbides and nitrides (MXenes), *Adv. Mater.*, 2018, **30**, 1804779.

202 Z. Lin, J. Liu, W. Peng, Y. Zhu, Y. Zhao, K. Jiang, M. Peng and Y. Tan, Highly stable 3D Ti3C2T x MXene-based foam architectures toward high-performance terahertz radiation shielding, *ACS Nano*, 2020, **14**, 2109–2117.

203 X. Lin, Z. Li, J. Qiu, Q. Wang, J. Wang, H. Zhang and T. Chen, Fascinating MXene nanomaterials: emerging opportunities in the biomedical field, *Biomater. Sci.*, 2021, **9**, 5437–5471.

204 Y.-Z. Zhang, J. K. El-Demellawi, Q. Jiang, G. Ge, H. Liang, K. Lee, X. Dong and H. N. Alshareef, MXene hydrogels: fundamentals and applications, *Chem. Soc. Rev.*, 2020, **49**, 7229–7251.

205 S. S. Siwal, K. Sheoran, K. Mishra, H. Kaur, A. K. Saini, V. Saini, D.-V. N. Vo, H. Y. Nezhad and V. K. Thakur, Novel synthesis methods and applications of MXene-based nanomaterials (MBNs) for hazardous pollutants degradation: Future perspectives, *Chemosphere*, 2022, **293**, 133542.

206 X. Li, Z. Huang, C. E. Shuck, G. Liang, Y. Gogotsi and C. Zhi, MXene chemistry, electrochemistry and energy storage applications, *Nat. Rev. Chem.*, 2022, 1–16.

207 A. Maleki, M. Ghomi, N. Nikfarjam, M. Akbari, E. Sharifi, M. A. Shahbazi, M. Kermanian, M. Seyedhamzeh, E. Nazarzadeh Zare and M. Mehrali, Biomedical Applications of MXene-Integrated Composites: Regenerative Medicine, Infection Therapy, Cancer Treatment, and Biosensing, *Adv. Funct. Mater.*, 2022, **32**, 2203430.

208 J. Meng, Z. An, Y. Liu, X. Sun and J. Li, MXene-based hydrogels towards the photothermal applications, *J. Phys. D: Appl. Phys.*, 2022, **55**, 374003.

209 P. P. He, X. Du, Y. Cheng, Q. Gao, C. Liu, X. Wang, Y. Wei, Q. Yu and W. Guo, Thermal-Responsive MXene-DNA Hydrogel for Near-Infrared Light Triggered Localized Photothermal-Chemo Synergistic Cancer Therapy, *Small*, 2022, **18**, 2200263.

210 Y. Li, M. Han, Y. Cai, B. Jiang, Y. Zhang, B. Yuan, F. Zhou and C. Cao, Muscle-inspired MXene/PVA hydrogel with high toughness and photothermal therapy for promoting bacteria-infected wound healing, *Biomater. Sci.*, 2022, **10**, 1068–1082.

211 Y. Li, Y. Wang, J. Lu, W. Wang and D. Wang, Synergistically Photothermal Au Nanoprisms@ MXene Enable Adaptive Solar Modulation of HA-PNIPAM Hydrogels for Smart Window, *Chem. Eng. J.*, 2023, 141299.

212 P. Xue, C. Valenzuela, S. Ma, X. Zhang, J. Ma, Y. Chen, X. Xu and L. Wang, Highly Conductive MXene/PEDOT: PSS-Integrated Poly(N-Isopropylacrylamide) Hydrogels for Bioinspired Somatosensory Soft Actuators, *Adv. Funct. Mater.*, 2023, **33**, 2214867.

213 N. Tao, D. Zhang, X. Li, D. Lou, X. Sun, C. Wei, J. Li, J. Yang and Y.-N. Liu, Near-infrared light-responsive hydrogels via peroxide-decorated MXene-initiated polymerization, *Chem. Sci.*, 2019, **10**, 10765–10771.

214 J. Meng, J. Luo, H. Wang, Y. Quan, J. Li and X. Sun, Silver decorated MXene Nanosheet as a Radical Initiator for Polymerization and Multifunctional Hydrogel, *Chem. Commun.*, 2022, **58**, 6821–6824.

215 G. Ge, Y.-Z. Zhang, W. Zhang, W. Yuan, J. K. El-Demellawi, P. Zhang, E. Di Fabrizio, X. Dong and H. N. Alshareef, Ti3C2T x MXene-Activated Fast Gelation of Stretchable and Self-Healing Hydrogels: A Molecular Approach, *ACS Nano*, 2021, **15**, 2698–2706.

216 P. Xue, H. K. Bisoyi, Y. Chen, H. Zeng, J. Yang, X. Yang, P. Lv, X. Zhang, A. Priimagi and L. Wang, Near-infrared light-driven shape-morphing of programmable anisotropic hydrogels enabled by MXene nanosheets, *Angew. Chem., Int. Ed.*, 2021, **60**, 3390–3396.

217 T. Huber, J. Müssig, O. Curnow, S. Pang, S. Bickerton and M. P. Staiger, A critical review of all-cellulose composites, *J. Mater. Sci.*, 2012, **47**, 1171–1186.

218 R. J. Moon, A. Martini, J. Nairn, J. Simonsen and J. Youngblood, Cellulose nanomaterials review: structure, properties and nanocomposites, *Chem. Soc. Rev.*, 2011, **40**, 3941–3994.

219 S. Iwamoto, K. Abe and H. Yano, The effect of hemicelluloses on wood pulp nanofibrillation and nanofiber network characteristics, *Biomacromolecules*, 2008, **9**, 1022–1026.

220 M. Nogi, S. Iwamoto, A. N. Nakagaito and H. Yano, Optically transparent nanofiber paper, *Adv. Mater.*, 2009, **21**, 1595–1598.

221 A. J. Onyianta, D. O'Rourke, D. Sun, C.-M. Popescu and M. Dorris, High aspect ratio cellulose nanofibrils from macroalgae Laminaria hyperborea cellulose extract via a zero-waste low energy process, *Cellulose*, 2020, **27**, 7997–8010.

222 O. M. Vanderfleet and E. D. Cranston, Production routes to tailor the performance of cellulose nanocrystals, *Nat. Rev. Mater.*, 2021, **6**, 124–144.

223 N. L. Garcia de Rodriguez, W. Thielemans and A. Dufresne, Sisal cellulose whiskers reinforced polyvinyl acetate nanocomposites, *Cellulose*, 2006, **13**, 261–270.

224 X. Feng, C. Wang, S. Shang, H. Liu, X. Huang, J. Jiang and H. Zhang, Multicolor fluorescent cellulose hydrogels actuators: Lanthanide-ligand metal coordination, synergetic color-changing and shape-morphing, and antibacterial activity, *Chem. Eng. J.*, 2022, **450**, 138356.

225 O. Fourmann, M. K. Hausmann, A. Neels, M. Schubert, G. Nyström, T. Zimmermann and G. Siqueira, 3D printing of shape-morphing and antibacterial anisotropic nanocellulose hydrogels, *Carbohydr. Polym.*, 2021, **259**, 117716.

226 S. Spoljaric, A. Genovese and R. A. Shanks, Polypropylene–microcrystalline cellulose composites with enhanced compatibility and properties, *Composites, Part A*, 2009, **40**, 791–799.

227 A. Isogai and Y. Zhou, Diverse nanocelluloses prepared from TEMPO-oxidized wood cellulose fibers: Nanonetworks, nanofibers, and nanocrystals, *Curr. Opin. Solid State Mater. Sci.*, 2019, **23**, 101–106.

228 T. Saito, Y. Nishiyama, J.-L. Putaux, M. Vignon and A. Isogai, Homogeneous suspensions of individualized microfibrils from TEMPO-catalyzed oxidation of native cellulose, *Biomacromolecules*, 2006, **7**, 1687–1691.

229 M. C. Mulakkal, R. S. Trask, V. P. Ting and A. M. Seddon, Responsive cellulose-hydrogel composite ink for 4D printing, *Mater. Des.*, 2018, **160**, 108–118.

230 J. Espín, L. Garzón-Tovar, A. Carné-Sánchez, I. Imaz and D. Maspoch, Photothermal activation of metal–organic frameworks using a UV–vis light source, *ACS Appl. Mater. Interfaces*, 2018, **10**, 9555–9562.

231 X. Zhang, P. Xue, X. Yang, C. Valenzuela, Y. Chen, P. Lv, Z. Wang, L. Wang and X. Xu, Near-Infrared Light-Driven Shape-Programmable Hydrogel Actuators Loaded with Metal–Organic Frameworks, *ACS Appl. Mater. Interfaces*, 2022, **14**, 11834–11841.

232 L. Zong, X. Li, X. Han, L. Lv, M. Li, J. You, X. Wu and C. Li, Activation of actuating hydrogels with WS2 nanosheets for biomimetic cellular structures and steerable prompt deformation, *ACS Appl. Mater. Interfaces*, 2017, **9**, 32280–32289.

233 J. Zhao and J. Bae, Microphase Separation-Driven Sequential Self- Folding of Nanocomposite Hydrogel/Elastomer Actuators, *Adv. Funct. Mater.*, 2022, **32**, 2200157.

234 H. Son, E. Byun, Y. J. Yoon, J. Nam, S. H. Song and C. Yoon, Untethered Actuation of Hybrid Hydrogel Gripper via Ultrasound, *ACS Macro Lett.*, 2020, **9**, 1766–1772.

235 D. C. Tuncaboylu, M. Sari, W. Oppermann and O. Okay, Tough and Self-Healing Hydrogels Formed via Hydrophobic Interactions, *Macromolecules*, 2011, **44**, 4997–5005.

236 U. Gulyuz and O. Okay, Self-Healing Poly(acrylic acid) Hydrogels with Shape Memory Behavior of High Mechanical Strength, *Macromolecules*, 2014, **47**, 6889–6899.

237 G. Akay, A. Hassan-Raeisi, D. C. Tuncaboylu, N. Orakdogen, S. Abdurrahmanoglu, W. Oppermann and O. Okay, Self-healing hydrogels formed in catanionic surfactant solutions, *Soft Matter*, 2013, **9**, 2254–2261.

238 M. Yang, C. Liu, Z. Li, G. Gao and F. Liu, Temperature-Responsive Properties of Poly(acrylic acid-*co*-acrylamide) Hydrophobic Association Hydrogels with High Mechanical Strength, *Macromolecules*, 2010, **43**, 10645–10651.

239 G.-l Du, Y. Cong, L. Chen, J. Chen and J. Fu, Tough and multi-responsive hydrogels based on core-shell structured macro-crosslinkers, *Chin. J. Polym. Sci.*, 2017, **35**, 1286–1296.

240 E. Lee, D. Kim, H. Kim and J. Yoon, Photothermally driven fast responding photo-actuators fabricated with comb-type hydrogels and magnetite nanoparticles, *Sci. Rep.*, 2015, **5**, 15124.

241 J. Bae, J. Lawrence, C. Miesch, A. Ribbe, W. Li, T. Emrick, J. Zhu and R. C. Hayward, Multifunctional nanoparticle-loaded spherical and wormlike micelles formed by interfacial instabilities, *Adv. Mater.*, 2012, **24**, 2735–2741.

242 A. Saddique, H. M. Lee, J. C. Kim, J. Bae and I. W. Cheong, Cellulose nanocrystal nanocomposites capable of low-temperature and fast self-healing performance, *Carbohydr. Polym.*, 2022, **296**, 119973.

243 C. F. Dai, C. Du, Y. Xue, X. N. Zhang, S. Y. Zheng, K. Liu, Z. L. Wu and Q. Zheng, Photodirected Morphing Structures of Nanocomposite Shape Memory Hydrogel with High Stiffness and Toughness, *ACS Appl. Mater. Interfaces*, 2019, **11**, 43631–43640.

244 Y. Wang, C. Song, X. Yu, L. Liu, Y. Han, J. Chen and J. Fu, Thermo-responsive hydrogels with tunable transition temperature crosslinked by multifunctional graphene oxide nanosheets, *Compos. Sci. Technol.*, 2017, **151**, 139–146.

245 J. Liu, C. Chen, C. He, J. Zhao, X. Yang and H. Wang, Synthesis of Graphene Peroxide and Its Application in Fabricating Super Extensible and Highly Resilient Nanocomposite Hydrogels, *ACS Nano*, 2012, **6**, 8194–8202.

246 F. A. Plamper and W. Richtering, Functional Microgels and Microgel Systems, *Acc. Chem. Res.*, 2017, **50**, 131–140.

247 A. Ahiabu and M. J. Serpe, Rapidly Responding pH- and Temperature-Responsive Poly(*N*-Isopropylacrylamide)-Based Microgels and Assemblies, *ACS Omega*, 2017, **2**, 1769–1777.

248 L. W. Xia, R. Xie, X. J. Ju, W. Wang, Q. Chen and L. Y. Chu, Nano-structured smart hydrogels with rapid response and high elasticity, *Nat. Commun.*, 2013, **4**, 2226.

249 J. H. Na, A. A. Evans, J. Bae, M. C. Chiappelli, C. D. Santangelo, R. J. Lang, T. C. Hull and R. C. Hayward, Programming reversibly self-folding origami with micropatterned photocrosslinkable polymer trilayers, *Adv. Mater.*, 2015, **27**, 79–85.

250 M. Pezzulla, S. A. Shillig, P. Nardinocchi and D. P. Holmes, Morphing of geometric composites via residual swelling, *Soft Matter*, 2015, **11**, 5812–5820.

251 H. Therien-Aubin, Z. L. Wu, Z. Nie and E. Kumacheva, Multiple shape transformations of composite hydrogel sheets, *J. Am. Chem. Soc.*, 2013, **135**, 4834–4839.

252 J. Yin, W. Fan, Z. Xu, J. Duan, Y. Xia, Z. Nie and K. Sui, Precisely Defining Local Gradients of Stimuli-Responsive Hydrogels for Complex 2D-to-4D Shape Evolutions, *Small*, 2022, **18**, e2104440.

253 J. Uribe-Gomez, A. Posada-Murcia, A. Shukla, M. Ergin, G. Constante, I. Apsite, D. Martin, M. Schwarzer, A. Caspari and A. Synytska, Shape-morphing fibrous hydrogel/elastomer bilayers fabricated by a combination of 3D printing and melt electrowriting for muscle tissue regeneration, *ACS Appl. Bio Mater.*, 2021, **4**, 1720–1730.

254 Y. Tan, D. Wang, H. Xu, Y. Yang, W. An, L. Yu, Z. Xiao and S. Xu, A Fast, Reversible, and Robust Gradient Nanocomposite Hydrogel Actuator with Water-Promoted Thermal Response, *Macromol. Rapid Commun.*, 2018, **39**, 1700863.

255 Y. Liu, M. Takafuji, H. Ihara, M. Zhu, M. Yang, K. Gu and W. Guo, Programmable responsive shaping behavior induced by visible multi-dimensional gradients of magnetic nanoparticles, *Soft Matter*, 2012, **8**, 3295–3299.

256 J. Lin, Y. Han, Y. Cui, W. Zhao and C. Chang, Ionic coordination strengthening of temperature-driven gradient hydrogel actuators with rapid responsiveness, *Composites, Part B*, 2022, **245**, 110210.

257 W. Connacher, N. Zhang, A. Huang, J. Mei, S. Zhang, T. Gopesh and J. Friend, Micro/nano acoustofluidics: materials, phenomena, design, devices, and applications, *Lab Chip*, 2018, **18**, 1952–1996.

258 M. Li, J. Mei, J. Friend and J. Bae, Acousto-Photolithography for Programmable Shape Deformation of Composite Hydrogel Sheets, *Small*, 2022, **18**, e2204288.

259 S. Sant, M. J. Hancock, J. P. Donnelly, D. Iyer and A. Khademhosseini, Biomimetic gradient hydrogels for tissue engineering, *Can. J. Chem. Eng.*, 2010, **88**, 899–911.

260 D. Ji, S. Choi and J. Kim, A Hydrogel-Film Casting to Fabricate Platelet-Reinforced Polymer Composite Films Exhibiting Superior Mechanical Properties, *Small*, 2018, **14**, 1801042.

261 A. P. Piedade and A. C. Pinho, in *Smart Materials in Additive Manufacturing*, ed. M. Bodaghi and A. Zolfagharian, Elsevier, 2022, pp. 151–192.

262 D. Kim, A. Jo, K. B. C. Imani, D. Kim, J. W. Chung and J. Yoon, Microfluidic fabrication of multistimuli-responsive tubular hydrogels for cellular scaffolds, *Langmuir*, 2018, **34**(14), 4351–4359.

263 Y. Li, L. Liu, H. Xu, Z. Cheng, J. Yan and X.-M. Xie, Biomimetic Gradient Hydrogel Actuators with Ultrafast Thermo-Responsiveness and High Strength, *ACS Appl. Mater. Interfaces*, 2022, **14**, 32541–32550.

264 L. Liu, C. Qiao, H. An and D. Pasini, Encoding kirigami bi-materials to morph on target in response to temperature, *Sci. Rep.*, 2019, **9**, 19499.

265 Z. Jiang, M. L. Tan, M. Taheri, Q. Yan, T. Tsuzuki, M. G. Gardiner, B. Diggle and L. A. Connal, Strong, Self-Healable, and Recyclable Visible-Light-Responsive Hydrogel Actuators, *Angew. Chem., Int. Ed.*, 2020, **59**, 7049–7056.

266 C. Zhou, S. Dai, X. Zhou, H. Zhu, G. Cheng and J. Ding, Ethanol stimuli-responsive toughening PNIPAM/PVA self-healing hydrogel thermal actuator, *New J. Chem.*, 2023, **47**, 5825–5831.

267 M. P. H. Pedige, T.-A. Asoh, Y.-I. Hsu and H. Uyama, Stimuli-responsive composite hydrogels with three-dimensional stability prepared using oxidized cellulose nanofibers and chitosan, *Carbohydr. Polym.*, 2022, **278**, 118907.

268 R. C. P. Verpaalen, M. G. Debije, C. W. M. Bastiaansen, H. Halilović, T. A. P. Engels and A. P. H. J. Schenning, Programmable helical twisting in oriented humidity-responsive bilayer films generated by spray-coating of a chiral nematic liquid crystal, *J. Mater. Chem. A*, 2018, **6**, 17724–17729.

269 E.-J. Nam, Y. Kwon, Y. Ha and S. R. Paik, Fabrication of a Dual Stimuli-Responsive Assorted Film Comprising Magnetic- and Gold-Nanoparticles with a Self-Assembly Protein of α-Synuclein, *ACS Appl. Bio Mater.*, 2021, **4**, 1863–1875.

270 G. Stoychev, L. Guiducci, S. Turcaud, J. W. C. Dunlop and L. Ionov, Hole-Programmed Superfast Multistep Folding of Hydrogel Bilayers, *Adv. Funct. Mater.*, 2016, **26**, 7733–7739.

271 D. Guzman-Villanueva, H. D. C. Smyth, D. Herrera-Ruiz and I. M. El-Sherbiny, A novel aerosol method for the production of hydrogel particles, *J. Nanomater.*, 2011, **2011**, 1–10.

272 W. H. Kim, Y. Han, Y. H. Rhie, N.-I. Won and Y. H. Na, Spray Coating of Nanosilicate-Based Hydrogel on Concrete, *Adv. Mater. Interfaces*, 2022, **9**, 2201664.

273 M. G. Buonomenna, in *Smart Composite Coatings and Membranes*, ed. M. F. Montemor, Woodhead Publishing, 2016, pp. 371–419.

274 Y. Yu, J. Wang, X. Wang, Y. Huang, R. Li, Y. Wang, K. Ren and J. Ji, A Tough, Slippery, and Anticoagulant Double-Network Hydrogel Coating, *ACS Appl. Polym. Mater.*, 2022, **4**, 5941–5951.

275 X. Zhang, X. Xu, L. Chen, C. Zhang and L. Liao, Multi-responsive hydrogel actuator with photo-switchable color changing behaviors, *Dyes Pigm.*, 2020, **174**, 108042.

276 Y. Cheng, K. Ren, D. Yang and J. Wei, Bilayer-type fluorescence hydrogels with intelligent response serve as temperature/pH driven soft actuators, *Sens. Actuators, B*, 2018, **255**, 3117–3126.

277 Y. Cheng, C. Huang, D. Yang, K. Ren and J. Wei, Bilayer hydrogel mixed composites that respond to multiple stimuli for environmental sensing and underwater actuation, *J. Mater. Chem. B*, 2018, **6**, 8170–8179.

278 J. Zhang, L. Zheng, Z. Wu, L. Wang and Y. Li, Thermo-responsive bilayer hydrogel with switchable bending directions as soft actuator, *Polymer*, 2022, **253**, 124998.

279 Q. Zhao, Y. Liang, L. Ren, Z. Yu, Z. Zhang, F. Qiu and L. Ren, Design and fabrication of nanofibrillated cellulose-containing bilayer hydrogel actuators with temperature and near infrared laser responses, *J. Mater. Chem. B*, 2018, **6**, 1260–1271.

280 Y. Li, W. Zheng, B. Li, J. Dong, G. Gao and Z. Jiang, Double-layer temperature-sensitive hydrogel fabricated by 4D printing with fast shape deformation, *Colloids Surf., A*, 2022, **648**, 129307.

281 A. K. Bastola and M. Hossain, The shape – morphing performance of magnetoactive soft materials, *Mater. Des.*, 2021, **211**, 110172.

282 P. Jiang, Z. Ji, X. Zhang, Z. Liu and X. Wang, Recent advances in direct ink writing of electronic components and functional devices, *Prog. Addit. Manuf*, 2017, **3**, 65–86.

283 X. Kuang, D. J. Roach, J. Wu, C. M. Hamel, Z. Ding, T. Wang, M. L. Dunn and H. J. Qi, Advances in 4D Printing: Materials and Applications, *Adv. Funct. Mater.*, 2018, 1–23.

284 X. Li, Y. Yang, Y. Zhang, T. Wang, Z. Yang, Q. Wang and X. Zhang, Dual-method molding of 4D shape memory polyimide ink, *Mater. Des.*, 2020, **191**, 108606.

285 M. Falahati, P. Ahmadvand, S. Safaee, Y.-C. Chang, Z. Lyu, R. Chen, L. Li and Y. Lin, Smart polymers and nanocomposites for 3D and 4D printing, *Mater. Today*, 2020, **40**, 215–245.

286 G. Liu, Y. Zhao, G. Wu and J. Lu, Origami and 4D Printing of Elastomer-Derived Ceramic Structures, *Sci. Adv.*, 2018, **4**, eaat0641.

287 P. Jiang, Z. Ji, C. Yan, X. Wang and F. Zhou, High compressive strength metallic architectures prepared via polyelectrolyte-brush assisted metal deposition on 3D printed lattices, *Nano-Struct. Nano-Objects.*, 2018, **16**, 420–427.

288 P. Cao, L. Tao, J. Gong, T. Wang, Q. Wang, J. Ju and Y. Zhang, 4D Printing of a Sodium Alginate Hydrogel with Step-Wise Shape Deformation Based on Variation of Cross-linking Density, *ACS Appl. Polym. Mater.*, 2021, **3**, 6167–6175.

289 S. Tibbits, 4D Printing: Multi-Material Shape Change, *Archit. Des.*, 2014, **84**, 116–121.

290 F. Puza and K. Lienkamp, 3D Printing of Polymer Hydrogels—From Basic Techniques to Programmable Actuation, *Adv. Funct. Mater.*, 2022, **32**, 2205345.

291 K. Tian, J. Bae, S. E. Bakarich, C. Yang, R. D. Gately and G. M. Spinks, M. In Het Panhuis, Z. Suo and J. J. Vlassak, 3D Printing of Transparent and Conductive Heterogeneous Hydrogel-Elastomer Systems, *Adv. Mater.*, 2017, **29**, 1604827.

292 A. B. Baker, S. R. G. Bates, T. M. Llewellyn-Jones, L. P. B. Valori, M. P. M. Dicker and R. S. Trask, 4D printing with robust thermoplastic polyurethane hydrogel-elastomer trilayers, *Mater. Des.*, 2019, **163**, 107544.

293 Q. Ge, Z. Chen, J. Cheng, B. Zhang, Y.-F. Zhang, H. Li, X. He, C. Yuan, J. Liu, S. Magdassi and S. Qu, 3D printing of highly stretchable hydrogel with diverse UV curable polymers, *Sci. Adv.*, 2021, **7**, eaba4261.

294 Z. Ji, C. Yan, B. Yu, X. Zhang, M. Cai, X. Jia, X. Wang and F. Zhou, 3D printing of hydrogel architectures with complex and controllable shape deformation, *Adv. Mater. Technol.*, 2019, **4**, 1800713.

295 J. H. Na, N. P. Bende, J. Bae, C. D. Santangelo and R. C. Hayward, Grayscale gel lithography for programmed buckling of non-Euclidean hydrogel plates, *Soft Matter*, 2016, **12**, 4985–4990.

296 M. A. S. R. Saadi, A. Maguire, N. T. Pottackal, M. S. H. Thakur, M. M. Ikram, A. J. Hart, P. M. Ajayan and M. M. Rahman, Direct Ink Writing: A 3D Printing Technology for Diverse Materials, *Adv. Mater.*, 2022, **34**, 2108855.

297 A. Ambrosi and M. Pumera, 3D-printing technologies for electrochemical applications, *Chem. Soc. Rev.*, 2016, **45**, 2740–2755.

298 R. V. Pazhamannil, V. N. Jishnu Namboodiri, P. Govindan and A. Edacherian, Property enhancement approaches of fused filament fabrication technology: A review, *Polym. Eng. Sci.*, 2022, **62**, 1356–1376.

299 W. Li, M. Wang, H. Ma, F. A. Chapa-Villarreal, A. O. Lobo and Y. S. Zhang, Stereolithography apparatus and digital light processing-based 3D bioprinting for tissue fabrication, *iScience*, 2023, **26**, 106039.
300 H. Ding, M. Dong, Q. Zheng and Z. L. Wu, Digital light processing 3D printing of hydrogels: a minireview, *Mol. Syst. Des. Eng.*, 2022, **7**, 1017–1029.
301 Y. Dong, S. Wang, Y. Ke, L. Ding, X. Zeng, S. Magdassi and Y. Long, 4D Printed Hydrogels: Fabrication, Materials, and Applications, *Adv. Mater. Technol.*, 2020, **5**, 2000034.
302 A. Vaseashta, D. Demir, B. Sakım, M. Aşık and N. Bölgen, in *Electrospun Nanofibers: Principles, Technology and Novel Applications*, ed. A. Vaseashta and N. Bölgen, Springer International Publishing, Cham, 2022, pp. 631–655.
303 L. Liu, A. Ghaemi, S. Gekle and S. Agarwal, One-Component Dual Actuation: Poly(NIPAM) Can Actuate to Stable 3D Forms with Reversible Size Change, *Adv. Mater.*, 2016, **28**, 9792–9796.
304 O. Nechyporchuk, T. Yang Nilsson, H. Ulmefors and T. Köhnke, Wet Spinning of Chitosan Fibers: Effect of Sodium Dodecyl Sulfate Adsorption and Enhanced Dope Temperature, *ACS Appl. Polym. Mater.*, 2020, **2**, 3867–3875.
305 T. Chen, H. Bakhshi, L. Liu, J. Ji and S. Agarwal, Combining 3D Printing with Electrospinning for Rapid Response and Enhanced Designability of Hydrogel Actuators, *Adv. Funct. Mater.*, 2018, **28**, 1800514.
306 Q. Zheng, Z. Jiang, X. Xu, C. Xu, M. Zhu, C. Chen and F. Fu, Bio-Inspired Bicomponent Fiber with Multistimuli Response to Infrared Light and Humidity for Smart Actuators, *ACS Appl. Polym. Mater.*, 2021, **3**, 3131–3141.
307 J. J. Park, P. Won and S. H. Ko, A Review on Hierarchical Origami and Kirigami Structure for Engineering Applications, *Int. J. Precis. Eng. Manuf. – Green Technol.*, 2019, **6**, 147–161.
308 Q. Zhang, J. Wommer, C. O'Rourke, J. Teitelman, Y. Tang, J. Robison, G. Lin and J. Yin, Origami and kirigami inspired self-folding for programming three-dimensional shape shifting of polymer sheets with light, *Extreme Mech. Lett.*, 2017, **11**, 111–120.
309 T. S. Shim, S.-H. Kim, C.-J. Heo, H. C. Jeon and S.-M. Yang, Controlled Origami Folding of Hydrogel Bilayers with Sustained Reversibility for Robust Microcarriers, *Angew. Chem., Int. Ed.*, 2012, **51**, 1420–1423.
310 W. Fan, C. Shan, H. Guo, J. Sang, R. Wang, R. Zheng, K. Sui and Z. Nie, Dual-gradient enabled ultrafast biomimetic snapping of hydrogel materials, *Sci. Adv.*, 2019, **5**, eaav7174.
311 I. A. Choudhury and S. Shirley, Laser cutting of polymeric materials: An experimental investigation, *Opt. Laser Technol.*, 2010, **42**, 503–508.
312 A. K. Brooks, S. Chakravarty, M. Ali and V. K. Yadavalli, Kirigami-Inspired Biodesign for Applications in Healthcare, *Adv. Mater.*, 2022, **34**, 2109550.
313 X. P. Hao, Z. Xu, C. Y. Li, W. Hong, Q. Zheng and Z. L. Wu, Kirigami-Design-Enabled Hydrogel Multimorphs with Application as a Multistate Switch, *Adv. Mater.*, 2020, **32**, 2000781.
314 E. Ruel-Gariepy and J.-C. Leroux, In situ-forming hydrogels—review of temperature-sensitive systems, *Eur. J. Pharm. Biopharm.*, 2004, **58**, 409–426.
315 C. Wu and X. Wang, Globule-to-coil transition of a single homopolymer chain in solution, *Phys. Rev. Lett.*, 1998, **80**, 4092.
316 R. Bernstein, C. Cruz, D. Paul and J. Barlow, LCST behavior in polymer blends, *Macromolecules*, 1977, **10**, 681–686.
317 F. Liu, S. Jiang, L. Ionov and S. Agarwal, Thermophilic films and fibers from photo cross-linkable UCST-type polymers, *Polym. Chem.*, 2015, **6**, 2769–2776.
318 E. Clark and J. Lipson, LCST and UCST behavior in polymer solutions and blends, *Polymer*, 2012, **53**, 536–545.
319 J. Bae, J.-H. Na, C. D. Santangelo and R. C. Hayward, Edge-defined metric buckling of temperature-responsive hydrogel ribbons and rings, *Polymer*, 2014, **55**, 5908–5914.
320 J. Bae, N. P. Bende, A. A. Evans, J.-H. Na, C. D. Santangelo and R. C. Hayward, Programmable and reversible assembly of soft capillary multipoles, *Mater. Horiz.*, 2017, **4**, 228–235.
321 F. Doberenz, K. Zeng, C. Willems, K. Zhang and T. Groth, Thermoresponsive polymers and their biomedical application in tissue engineering–a review, *J. Mater. Chem. B*, 2020, **8**, 607–628.
322 M. Heskins and J. E. Guillet, Solution properties of poly(*N*-isopropylacrylamide), *J. Macromol. Sci., Chem.*, 1968, **2**, 1441–1455.
323 X. Zhang, L. Zhou, X. Zhang and H. Dai, Synthesis and solution properties of temperature-sensitive copolymers based on NIPAM, *J. Appl. Polym. Sci.*, 2010, **116**, 1099–1105.
324 T. H. Kim, J. G. Choi, J. Y. Byun, Y. Jang, S. M. Kim, G. M. Spinks and S. J. Kim, Biomimetic Thermal-sensitive Multi-transform Actuator, *Sci. Rep.*, 2019, **9**, 7905.
325 S. So and R. C. Hayward, Tunable upper critical solution temperature of poly(*N*-isopropylacrylamide) in ionic liquids for sequential and reversible self-folding, *ACS Appl. Mater. Interfaces*, 2017, **9**, 15785–15790.
326 X. Z. Zhang, D. Q. Wu and C. C. Chu, Effect of the crosslinking level on the properties of temperature-sensitive poly(N-isopropylacrylamide) hydrogels, *J. Polym. Sci., Part B: Polym. Phys.*, 2003, **41**, 582–593.
327 C. Yoon, R. Xiao, J. Park, J. Cha, T. D. Nguyen and D. H. Gracias, Functional stimuli responsive hydrogel devices by self-folding, *Smart Mater. Struct.*, 2014, **23**, 094008.
328 G. Stoychev, A. Kirillova and L. Ionov, Light-responsive shape-changing polymers, *Adv. Opt. Mater.*, 2019, **7**, 1900067.
329 J. Yang, X. Zhang, X. Zhang, L. Wang, W. Feng and Q. Li, Beyond the visible: bioinspired infrared adaptive materials, *Adv. Mater.*, 2021, **33**, 2004754.
330 Y.-L. Zhao and J. F. Stoddart, Azobenzene-Based Light-Responsive Hydrogel System, *Langmuir*, 2009, **25**, 8442–8446.
331 I. Tomatsu, K. Peng and A. Kros, Photoresponsive hydrogels for biomedical applications, *Adv. Drug Delivery Rev.*, 2011, **63**, 1257–1266.
332 Q. Si, Y. Feng, W. Yang, L. Fu, Q. Yan, L. Dong, P. Long and W. Feng, Controllable and stable deformation of a self-healing photo-responsive supramolecular assembly for an

optically actuated manipulator arm, *ACS Appl. Mater. Interfaces*, 2018, **10**, 29909–29917.

333 C. Li, Y. Xue, M. Han, L. C. Palmer, J. A. Rogers, Y. Huang and S. I. Stupp, Synergistic photoactuation of bilayered spiropyran hydrogels for predictable origami-like shape change, *Matter*, 2021, **4**, 1377–1390.

334 M. Irie and D. Kunwatchakun, Photoresponsive polymers. 8. Reversible photostimulated dilation of polyacrylamide gels having triphenylmethane leuco derivatives, *Macromolecules*, 1986, **19**, 2476–2480.

335 H. Patel, J. Chen, Y. Hu and A. Erturk, Photo-responsive hydrogel-based re-programmable metamaterials, *Sci. Rep.*, 2022, **12**, 13033.

336 G. Fang, X. Yang, S. Chen, Q. Wang, A. Zhang and B. Tang, Cyclodextrin-based host–guest supramolecular hydrogels for local drug delivery, *Coord. Chem. Rev.*, 2022, **454**, 214352.

337 G. Liu, Q. Yuan, G. Hollett, W. Zhao, Y. Kang and J. Wu, Cyclodextrin-based host–guest supramolecular hydrogel and its application in biomedical fields, *Polym. Chem.*, 2018, **9**, 3436–3449.

338 J. Chen, J. Huang, H. Zhang and Y. Hu, A photoresponsive hydrogel with enhanced photoefficiency and the decoupled process of light activation and shape changing for precise geometric control, *ACS Appl. Mater. Interfaces*, 2020, **12**, 38647–38654.

339 L. Hines, K. Petersen, G. Z. Lum and M. Sitti, Soft actuators for small-scale robotics, *Adv. Mater.*, 2017, **29**, 1603483.

340 Z. Li, J. Cai, M. Wei and J. Chen, An UV-photo and ionic dual responsive interpenetrating network hydrogel with shape memory and self-healing properties, *RSC Adv.*, 2022, **12**, 15105–15114.

341 Z. Tang, Z. Gao, S. Jia, F. Wang and Y. Wang, Graphene-based polymer bilayers with superior light-driven properties for remote construction of 3D structures, *Adv. Sci.*, 2017, **4**, 1600437.

342 D. Kim, H. S. Lee and J. Yoon, Highly bendable bilayer-type photo-actuators comprising of reduced graphene oxide dispersed in hydrogels, *Sci. Rep.*, 2016, **6**, 20921.

343 S. Li, Z. Cai, J. Han, Y. Ma, Z. Tong, M. Wang, L. Xiao, S. Jia and X. Chen, Fast-response photothermal bilayer actuator based on poly(*N*-isopropylacrylamide)–graphene oxide–hydroxyethyl methacrylate/polydimethylsiloxane, *RSC Adv.*, 2023, **13**, 18090–18098.

344 H. Kim, J. H. Kang, Y. Zhou, A. S. Kuenstler, Y. Kim, C. Chen, T. Emrick and R. C. Hayward, Light-driven shape morphing, assembly, and motion of nanocomposite gel surfers, *Adv. Mater.*, 2019, **31**, 1900932.

345 R. V. Kulkarni and S. Biswanath, Electrically responsive smart hydrogels in drug delivery: a review, *J. Appl. Biomater. Biomech.*, 2007, **5**, 125–139.

346 M.-Y. Choi, Y. Shin, H. S. Lee, S. Y. Kim and J.-H. Na, Multipolar spatial electric field modulation for freeform electroactive hydrogel actuation, *Sci. Rep.*, 2020, **10**, 1–8.

347 J. Ko, C. Kim, D. Kim, Y. Song, S. Lee, B. Yeom, J. Huh, S. Han, D. Kang and J.-S. Koh, High-performance electrified hydrogel actuators based on wrinkled nanomembrane electrodes for untethered insect-scale soft aquabots, *Sci. Robot.*, 2022, **7**, eabo6463.

348 S. Martel, J.-B. Mathieu, O. Felfoul, A. Chanu, E. Aboussouan, S. Tamaz, P. Pouponneau, L. H. Yahia, G. Beaudoin, G. Soulez and M. Mankiewicz, Automatic navigation of an untethered device in the artery of a living animal using a conventional clinical magnetic resonance imaging system, *Appl. Phys. Lett.*, 2007, **90**, 114105.

349 X. Hu, G. Nian, X. Liang, L. Wu, T. Yin, H. Lu, S. Qu and W. Yang, Adhesive Tough Magnetic Hydrogels with High Fe3O4 Content, *ACS Appl. Mater. Interfaces*, 2019, **11**, 10292–10300.

350 S. R. Goudu, I. C. Yasa, X. Hu, H. Ceylan, W. Hu and M. Sitti, Biodegradable Untethered Magnetic Hydrogel Milli-Grippers, *Adv. Funct. Mater.*, 2020, **30**, 2004975.

351 J. Tang, Z. Tong, Y. Xia, M. Liu, Z. Lv, Y. Gao, T. Lu, S. Xie, Y. Pei, D. Fang and T. J. Wang, Super tough magnetic hydrogels for remotely triggered shape morphing, *J. Mater. Chem. B*, 2018, **6**, 2713–2722.

352 D. E. P. Klenam, G. Egowan, M. O. Bodunrin, J. W. van der Merwe, N. Rahbar and W. Soboyejo, in *Comprehensive Structural Integrity*, ed. M. H. F. Aliabadi and W. O. Soboyejo, Elsevier, Oxford, 2nd edn, 2023, 50–90.

353 M. Saadli, D. L. Braunmiller, A. Mourran and J. J. Crassous, Thermally and Magnetically Programmable Hydrogel Microactuators, *Small*, 2023, **19**, 2207035.

354 J. Tang, B. Sun, Q. Yin, M. Yang, J. Hu and T. Wang, 3D printable, tough, magnetic hydrogels with programmed magnetization for fast actuation, *J. Mater. Chem. B*, 2021, **9**, 9183–9190.

355 A. K. Bastola, N. Rodriguez, M. Behl, P. Soffiatti, N. P. Rowe and A. Lendlein, Cactus-inspired design principles for soft robotics based on 3D printed hydrogel-elastomer systems, *Mater. Des.*, 2021, **202**, 109515.

356 C. Li, G. C. Lau, H. Yuan, A. Aggarwal, V. L. Dominguez, S. Liu, H. Sai, L. C. Palmer, N. A. Sather and T. J. Pearson, Fast and programmable locomotion of hydrogel-metal hybrids under light and magnetic fields, *Sci. Robot.*, 2020, **5**, eabb9822.

357 A. D. Drozdov, Swelling of pH-responsive cationic gels: Constitutive modeling and structure–property relations, *Int. J. Solids Struct.*, 2015, **64–65**, 176–190.

358 Y. Xiang, C. Liu, S. Ma, X. Wang, L. Zhu and C. Bao, Stimuli-Responsive Peptide Self-Assembly to Construct Hydrogels with Actuation and Shape Memory Behaviors, *Adv. Funct. Mater.*, 2023, 2300416.

359 R. Wang, Y. Zhang, W. Lu, B. Wu, S. Wei, S. Wu, W. Wang and T. Chen, Bio-inspired Structure-editing Fluorescent Hydrogel Actuators for Environment-interactive Information Encryption, *Angew. Chem., Int. Ed.*, 2023, **62**, e202300417.

360 L. Wang, F. Liu, J. Qian, Z. Wu and R. Xiao, Multi-responsive PNIPAM-PEGDA hydrogel composite, *Soft Matter*, 2021, **17**, 10421–10427.

361 D. Zhang, Y. Tang, K. Zhang, Y. Xue, S. Y. Zheng, B. Wu and J. Zheng, Multiscale bilayer hydrogels enabled by macrophase separation, *Matter*, 2023, **6**, 1484–1502.

362 Y. Lee, W. Song and J.-Y. Sun, Hydrogel soft robotics, *Mater. Today Phys.*, 2020, **15**, 100258.

363 Y. Chen, Y. Zhang, H. Li, J. Shen, F. Zhang, J. He, J. Lin, B. Wang, S. Niu and Z. Han, Bioinspired hydrogel actuator for soft robotics: Opportunity and challenges, *Nano Today*, 2023, **49**, 101764.

364 A. López-Díaz, A. Martín-Pacheco, A. M. Rodríguez, M. A. Herrero, A. S. Vázquez and E. Vázquez, Concentration Gradient-Based Soft Robotics: Hydrogels Out of Water, *Adv. Funct. Mater.*, 2020, **30**, 2004417.

365 X. Liu, M. Gao, J. Chen, S. Guo, W. Zhu, L. Bai, W. Zhai, H. Du, H. Wu and C. Yan, Recent Advances in Stimuli-Responsive Shape-Morphing Hydrogels, *Adv. Funct. Mater.*, 2022, **32**, 2203323.

366 B. Ying and X. Liu, Skin-like hydrogel devices for wearable sensing, soft robotics and beyond, *iScience*, 2021, **24**, 103174.

367 Y. Jian, B. Wu, X. Yang, Y. Peng, D. Zhang, Y. Yang, H. Qiu, H. Lu, J. Zhang and T. Chen, Stimuli-responsive hydrogel sponge for ultrafast responsive actuator, *Supramol. Mater.*, 2022, **1**, 100002.

368 Y. Zhao, C. Xuan, X. Qian, Y. Alsaid, M. Hua, L. Jin and X. He, Soft phototactic swimmer based on self-sustained hydrogel oscillator, *Sci. Robot.*, 2019, **4**, eaax7112.

369 Y. Sun, X. Le, S. Zhou and T. Chen, Recent Progress in Smart Polymeric Gel-based Information Storage for Anti-counterfeiting, *Adv. Mater.*, 2022, **34**, 2201262.

370 C. Yang, H. Xiao, L. Tang, Z. Luo, Y. Luo, N. Zhou, E. Liang, G. Wang and J. Tang, A 3D multistage information encryption platform with self-erasure function based on a synergistically shape-deformable and AIE fluorescence-tunable hydrogel, *Mater. Horiz.*, 2023, **10**, 2496–2505.

371 X. Du, H. Cui, B. Sun, J. Wang, Q. Zhao, K. Xia, T. Wu and M. S. Humayun, Photothermally Triggered Shape-Adaptable 3D Flexible Electronics, *Adv. Mater. Technol.*, 2017, **2**, 1700120.

372 A. D. Lantada, J. G. Korvink and M. Islam, Taxonomy for engineered living materials, *Cell Rep. Phys. Sci.*, 2022, **3**, 100807.

373 L. K. Rivera-Tarazona, M. S. Kalairaj, T. Corazao, M. Javed, P. E. Zimmern, S. Subashchandrabose and T. H. Ware, Controlling shape morphing and cell release in engineered living materials, *Biomater. Adv.*, 2022, **143**, 213182.

374 J. Qin, K. Chu, Y. Huang, X. Zhu, J. Hofkens, G. He, I. P. Parkin, F. Lai and T. Liu, The bionic sunflower: a bio-inspired autonomous light tracking photocatalytic system, *Energy Environ. Sci.*, 2021, **14**, 3931–3937.

375 A. Ding, O. Jeon, R. Tang, Y. B. Lee, S. J. Lee and E. Alsberg, Cell-Laden Multiple-Step and Reversible 4D Hydrogel Actuators to Mimic Dynamic Tissue Morphogenesis, *Adv. Sci.*, 2021, **8**, 2004616.